

SOFTWARE DEVELOPMENT FOR ANALYZING FLUID TRANSIENTS IN  
PIPELINES

A THESIS SUBMITTED TO  
THE GRADUATE SCHOOL OF NATURAL AND APPLIED SCIENCES  
OF  
MIDDLE EAST TECHNICAL UNIVERSITY

BY

SABER HABIBI TOPRAGHHALEH

IN PARTIAL FULFILLMENT OF THE REQUIREMENTS  
FOR  
THE DEGREE OF MASTER OF SCIENCE  
IN  
CIVIL ENGINEERING

AUGUST 2020



Approval of the thesis:

**SOFTWARE DEVELOPMENT FOR ANALYZING FLUID TRANSIENTS  
IN PIPELINES**

submitted by **SABER HABIBI TOPRAGHGHALEH** in partial fulfillment of the requirements for the degree of **Master of Science in Civil Engineering Department, Middle East Technical University** by,

Prof. Dr. Halil Kalıpçılar

Dean, Graduate School of **Natural and Applied Sciences**

---

Prof. Dr. Ahmet Türer

Head of the Department, **Civil Engineering**

---

Prof. Dr. Zafer Bozkuş

Supervisor, **Civil Engineering, METU**

---

**Examining Committee Members:**

Prof. Dr. İsmail Aydın

Civil Engineering, METU

---

Prof. Dr. Zafer Bozkuş

Civil Engineering, METU

---

Assoc. Prof. Dr. Elif Oğuz

Civil Engineering, METU

---

Assoc. Prof. Dr. Yakup Darama

Civil Engineering, Atılım University

---

Assist. Prof. Dr. Ali Ersin Dinçer

Civil Engineering, Abdullah Gül University

---

Date: 05.08.2020

**I hereby declare that all information in this document has been obtained and presented in accordance with academic rules and ethical conduct. I also declare that, as required by these rules and conduct, I have fully cited and referenced all material and results that are not original to this work.**

Name, Last name : Saber Habibi Topraghghaleh

Signature :

## **ABSTRACT**

### **SOFTWARE DEVELOPMENT FOR ANALYZING FLUID TRANSIENTS IN PIPELINES**

Habibi Topraghaleh, Saber  
Master of Science, Civil Engineering  
Supervisor : Prof. Dr. Zafer Bozkus

August 2020, 105 pages

A computer program is developed to analyze and simulate fluid transients in hydraulic systems contributing to finding practical solutions for unsteady flow conditions in pipelines. This program is built up using C sharp programming language in the visual studio platform. In the software, the method of characteristics is used for solving the non-linear partial differential equations of the transient flow. This software's primary purpose is to find quick solutions for a phenomenon called water hammer, which has been a severe problem for hydraulics engineers. The term water hammer in pipes is used for the condition in which pressure waves are created when the boundary conditions caused a moving fluid to experience a sudden change in its flow rate. This problem could be very damaging, and sometimes it leads to deadly consequences, and at the designing stage to provide safety, this phenomenon must be taken into account for pipelines. A number of boundary conditions can cause these sudden changes in the flow rate. Some of these conditions are opening or closing valves, pump trip, turbine load rejection or acceptance, etc. Solving and finding solutions manually for this phenomenon is very tedious and time-consuming work. As a result, a number of softwares have been developed in the world to tackle this

important issue. The present study is one of them to address the problem efficiently and accurately. For the time being, a new software has been developed in this study with some limited but important boundary conditions. The results of the number of problems tested indicate its correctness. It is hoped that it would be enriched in future studies with additional boundary conditions.

Keywords: Pipelines, Water hammer, Fluid transients, Software development, Boundary Conditions

## ÖZ

### **BORU HATLARINDA ZAMANA BAĞLI DEĞİŞEN AKIMLARIN ANALİZİ İÇİN YAZILIM GELİŞTİRME**

Habibi Topraghhaleh, Saber  
Yüksek Lisans, İnşaat Mühendisliği  
Tez Yöneticisi: Prof. Dr. Zafer Bozkuş

Ağustos 2020, 105 sayfa

Hidrolik sistemlerdeki zamana bağlı değişen (ZBD) akımları analiz etmek ve simüle etmek için, boru hatlarındaki bu tür akış koşulları için pratik çözümler bulmaya katkıda bulunan bir bilgisayar programı geliştirilmiştir. Bu program, visual studio platformunda C sharp programlama dili kullanılarak oluşturulmuştur. Yazılımda, ZBD akışın doğrusal olmayan kısmi diferansiyel denklemlerini çözmek için Karakteristikler Metodu kullanılmıştır. Bu yazılımın birincil amacı, Hidrolik mühendisleri için borularda ciddi bir sorun olan su darbesi adı verilen bir olgu için hızlı çözümler bulmasıdır. Su darbesi terimi, hareket eden bir akışkanın akış hızında sınır koşulları ani bir değişiklik yarattığında ortaya çıkan basınç dalgalarının olduğu durum için kullanılır. Bu sorun çok zararlı olabilir ve bazen ölümcül sonuçlara yol açabilir ve tasarım aşamasında güvenlik sağlamak için bu olgu boru hatları için dikkate alınmalıdır. Bir dizi sınır koşulu, akış hızında bu ani değişikliklere neden olabilir. Bu koşullardan bazıları vanaları açma veya kapatma, ani pompa güç kaybı, türbin yükünün reddedilmesi veya kabulü vs olabilir. Bu olgu için el hesapları ile çözüm bulmak çok yorucu ve zaman alıcı bir iştir. Sonuç olarak, bu önemli sorunun üstesinden gelmek için dünyada çeşitli yazılımlar geliştirilmiştir. Bu çalışma, sorunu etkin ve doğru bir şekilde ele alan yazılımlardan biridir. Şimdilik, bu çalışmada az

sayıda ancak önemli sınır koşullarıyla yeni bir yazılım geliştirilmiştir. Test edilen bir kaç problem örneğinin sonuçları yazılımın doğruluğunu kanıtlamaktadır. Ek sınır koşulları ile gelecekteki çalışmalarda bu yazılımın zenginleştirileceği ümit edilmektedir.

Anahtar Kelimeler: Boru hatları, Su darbesi, Zamana Bağlı Değişen Akım, Yazılım geliştirme, Sınır Koşulları

To My Family

## ACKNOWLEDGMENTS

I would like to express my deepest gratitude to Prof. Dr. Zafer Bozkuş for his support, guidance, advice, criticism, encouragement, and insight throughout the research. It is a real honor to work with him. This thesis could not have been completed without his help.

I also would like to thank the jury members of my thesis, Prof. Dr. Ismail Aydın, Assoc. Prof. Dr. Yakup Darama, Assoc. Prof. Dr. Elif Oğuz and Assist. Prof. Dr. Ali Ersin Dinçer for their contributions to improving the quality of the thesis.

I really appreciate my family. Thanks to my father Ali Habibi and my lovely mother Parvin Danandeh for their love and support even we have a long distance. My brilliant and beautiful sister Mahsa Habibi deserves special thanks. They have a main role on every success of my life.

## TABLE OF CONTENTS

ABSTRACT.....	v
ÖZ .....	vii
ACKNOWLEDGMENTS .....	x
TABLE OF CONTENTS.....	xi
LIST OF TABLES .....	xiv
LIST OF FIGURES .....	xv
LIST OF SYMBOLS .....	xix
CHAPTERS	
1 INTRODUCTION .....	1
1.1 General .....	1
1.2 Literature Survey .....	2
1.3 Aim of the Thesis .....	4
2 TRANSIENT FLOW .....	7
2.1 Definition of Transient Flow .....	7
2.2 Arithmetic Derivation of the Transient Flow Equations .....	8
2.3 Governing Differential Equations in Unsteady Pipe Flow.....	15
2.4 Method of Characteristics (MOC).....	16
2.4.1 Characteristics Equations .....	17
2.4.2 Time Discretization of Compatibility Equations .....	20
3 BOUNDARY CONDITIONS .....	25
3.1 Pipe Section.....	25

3.2	Series Pipes Connections .....	26
3.3	Upstream Reservoir with Constant Head.....	27
3.4	Upstream Reservoir with Variable Head .....	27
3.5	Single Centrifugal Pump.....	28
3.5.1	Events Following a Complete Power Failure .....	29
3.5.2	Dimensionless Pump Characteristics .....	30
3.5.3	Transient Equations for Pump Failure.....	33
3.5.4	Pumps with Discharge valve .....	38
3.5.5	Single Pump Boundary .....	39
3.6	Downstream Valve .....	40
3.7	Downstream Dead End .....	42
3.8	Surge Tank.....	42
4	THE SOFTWARE.....	45
4.1	User Interface Library.....	45
4.1.1	Main User Interface .....	45
4.1.2	Design Canvas .....	46
4.1.3	Engineering Libraries .....	48
4.1.4	Wave Speed Calculator .....	50
4.1.5	Object Properties Panel .....	51
4.1.6	Messages Box .....	52
4.1.7	Initial Conditions .....	52
4.1.8	Graphical and Tabular Result Forms.....	53
4.2	Object Elements and Properties .....	58
4.2.1	Pipe Object .....	58

4.2.2	Reservoir Object .....	59
4.2.3	Valve Object .....	61
4.2.4	Pump Object.....	63
4.2.5	Dead End Object .....	64
4.2.6	Surge Tank Object .....	65
5	Validation of the Software .....	67
5.1	Single Pipe Scenario.....	67
5.1	Series Pipes Scenario .....	73
5.1.1	Series Pipes Comparison for a Case Study by Wylie & Streeter.....	73
5.1.2	Series Pipes Comparison for a Case Study by Chaudhry .....	78
5.2	Pump Failure Scenarios.....	83
5.2.1	Pump Failure without Discharge valve .....	84
5.2.2	Pump Failure with Discharge valve Closing Gradually .....	87
5.2.3	Pump Failure with Discharge valve Closing Suddenly .....	90
5.3	Surge Tank Computation .....	92
5.4	Closure on the Cases .....	94
6	CONCLUSIONS.....	95
	REFERENCES .....	97
	APPENDICES	
A.	USER MANUAL .....	99

## LIST OF TABLES

### TABLES

Table 3.1 <i>Pump operation zones</i> .....	32
Table 4.1: <i>Young's Modulus of elasticity and Poisson's ratio for available pipe materials in the material collection, Chaudhry (1979)</i> .....	48
Table 4.2 <i>Available materials in the liquid collection of the software</i> .....	49
Table 5.1: <i>Single Pipe comparison at valve end (S-Hammer &amp; Wylie-Streeter)</i> ....	71
Table 5.2 <i>H vs. Time comparison for series pipes (Wylie-Streeter vs. S-Hammer)</i>	75
Table 5.3 <i>Q vs. Time comparison for series pipes (Wylie-Streeter vs. S-Hammer)</i>	76
Table 5.4 <i>H vs. Time comparison for series pipes (Chaudhry vs. S-Hammer)</i> .....	80
Table 5.5 <i>Q vs. Time comparison for series pipes (Chaudhry vs. S-Hammer)</i> .....	80
Table 5.6 <i>Input data for pump failure transient simulation</i> .....	84
Table 5.7 <i>Simple surge tank result comparisons</i> .....	94

## LIST OF FIGURES

### FIGURES

<i>Figure 2.1.</i> The pipeline system with a reservoir at upstream and a suddenly closed valve at downstream, Streeter & Wylie (1967).....	8
<i>Figure 2.2.</i> Implementation of the momentum equation to the control volume, Streeter & Wylie (1967, 1993).....	9
<i>Figure 2.3.</i> Continuity relations in a pipeline, Streeter & Wylie (1967).....	11
<i>Figure 2.4.</i> Circumferential pipe stress forces because of water hammer.....	13
<i>Figure 2.5.</i> Selected control volume for the continuity and momentum equations	15
<i>Figure 2.6.</i> Characteristic lines in the x-t plane.....	19
<i>Figure 2.7.</i> Characteristics lines for the nodal solution.....	21
<i>Figure 3.1.</i> Series junction boundary condition.....	26
<i>Figure 3.2.</i> Upstream reservoir with variable head.....	28
<i>Figure 3.3.</i> Polar diagram for $\alpha$ and $v$ .....	32
<i>Figure 3.4.</i> Pump characteristic curves for $N_s = 1800$ rpm.....	33
<i>Figure 3.5.</i> Schematic view of a pump boundary with its discharge valve.....	34
<i>Figure 3.6.</i> Replacement of WH curve with a straight line.....	35
<i>Figure 3.7.</i> Simple surge tank.....	42
<i>Figure 4.1.</i> The main user interface of the software.....	46
<i>Figure 4.2.</i> An example of all the objects drawn in the design canvas.....	47
<i>Figure 4.3.</i> Material library interface.....	49
<i>Figure 4.4.</i> Liquid library interface.....	50
<i>Figure 4.5.</i> Wave speed calculator result for the information provided.....	51
<i>Figure 4.6.</i> Scheme of the object properties Panel.....	52
<i>Figure 4.7.</i> Message box panel.....	52
<i>Figure 4.8.</i> Initial conditions window.....	53
<i>Figure 4.9.</i> Time-based tabular view of the results.....	54
<i>Figure 4.10.</i> Pipe-based tabular view of the results.....	54
<i>Figure 4.11.</i> Time dependent graphical chart windows form.....	55

<i>Figure 4.12.</i> A feature of the graphical charts form.....	57
<i>Figure 4.13.</i> Animation graphical chart windows form .....	57
<i>Figure 4.14.</i> A scheme of pipe series and Pipe series property panel in the software .....	59
<i>Figure 4.15.</i> symbols of upstream and downstream reservoirs and upstream reservoir object properties panel .....	60
<i>Figure 4.16.</i> Valve objects view and its properties panel .....	61
<i>Figure 4.17.</i> Valve object closure setting window .....	62
<i>Figure 4.18.</i> A sample of a system pumping water from an upstream lower reservoir to a downstream upper reservoir .....	64
<i>Figure 4.19.</i> A single pump boundary object Properties.....	64
<i>Figure 4.20.</i> Dead end boundary view of the software .....	65
<i>Figure 4.21.</i> Surge tank added to the system in the design stage.....	65
<i>Figure 4.22.</i> Surge tank analysis window .....	66
<i>Figure 5.1.</i> The definition of a water system with a Single Pipe .....	67
<i>Figure 5.2.</i> (a) Single pipeline design (b) analyze input data of the software .....	68
<i>Figure 5.3.</i> Objects properties inputs, (a) Valve Object properties, (b) Reservoir object properties, (c) Valve closure setting, and (d) Pipe object properties.....	69
<i>Figure 5.4.</i> Tabular view of results obtained for single pipe application.....	70
<i>Figure 5.5.</i> Graphical results obtained at valve end for single pipe application .....	70
<i>Figure 5.6.</i> Single pipe comparison (H vs. Time) and (Q vs. Time) at valve end ..	72
<i>Figure 5.7.</i> Series pipes case study, Wylie and Streeter (1978).....	73
<i>Figure 5.8.</i> S-Hammer schematic view and the properties of the pipes of a case study by Wylie & Streeter .....	74
<i>Figure 5.9.</i> H vs. Time comparison at valve end (Wylie-Streeter vs. S-Hammer).	77
<i>Figure 5.10.</i> Q vs. Time comparison at valve end (Wylie-Streeter vs. S-Hammer)	77
<i>Figure 5.11.</i> Series pipes case study by Chaudhry (1979) .....	78
<i>Figure 5.12.</i> Manual valve closure data entry .....	79
<i>Figure 5.13.</i> S-Hammer view and pipes properties of a case study by Chaudhry ..	79
<i>Figure 5.14.</i> H vs. Time at valve end (Chaudhry vs. Present study).....	82

<i>Figure 5.15.</i> Q vs. Time at the reservoir (Chaudhry vs. Present study) .....	82
<i>Figure 5.16.</i> The hydraulic model for pump failure transient simulation.....	83
<i>Figure 5.17.</i> H vs. Time chart for pump failure with no discharge valve, at x = 0 m .....	85
<i>Figure 5.18.</i> Q vs. Time chart for pump failure with no discharge valve, at x = 0 m .....	85
<i>Figure 5.19.</i> H vs. Time chart for the pump with no discharge valve, at x = 1575 m .....	86
<i>Figure 5.20.</i> Q vs. Time chart for the pump with no discharge valve, at x = 1575 m .....	86
<i>Figure 5.21.</i> S-Hammer valve closure setting for the pump trip with a valve.....	87
<i>Figure 5.22.</i> H vs. Time chart for pump failure transient event with a discharge valve and $t_c = 8$ s, at x = 0 m.....	88
<i>Figure 5.23.</i> Discharge vs. Time chart for pump failure transient event with a discharge valve and $t_c = 8$ seconds, at x = 0 m .....	88
<i>Figure 5.24.</i> H vs. Time chart for pump failure transient event with a discharge valve and $t_c = 8$ seconds, at x = 1575 m.....	89
<i>Figure 5.25.</i> Q vs. Time chart for pump failure transient event with a discharge valve and $t_c = 8$ seconds, at x = 1575 m.....	89
<i>Figure 5.26.</i> H vs. Time chart for pump failure transient event with a discharge valve closing suddenly at x = 0 m.....	90
<i>Figure 5.27.</i> Q vs. Time chart for pump failure transient event with a discharge valve closing suddenly at x = 0 m.....	90
<i>Figure 5.28.</i> H vs. Time chart for pump failure transient event with a discharge valve closing suddenly, at x = 1575 m.....	91
<i>Figure 5.29.</i> Q vs. Time chart for pump failure transient event with a discharge valve closing suddenly, at x = 1575 m.....	91
<i>Figure 5.30.</i> Simple surge tank model (Cofcof, 2011) .....	93
<i>Figure 5.31.</i> Simple surge tank simulations of S-Hammer .....	93
<i>Figure A.1.</i> New project windows form .....	99

<i>Figure A.2.</i> Design tab and design components list .....	99
<i>Figure A.3.</i> A sample hydraulic system drawn in S-Hammer.....	100
<i>Figure A.4.</i> Pipe properties inserted to a sample model.....	100
<i>Figure A.5.</i> Initial conditions options of a sample model .....	101
<i>Figure A.6.</i> Valve closure setting of a sample model.....	101
<i>Figure A.7.</i> Messages printed for an example model .....	102
<i>Figure A.8.</i> Properties of example model after analysis .....	102
<i>Figure A.9.</i> Time-based table results for the example model.....	103
<i>Figure A.10.</i> Pipe-based table results for the example model.....	103
<i>Figure A.11.</i> Time-dependent graphical chart for the example model.....	104
<i>Figure A.12.</i> Animative chart result for the example model.....	105

## LIST OF SYMBOLS

### SYMBOLS

A	Cross-Sectional Area of the Pipe ( $\text{m}^2$ )
$A_g$	Valve Opening Area ( $\text{m}^2$ )
a	Speed of Sound (m/s)
$C^+$ , $C^-$	Positive and Negative Characteristics Equations
$C_D$	Discharge Coefficient
D	Diameter of the Pipe (m)
E	Modulus of Elasticity of the Pipe Material (GPA)
e	Pipe Wall Thickness (mm)
$E_m$	A Constant for Valve Closure
f	Friction Factor
g	Gravitational Acceleration ( $\text{m/s}^2$ )
H	Piezometric Head (m)
$H_R$	Rated Head (m)
K	Bulk's Modulus of Elasticity of Fluid (GPA)
L	Pipeline Length (m)
N	Number of Nodes
$N_R$	Rated Rotational Speed (rpm)
P	Pressure (kPa)
Q	Flow Discharge ( $\text{m}^3/\text{s}$ )

$Q_R$	Rated Discharge ( $m^3/s$ )
$T_R$	Rated Torque (N.m)
$t$	Time (seconds)
$t_c$	Valve closure time (seconds)
$V$	Velocity (m/s)
$\nabla$	Control Volume ( $m^3$ )
WB, WH	Nondimensional pump characteristics
$WR^2$	Inertia Momentum of Rotating Parts of the Pump ( $Nm^2$ )
$\Delta x$	Reach Length (m)
$\Delta t$	Time Increment (seconds)
$z$	Elevation Head (m)
$\gamma$	Specific Weight ( $N/m^3$ )
$\lambda$	Multiplier of the Combination of Transient Equations
$\eta_R$	Rated Pump Efficiency
$\mu$	Absolute Viscosity
$\rho$	Density ( $kg/m^3$ )
$\tau$	Nondimensional Valve Opening
$\omega$	Circular frequency (Degrees)

# CHAPTER 1

## INTRODUCTION

### 1.1 General

Numerous reasons can cause the disturbance in the steady-state of the flow in pipelines. When velocity changes at a fixed point in space, local accelerations or decelerations create supplementary mass forces in a transient flow, and this phenomenon causes corresponding changes in pressure. These can manifest themselves as prominent short-term pressure increases or decreases resulting from the sudden closing of valves, power failure of pumps and turbines, pump trips, or increased pressure losses caused by pulsating flow. This extreme situation is, in general, called water hammer due to hammering sound in pipes.

Water hammer is synonymous with the unsteady hydraulic problems that mostly occurs in the penstocks of hydropower plants, fluid transmissions, pumped discharge lines, pipelines, and water distribution networks. This unsteady condition produces substantial pressure surges or waves in the system. The pressure fluctuations and resultant maximum pressures cause incredibly high loads for the system. In other cases, extremely low pressures can be generated, too. Without considering this phenomenon, such massive catastrophes can result in pipe collapse, pipe bursting, pump destruction, and even death. For instance, one of the most severe dramatic accidents happened in Sayano-Shushenskaya hydropower plant in Russia on 17 August 2008. According to Seleznev et al. (2014), one of the hydroelectric generators was utterly destroyed because of the sudden turbine closure initiated by some debris in the flow. There was severe damage to all of the generators in the plant, and the turbine hall building was completely destroyed. Consequently, 76 people died, and the financial loss was more than \$310 million.

## 1.2 Literature Survey

Studying hydraulic transients have become a special interest among the researchers over the last century due to its important character as well as its mathematical challenge. To solve transient flows, various methods have been developed to date, some of which are arithmetic, algebraic, implicit, graphical, linear analysis, and method of characteristics, (MOC).

Streeter and Wylie (1967, 1993) are the early pioneers who developed and applied the method of characteristics for analyzing the unsteady pipe flow. They outlined the principals of this method in detail by expressing the continuity and conservation of momentum equations in the form of partial differential form. They provided a number of unsteady pipe solutions in FORTRAN language.

Karney (1984) developed a network program for predicting fluid transients in complex systems such as large water distribution networks and arbitrary geometry networks. This program can solve many boundary conditions at the same time. The verification of the algorithm is tested by experimental data, and MOC is used in the procedure.

Karney and McInnis (1992) suggested a new calculation of transients in simple pipe networks by adding extensions to the conservative MOC. They calculated the mathematical basis, including friction loss and various boundary conditions. The effects of frictions losses and other minor losses are considered in both pipe connections and control devices. Hence, this model is validated for small pipe systems but with subsuming a variety of devices.

Thorley (2004) presents some practical steps which could be taken to overcome the negative impacts of a transient event. He discussed the reasons for unsteady flow in the pipeline system along with the analyzing tools that can help to judge the potential effects of the flow. He suggested various protection and controlling devices and

strategies to suppress the cause of transient flow, as well as their mathematical expressions.

Koç (2007) developed a computer code written in C# programming language. The program analyzes transient events using the method of characteristics that is used to solve partial differential equations. The output of the code is arranged in tabular form for pressure head and discharge according to time increments, and it gives graphical representations of these values. There are also prompts for users, which warns about possible dangerous operation modes of the pipeline components.

Afshar and Rohani (2008) proposed an Implicit MOC to reduce the deficiencies and restrictions of the commonly used conventional MOC. They used an element-wise classification in equations for the system. The suitable equations which defined the behavior of the devices, including pipes, are collected to produce the final equations which can be solved for unknown heads and discharges. They solved two different transient problems, including pump failure and valve closure. Ultimately, they compared the results obtained from their method with the conventional methods.

Bozkuş (2008) performed a water-hammer analysis using MOC for the Çamlıdere-Ivedik Water Treatment Plant with multiple pipelines with different features. A FORTRAN program is used to simulate the transient event in the system for various conditions. Consequently, for considering the safety in case of a pipe break, to avoid pressure fluctuations in the pipelines, placing protection devices is recommended according to the results obtained. However, he just modified an existing program to perform the task.

A protective measurement has been studied by Calamak and Bozkus (2012). Researchers analyzed the reaction of the system caused by water hammer with a computer program using MOC and then run the code for three different protective measurement scenarios in a case study and compared the results. The cases are instant load rejection with the effect of a flywheel, pressure relief valve, and safety membranes. They did this method on small hydropower plants on the focus of the

safety of the system. In the analysis, head, power conditions, and discharge are assumed nominal.

Dinçer, A. E. (2013) investigated waterhammer problems in the penstocks of pumped-storage power plants. The results were also presented by Dinçer and Bozkuş (2016) They used an available code to solve transient events that are produced by sudden load rejection of the turbine, first with a surge tank and second without it. With the results obtained, they checked and compared the two scenarios to see the effect of protection devices.

Dursun S. (2013) studied numerically possible protection measures against water hammer in the Yeşilvadi Hydropower Plant. Again, an existing software was employed for the analyses under various scenarios, and the results were compared with the SCADA values obtained at the plant during operation. Good correlations were obtained.

Another study has been done by Dalgıç (2017), who focused on developing computer-based analyses for pipelines. He developed a computer program by using the method of characteristics which can solve equations of basic unsteady pipe flows, as mentioned previously. The developed software is named H-Hammer and operates with help from MS Excel, Visual Basic, and AutoCAD to analyze. Numerous boundary conditions are included in the study. For testing the software, he compared his results with those given in the well-known textbooks and concluded that they agreed well. However, his software depended on previous knowledge of AutoCAD, rendering it not so user-friendly.

### **1.3 Aim of the Thesis**

In this thesis, the main idea is to develop a brand new software to analyze and simulate the transient pipe flow conditions, which can help engineers to consider essential measures in order to avoid devastating pressure changes while water

hammer is happening. In order to do so, a windows-based software is deemed to be appropriate. To make it user-friendly, the software is independent of external programs. The program is presented with a user interface including designer canvas, database library, means for producing tables and graphics, wave speed and friction calculators, and other various features. Thoroughly performed simulations can help the engineers to design a safer system and find quick and correct solutions, mainly for water hammer problems. This program can guarantee safe control of the system, and engineers can judge genuinely using the knowledge of pressure and discharge information calculated using this software. Furthermore, the program is user-friendly and can be easily used by users whose knowledge about the subject is limited. The ultimate goal of this study is to develop a local computer software that can be used in Turkey to avoid buying costly programs from foreign companies.



## CHAPTER 2

### TRANSIENT FLOW

In this chapter, the transient flow features will be introduced first. Then, the transient flow equations will be derived.

#### 2.1 Definition of Transient Flow

The condition of flow consists of two states, steady and unsteady. In steady-state flow, the flow conditions at a point, including discharge, pressure, and velocity, do not vary over time. However, in a transient flow, the mentioned properties change at a point in space over time, or in other words, flow is time-dependent. The term "transient" is usually employed to indicate the evolution of the solution over time from an initial steady-state until it reaches the new steady-state condition. Between those steady-state conditions, the flow is unsteady. Before handling transient flow, the solution of the steady-state flow is needed. For solving the non-linear partial differential equations, the information of steady-state flow plays an essential role since the initial values are required to deal with the transients along with the boundary conditions.

The term, water hammer is used when a transient event occurs in close conduits. More detailed information will be discussed about the formulation of water hammer or transient flow.

## 2.2 Arithmetic Derivation of the Transient Flow Equations

The fundamental equations for transient flow are momentum and continuity equations. In this study, the solution is one dimensional, so the continuity and conservation of mass equations are derived for x-direction. Eq. (2.1) shows the integral form of the conservation of momentum equation written in the x-direction.

$$\sum F_x = \frac{d}{dt} \int_{CV} V \rho dV + \int_{CS} V \rho (\vec{V} \cdot \vec{n}) dA \quad (2.1)$$

Figure 2.1 illustrates a pipeline system with an upstream reservoir and a valve at its downstream. In this case, an abrupt stoppage in the system caused by the valve disturbs the flowing fluid with  $V_0$  towards downstream. Hence, a pressure surge wave produced by the valve propagates towards upstream. This surge wave is also known as the acoustic wave, “a” has the speed of sound.

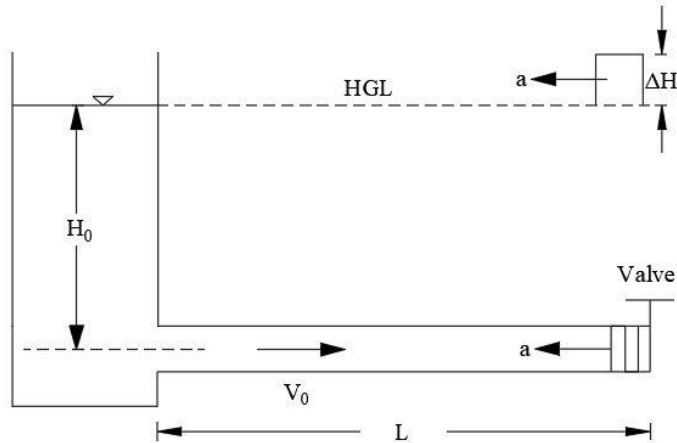


*Figure 2.1.* The pipeline system with a reservoir at upstream and a suddenly closed valve at downstream, Streeter & Wylie (1967)

The momentum equation is implemented to the control volume in Figure 2.1 and is shown in Figure 2.2.

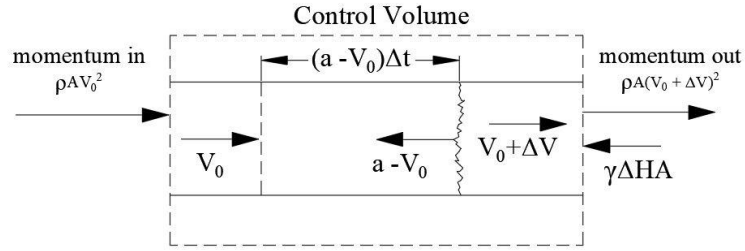


Figure 2.2. Implementation of the momentum equation to the control volume, Streeter & Wylie (1967, 1993)

By applying the forces according to Eq. (2.1), the unsteady part of the system representing the change of the internal momentum is written below.

$$\frac{d}{dt} \int_{CV} V \rho dV = \rho \frac{A(a - V_0)}{\Delta t} \Delta t (V_0 + \Delta V - V_0) = \rho A(a - V_0) \Delta V \quad (2.2)$$

Hence the momentum fluxes that are available across the control surface are written below:

$$\int_{CS} V \rho (\vec{V} \cdot \vec{n}) dA = \rho A (V_0 + \Delta V)^2 - \rho A V_0^2 \quad (2.3)$$

Finally, the combination of the Eqs. (2.2) and (2.3), gives the equation below.

$$\rho A(a - V_0) \Delta V + \rho A (V_0 + \Delta V)^2 - \rho A V_0^2 = -\gamma A \Delta H \quad (2.4)$$

In which,

$\rho$  = density of the fluid (kg/m<sup>3</sup>)

$A$  = cross-sectional area of the pipe (m)

$a$  = wave speed (m/s)

$V_0$  = initial velocity (m/s)

$\Delta V$  = change in the velocity (m/s)

$\gamma$  = specific weight of the fluid (N/m<sup>3</sup>)

$\Delta H$  = change in the head (m)

$g$  = gravitational acceleration ( $\text{m/s}^2$ )

In the equation obtained, the term  $\rho A(a-V_0)$ , which is the mass of fluid, has its change in velocity by  $\Delta V$  in one instant. Moreover, the quantity of the term  $\Delta V^2$  is so small that it can be neglected, so the simplified form of the equation is written below.

$$\Delta H = -\frac{a\Delta V}{g} \left( 1 + \frac{V_0}{a} \right) \approx -\frac{a\Delta V}{g} \quad (2.5)$$

In general, the wave speed is deficient compared to the initial velocity, so consequently, the term  $V_0/a$  can be omitted in the equation. Additionally, when the valve is closed by increments, Eq. (2.5) changes to the equation below.

$$\sum \Delta H = -\frac{a}{g} \sum \Delta V \quad (2.6)$$

It must be considered that both Eq. (2.5) and Eq. (2.6) are feasible when the wave surge travels to upstream and returns to the valve end in less than  $2L/a$  seconds in which  $L$  is the length of the pipe. In Figure 2.1 and 2.2, when the fluid stops moving,  $\Delta V = -V_0$  and  $\Delta H = aV_0/g$ . Consequently, a comprehensive equation can be written to describe the pressure changes in the system, so

$$\sum \Delta H = \pm \frac{a}{g} \sum \Delta V \quad (2.7)$$

The plus sign in the equation represents the pressure surges traveling downstream end, while the minus sign symbolizes the waves that move towards the upstream reservoir.

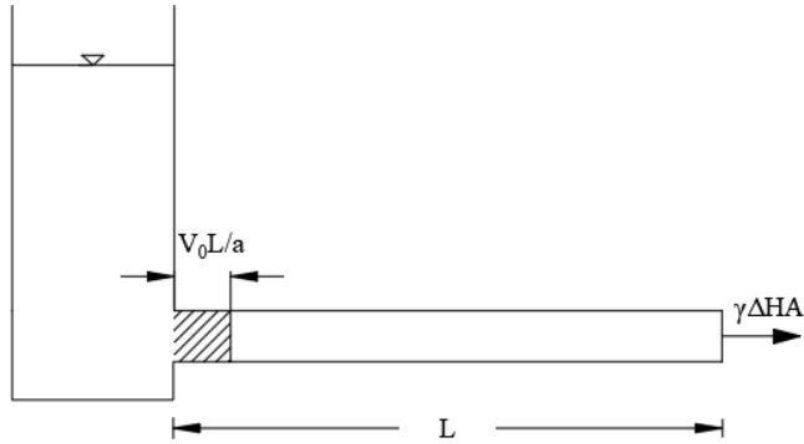


Figure 2.3. Continuity relations in a pipeline, Streeter & Wylie (1967)

Now, we can derive the wave speed equation with the help of continuity that is illustrated in Figure 2.3. By referring to Figure 2.1, when the valve at the downstream end stops instantaneously, the pipe length may be extended with increment  $\Delta s$ . This stretch is a result of high-pressure changes in the system and depends on the support type of the pipe. It is assumed that the stretch of the pipe happens when the wave moves the length in  $L/a$  seconds or similarly the velocity is  $\Delta s a / L$ . Hence, by the effect of the mass  $\rho A V_0 L/a$  entering, the change in velocity becomes  $\Delta V = \Delta s a / L - V_0$ . This process leads to a rise in the area of the pipe due to additional volume and pipe stretch. Mathematically, the continuity satisfaction of this process is shown in the equation below.

$$\rho A V_0 \frac{L}{A} = \rho L \Delta A + \rho A \Delta s + L A \Delta \rho \quad (2.8)$$

After considering  $\Delta V = \Delta s a / L - V_0$ , Eq. (2.13) is simplified.

$$-\frac{\Delta V}{a} = \frac{\Delta A}{A} + \frac{\Delta \rho}{\rho} \quad (2.9)$$

In Eq. (2.9),  $V_0$  is eliminated. Now, we can extract  $\Delta V$  by using Eq. (2.6).

$$a^2 = \frac{g\Delta H}{\frac{\Delta A}{A} + \frac{\Delta\rho}{\rho}} \quad (2.10)$$

The definition of the bulk modulus of elasticity is,

$$K = \frac{\Delta P}{\frac{\Delta\rho}{\rho}} = - \frac{\Delta P}{\frac{\Delta V}{V}} \quad (2.11)$$

Now, to obtain a new equation for wave speed, we can rearrange and simplify Eq. (2.10), so

$$a^2 = \frac{\frac{K}{\rho}}{1 + \left(\frac{K}{A}\right)\left(\frac{\Delta A}{\Delta P}\right)} \quad (2.12)$$

If the pipe wall is considerably thick, the extension in the pipe area will be so small that can be neglected, so the wave speed becomes,

$$a \approx \sqrt{\frac{K}{\rho}} \quad (2.13)$$

However, in the case of flexible pipes, in Eq. (2.12), the term 1 is minor, so it can be assumed unimportant.

$$a \approx \sqrt{\frac{A \Delta P}{\rho \Delta A}} \quad (2.14)$$

Moreover, in the case of thin wall pipes, the evaluation of  $\Delta A/(A \Delta P)$  depends on three support condition mentioned below:

- The pipe only anchored at the upstream end, case a
- The pipe anchored throughout against axial movements, case b
- The pipe anchored with expansion joints, case c

The difference that affects the wave speed equation from these three cases is in defining the Poisson's ratio,

$$\mu = -\frac{\text{lateral unit strain}}{\text{axial unit strain}} = -\frac{\xi}{\xi_1} \quad (2.15)$$

where,

$$\xi_r = \xi_2 + \xi = \xi_2 - \mu\xi_1 \quad (2.16)$$

Strain and stress are functions of the modulus of elasticity, E, thus

$$\xi_2 = \frac{\sigma_2}{E} \quad \xi_1 = \frac{\sigma_1}{E} \quad (2.17)$$

Where;

$\sigma_1$  = axial unit stress

$\sigma_2$  = lateral unit stress

To obtain the stresses generated by the water hammer, the realization of Figure 2.4 would be essential.

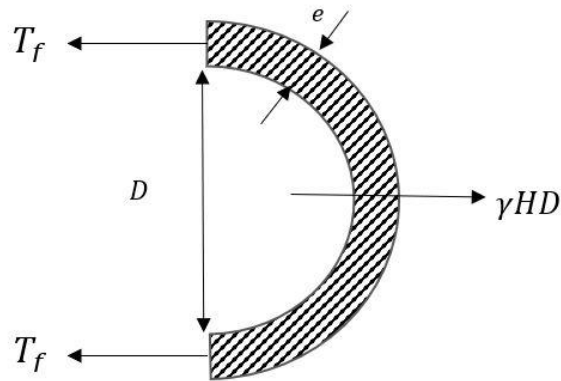


Figure 2.4. Circumferential pipe stress forces because of water hammer

where  $e$  = wall thickness and  $T_f$  = circumferential tensile force per unit of pipe.

Regarding Figure 2.4, tensile forces can be calculated for all three cases.

$$\sigma_2 = \frac{T_f}{e} = \frac{\gamma HD}{2e} \quad \text{or} \quad \Delta\sigma_2 = \frac{\gamma D\Delta H}{2e} = \frac{D\Delta P}{2e} \quad (2.18)$$

$$\sigma_1 = \frac{F}{A} = \frac{P\pi r^2}{2\pi r e} = \frac{DP}{4e} \quad (2.19)$$

Now, we can find the value of  $\Delta A/(A \Delta P)$  for all cases.

- Case a: in this case, the force on the valve that is closed will be the tensile stress, so

$$\sigma_1 = \frac{\gamma HA}{\pi D e} \quad \text{or} \quad \Delta\sigma_1 = \frac{D\Delta P}{4e} \quad (2.20)$$

Finally,

$$\frac{\Delta A}{A\Delta P} = \frac{2\Delta\xi_T}{\Delta P} = \frac{2}{\Delta PE} (\Delta\sigma_2 - \mu\Delta\sigma_1) = \frac{D}{Ee} \left(1 - \frac{\mu}{2}\right) \quad (2.21)$$

- Case b: in this case,  $\xi_1 = 0$ , and  $\sigma_1 = 0$ , thus

$$\frac{\Delta A}{A\Delta P} = \frac{2}{\Delta PE} (\Delta\sigma_2 - \mu^2\Delta\sigma_2) = \frac{D}{Ee} (1 - \mu^2) \quad (2.22)$$

- Case c: in this case, as the pipe anchored with expansion joints,  $\sigma_1 = 0$ , so

$$\frac{\Delta A}{A\Delta P} = \frac{2\Delta\sigma_2}{\Delta PE} = \frac{D}{Ee} \quad (2.23)$$

Consequently, we can obtain the final equation for the pressure wave speed.

$$a = \frac{\sqrt{K/\rho}}{\sqrt{1 + [(K/E)(D/E)]c_1}} \quad (2.24)$$

According to the cases discussed above,  $c_1$  represents the values that are shown below:

- Case a:  $c_1 = 1 - \frac{\mu}{2}$
- Case 2:  $c_1 = 1 - \mu^2$
- Case a:  $c_1 = 1$

### 2.3 Governing Differential Equations in Unsteady Pipe Flow

The water hammer analysis aims to determine fluid behavior throughout a transient event at a point in space and an instance of time. To achieve this goal, the conservation of mass and momentum equations must be applied. In this section, a control volume is used to derive partial differential equations for transient flow. The time rate of the momentum change in the hydraulic system must be equal to the sum of the forces applied to the control volume by its surrounding environment, according to Newton's second law. Figure 2.5 illustrates the parameters in a system used to derive momentum and continuity equations.

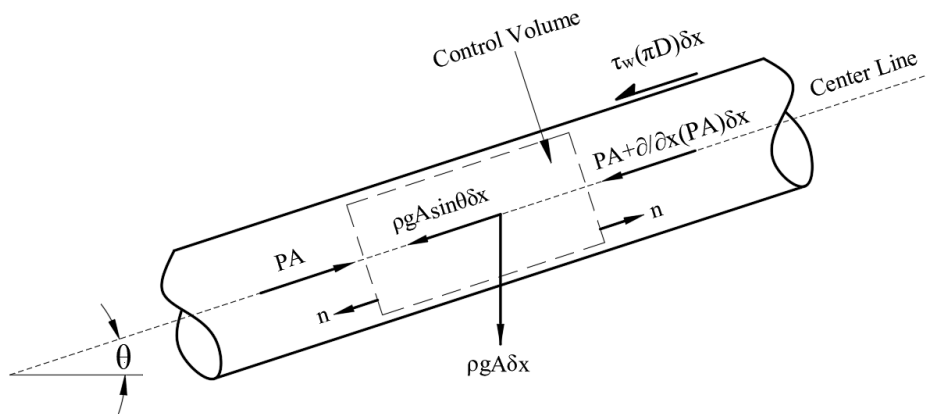


Figure 2.5. Selected control volume for the continuity and momentum equations

The assumptions made for the system above are;

- Flow is one-dimensional
- The liquid is slightly compressible
- Pipe wall is elastic

- The pressure is distributed uniformly at the surface of the control volume

By applying the conservation of mass and momentum principles, we can derive continuity and momentum equations.

$$\frac{\partial P}{\partial t} + V \frac{\partial P}{\partial x} + \rho a^2 \frac{\partial V}{\partial x} = 0 \quad (2.25)$$

$$\frac{\partial V}{\partial t} + V \frac{\partial V}{\partial x} + \frac{1}{\rho} \frac{\partial P}{\partial x} + g \sin \theta + \frac{4\tau_w}{\rho D} = 0 \quad (2.26)$$

In which,

P = Pressure (N/m<sup>2</sup>)

$\rho$  = Density of the fluid (kg/m<sup>3</sup>)

V = Flow velocity (m/s)

g = Gravitational acceleration (m/s<sup>2</sup>)

D = Diameter of the pipe (m)

a = Wave speed (m/s)

$\tau_w$  = wall shear stress (N/m<sup>2</sup>)

Eqs. (2.25) and (2.26) are continuity and momentum equations, respectively. While solving these equations, pressure and velocity must be calculated at any time and distance. Hence, solving these equations in a closed-form is impossible. There are various methods to solve these equations. In this study, the method of characteristics is selected to solve transient equations.

## 2.4 Method of Characteristics (MOC)

In this section, the use of MOC for solving transient flow is examined.

### 2.4.1 Characteristics Equations

An individual approach in previous sections derived the continuity and momentum equations. These two equations are non-linear, hyperbolic, partial differential equations in two dependent variables, velocity and pressure, and two independent variables, which are distance and time along the pipeline. These two non-linear partial differential equations can be transformed into four ordinary differential equations by the characteristics method to be explained below. Let us use labels  $L_1$  and  $L_2$  for the equations as follows:

$$L_1 = \frac{\partial P}{\partial t} + V \frac{\partial P}{\partial x} + \rho a^2 \frac{\partial V}{\partial x} = 0 \quad (2.27)$$

$$L_2 = \frac{\partial V}{\partial t} + V \frac{\partial V}{\partial x} + \frac{1}{\rho} \frac{\partial P}{\partial x} + g \sin \theta + \frac{4\tau_w}{\rho D} = 0 \quad (2.28)$$

As both of the equations are equal to 0, any linear combination of these two equations will again be equal to zero, i.e., these equations can be combined linearly with an unknown multiplier,  $\lambda$ , giving another equation.

$$L_1 + \lambda L_2 = \left[ \frac{\partial P}{\partial t} + V \frac{\partial P}{\partial x} + \rho a^2 \frac{\partial V}{\partial x} \right] + \lambda \left[ \frac{\partial V}{\partial t} + V \frac{\partial V}{\partial x} + \frac{1}{\rho} \frac{\partial P}{\partial x} + F \right] = 0 \quad (2.29)$$

Where

$$F = g \sin \theta + \frac{4\tau_w}{\rho D} \quad (2.30)$$

by rearranging the equation

$$\left[ \frac{\partial P}{\partial t} + \left( V + \frac{\lambda}{\rho} \right) \frac{\partial P}{\partial x} \right] + \lambda \left[ \frac{\partial V}{\partial t} + \left( V + \frac{\rho a^2}{\lambda} \right) \frac{\partial V}{\partial x} \right] + \lambda F = 0 \quad (2.31)$$

We know that  $P$  and  $V$  are a function of  $x$  and  $t$ , so we can use the chain rule from calculus to rewrite the terms.

$$\frac{dV}{dt} = \frac{\partial V}{\partial t} + \frac{\partial V}{\partial x} \frac{dx}{dt} \quad (2.32)$$

$$\frac{dP}{dt} = \frac{\partial P}{\partial t} + \frac{\partial P}{\partial x} \frac{dx}{dt} \quad (2.33)$$

To be able to validate the rule in Eqs. (2.32) and (2.33)

$$\frac{dx}{dt} = V + \frac{\lambda}{\rho} = V + \frac{\rho a^2}{\lambda} \quad (2.34)$$

Finally,

$$\frac{dP}{dt} + \lambda \frac{dV}{dt} + \lambda F = 0 \quad (2.35)$$

Now, we can find the  $\lambda$  value from Eqn. (2.34) by canceling V's on both sides;

$$\lambda = \pm \rho a \quad (2.36)$$

By substituting  $\lambda$  in Eq. (2.34), it can be rewritten as

$$\frac{dx}{dt} = V \pm a \quad (2.37)$$

If we compare the magnitude of acoustic wave speed to the flow velocity, there is a huge difference between them. Hence, we can neglect the V term, so that

$$\frac{dx}{dt} = \pm a \quad (2.38)$$

This shows the position change of the wave that is related to the change in time. Values of  $\lambda$  can be substituted into Eq. (2.35). This substitution leads to two sets of equations, which are named as  $C^+$  and  $C^-$  equations.

$$C^+ \begin{cases} \frac{1}{\rho} \frac{dP}{dt} + a \frac{dV}{dt} + aF = 0 \\ \frac{dx}{dt} = +a \end{cases} \quad (2.39)$$

$$C^- \begin{cases} \frac{1}{\rho} \frac{dP}{dt} - a \frac{dV}{dt} - aF = 0 \\ \frac{dx}{dt} = -a \end{cases} \quad (2.40)$$

Two real distinct values for  $\lambda$  are used to convert the original partial differential equations to two sets of total differential equations. The upper equations in the sets of Eqns. (2.39) and (2.40) are called compatibility equations, and they are valid when the lower equations, that is,  $dx/dt=a$  and  $dx/dt=-a$  are also valid, respectively. By considering the two independent variables  $x$  and  $t$  in a solution domain, a visualization of characteristics equations is shown in Figure 2.6.

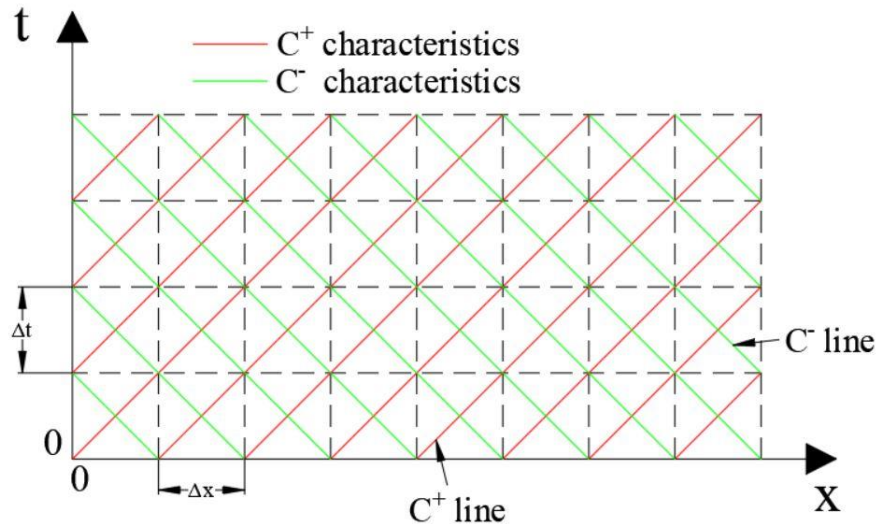


Figure 2.6. Characteristic lines in the  $x$ - $t$  plane

It should be mentioned that, according to Figure 2.6, to get the most accurate results and enable convergence, the so-called Courant condition must be satisfied. This condition expresses that

$$\frac{\Delta x}{\Delta t} \leq a \quad (2.41)$$

To make the solution of integration of compatibility equations easier, we can apply the shear stress that is defined by Darcy-Weisbach.

$$\tau_w = \frac{\rho f V |V|}{8} \quad (2.42)$$

As a consequence

$$F = g \sin \theta + f \frac{V |V|}{2D} \quad (2.43)$$

Now we can rearrange the Eqs. (2.39) and (2.40) in terms of head and velocity, so

$$C^+ \begin{cases} \frac{g}{a} \frac{dH}{dt} + \frac{dV}{dt} + \frac{fV |V|}{2D} = 0 \\ \frac{dx}{dt} = +a \end{cases} \quad (2.44)$$

$$C^- \begin{cases} -\frac{g}{a} \frac{dH}{dt} + \frac{dV}{dt} + \frac{fV |V|}{2D} = 0 \\ \frac{dx}{dt} = -a \end{cases} \quad (2.45)$$

Lastly, there are two unknown variables in the differential equations. These two unknowns are V and H in which H is the piezometric head, which is equal to  $z+P/\gamma$ . The time increments that are used in the analysis of the transient events are usually small. When solving these two equations simultaneously, a first-order finite-difference order is suggested by Wylie and Streeter (1978). However, when there are dominant friction losses in the pipeline, to get more accurate results, a second-order approximation is better to use. Hence, to avoid instability of the finite-difference scheme, second-order approximation should be used in such cases.

#### 2.4.2 Time Discretization of Compatibility Equations

For solving the characteristic equations, the equations should be discretized in the x-t plane, and solutions for every node should be found. To do so, a pipeline section is divided into N equal parts that form N+1 nodes to be solved for each time step. The

time increment for the calculation scheme can be calculated as  $\Delta t = \Delta x/a$ , which is called the courant condition. The solution domain can be shown in Figure 2.7.

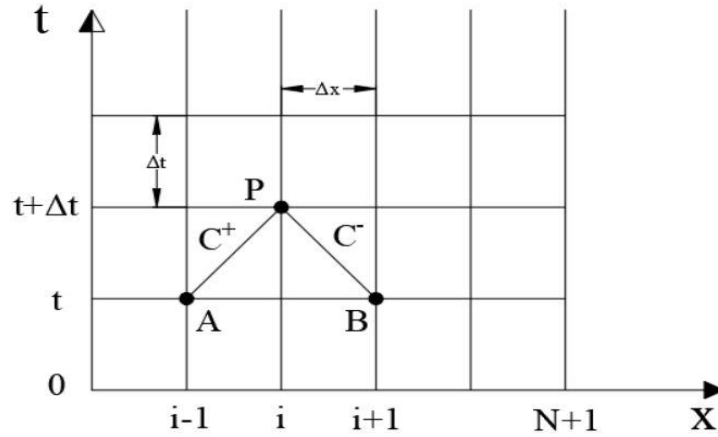


Figure 2.7. Characteristics lines for the nodal solution

If the values of dependent variables  $V$  and  $H$  are known at points  $A$  and  $B$ , then Eq. (2.44) can be integrated along the line  $AP$  on which the equation is valid. Then, as a result of integration, an equation in two unknowns,  $V$  and  $H$  at point  $P$  is obtained. Similarly, if the points of  $V$  and  $H$  are known at point  $B$  also, then Eq. (2.45) can be integrated along the line  $PB$  to have another equation with two unknowns  $V$  and  $H$  at point  $P$ . Then, the simultaneous solution of these two equations yields the condition at point  $P$  at a particular time.

Integration of equations can be handled by simple manipulation of equations just multiplying equation (2.44) by  $adt/g = dx/g$ , and pipeline area may be introduced to the equations in order to be able to obtain equations in terms of discharge,  $Q$ , instead of flow velocity,  $V$ .

$$\int_{H_A}^{H_P} dH + \frac{a}{gA} \int_{Q_A}^{Q_P} dQ + \frac{f}{2gDA^2} \int_{x_A}^{x_P} Q|Q| dx = 0 \quad (2.46)$$

It must be noted that a solution to the integral in the last term is unknown in advance, so an approximation is introduced to handle that term. This approximation is a first-order approximation for the evaluation of the last term and is insignificant as long as

the friction dominated flow is considered. With similar integration of equation (2.45) along with C<sup>-</sup> line, the following equations are obtained.

$$H_P - H_A + \frac{a}{gA} (Q_P - Q_A) + \frac{f \Delta x}{2gDA^2} Q_A |Q_A| = 0 \quad (2.47)$$

$$H_P - H_B - \frac{a}{gA} (Q_P - Q_B) - \frac{f \Delta x}{2gDA^2} Q_B |Q_B| = 0 \quad (2.48)$$

The above two equations are compatibility equations and are the fundamental relations describing transient in a pipe flow. The equations above can be solved for H<sub>P</sub>, and the below equations can be obtained.

$$C^+ : H_P = H_A - B(Q_P - Q_A) - RQ_A |Q_A| \quad (2.49)$$

$$C^- : H_P = H_B + B(Q_P - Q_B) + RQ_B |Q_B| \quad (2.50)$$

Where

$$B = \frac{a}{gA} \quad R = \frac{f \Delta x}{2gDA^2} \quad (2.51)$$

These equations must satisfy the steady-state conditions, which are, in fact, individual cases of transients. Since the original problem is the initial value and boundary value problem, the solution scheme should have a seed of initial values and should also have boundary values to be supplied. Initial values of the solution can always well be the steady-state values of flow variables as they are also special cases of transients. Boundary values can be obtained by defining distinct boundaries, and these boundaries will be considered in the following chapter.

For any interior intersection point, in other words, in every nodal point, the two compatibility equations are solved simultaneously for the unknowns head and discharge at that node. By introducing C<sub>P</sub> and C<sub>M</sub> to the Eqs. (2.49) and (2.50), they can be rewritten as the following

$$C^+ : H_{P_i} = C_P - BQ_{P_i} \quad (2.52)$$

$$C^- : H_{P_i} = C_M + BQ_{P_i} \quad (2.53)$$

$C_P$  and  $C_M$  are always known and constants. Their equations are written below.

$$C_P = H_{i-1} + BQ_{i-1} - RQ_{i-1} |Q_{i-1}| \quad (2.54)$$

$$C_M = H_{i+1} - BQ_{i+1} + RQ_{i+1} |Q_{i+1}| \quad (2.55)$$

After obtaining the above equations, head value at point P can be calculated by eliminating Q from equations (2.52) and (2.53). Then

$$H_{P_i} = (C_P + C_M) / 2 \quad (2.56)$$

Discharge at point P can then be calculated from either Eq. (2.52) or (2.53). It should be noted that all known values of H and Q are from the preceding time step, either the result of the previous calculation or the initial value given at the beginning of the solution.

The solution scheme requires the knowledge of the boundary values whenever the last and first boundaries of the pipe are reached. Thus boundary conditions should be defined and handled by special predefined functions.



## CHAPTER 3

### BOUNDARY CONDITIONS

The structure and details of transient equations were described in ‘Chapter 2’. In order to simulate a transient analysis in terms of head and flow rate, the compatibility equations are calculated in space and time across the nodal points throughout the pipeline. Now, to perform simulations for complex pipeline scenarios, there must be some relevant boundary conditions. The boundaries that are used in the development of the S-Hammer software are introduced and listed below:

- Single Pipe Section
- Series Pipes Connections
- Upstream Reservoir with Constant Head
- Upstream Reservoir with Variable Head
- Single Centrifugal Pump
- Downstream Valve
- Downstream Dead End
- Surge Tank

Explanation and equations related to these boundaries will be introduced in this chapter, and ultimately, different transient events can be simulated by using these boundary conditions.

#### 3.1 Pipe Section

To calculate the head and discharge values of nodal points in the interior pipe, Equations (2.52) and (2.53) are solved. Whenever the pipeline system of the solution domain consists of a single pipe with constant characteristics, the value for the pressure wave speed will have equal magnitude throughout the pipeline.

As the cross-sectional area and wave magnitude is equal along the pipe, Eq. (2.52) and Eq. (2.53) can be simplified. So,

$$H_{P_i} = \frac{1}{2}(C_P + C_M) \quad (3.1)$$

$$Q_{P_i} = \frac{(C_P - H_{P_i})}{B} \quad (3.2)$$

### 3.2 Series Pipes Connections

In the Series junction boundary condition, there are some differences when compared to a single pipe solution. When there is more than one pipe in a pipeline system, a series junction boundary solution is applied. In other words, the diameter, pipe material, and pipe thickness of the sequential pipes can change. Therefore, since the characteristics of pipes differ, the pressure wave speed varies. Hence, the transient solution is solved for each pipe. Figure 3.1 is an illustration of the series junction.

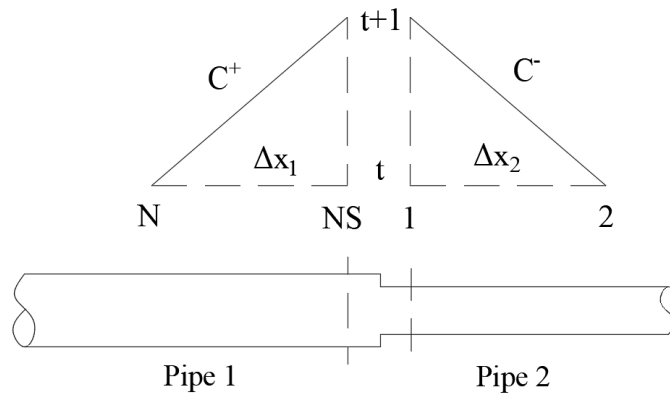


Figure 3.1. Series junction boundary condition

When solving the continuity expression, the junction that connects consecutive pipes has equal HGL elevation value. So this condition provides two equations for head and discharge of common elevation, and it is written in double-subscript notation.

$$Q_{P_{1,NS}} = Q_{P_{2,1}} \quad (3.3)$$

$$H_{P_{1,NS}} = H_{P_{2,1}} \quad (3.4)$$

The first script represents the pipe number, while the second one indicates the node number.

Now, the equations (3.3) and (3.4) are solved simultaneously with equations (2.52) and (2.53). So,

$$Q_{P_{2,1}} = \frac{C_{P_1} - C_{M_2}}{B_1 + B_2} \quad (3.5)$$

Where,

$$B_1 = \frac{a_1}{gA_1} \quad B_2 = \frac{a_2}{gA_2} \quad (3.6)$$

### 3.3 Upstream Reservoir with Constant Head

One of the boundary conditions during a transient event at the upstream end of the hydraulic system can be a reservoir. As upstream reservoirs are mostly large, the head value is assumed constant. Hence, at the start of the pipeline, the head value of the first node is taken from this boundary. So,

$$H_{P_1} = H_R \quad Q_R = \frac{(H_{P_1} - C_M)}{B} \quad (3.7)$$

Where  $H_R$  is the constant head value of the upstream reservoir.

### 3.4 Upstream Reservoir with Variable Head

Another boundary condition is when the head value of the upstream reservoir varies according to a known function, such as a sine wave. To find the head value of the

reservoir, there must be a definition that defines the value for the calculation time. The equation below shows the mathematical description of this boundary condition.

$$H_{P_1} = H_R + \Delta H \sin \omega t \quad (3.8)$$

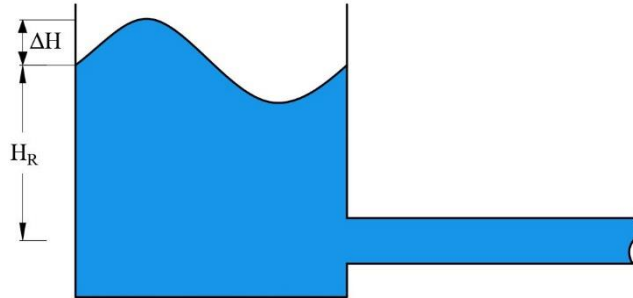


Figure 3.2. Upstream reservoir with variable head

Figure 3.2 shows a physical illustration of this type of boundary. In Eq. (3.8)  $\omega$  represents the circular frequency, and  $\Delta H$  is the amplitude of the wave. In terms of the discharge, Eq. (3.7) is used.

### 3.5 Single Centrifugal Pump

In most transient cases, one of the main reasons that produce transient surge is pump failure. Pump failure occurs when the pump starts up or stops inadvertently, or the valves operating with pumps close suddenly. This situation could happen in emergency shut-down or power failure events. Also, a wrong operation of the pumps may trigger a sequence of transient events. The pump inertia that rotates the parts is minor compared to the liquid inertia in the pump discharge line. This leads to a decrease in pump speed. Hence, in the hydraulic design stage, a careful examination must be considered.

To analyze the transient during a pump failure, the method of characteristics can be used. Two parameters are essential to be assembled into head and discharge equations in the analysis of centrifugal pumps. These parameters are pump head and pump torque variation. The development of a unique boundary condition for a pump

must be done. Therefore, change in the pump head and pump torque during the transient event can be calculated.

In this section, the first events when a complete power failure occurs are explained, and then a general view of dimensionless-homologous turbopump characteristics and their application are summarized. Finally, the boundary conditions of single pump stations are developed, Streeter & Wylie (1967).

### 3.5.1 Events Following a Complete Power Failure

The motor of the pump applies a torque on the rotating shaft. This torque generates the energy needed to rotate the impeller to derive the flow through the pump. This motion develops a total dynamic head that increases from the suction flange to the discharge flange of the pump. This total head is the energy increase per unit weight of the flowing fluid.

$$tdh = \frac{V_d^2}{2g} + \frac{P_d}{\gamma} + z_d - \left( \frac{V_s^2}{2g} + \frac{P_s}{\gamma} + z_s \right) \quad (3.9)$$

In Eq. (3.9), the subscripts d and s refer to discharge and suction flanges, respectively. When a power failure occurs in a pump, the rotational speed of the impeller reduces. This reduction results in reduced total dynamic head and produces positive and negative pressure waves. The positive waves propagate towards the upstream of the suction line, while the negative waves transmit to downstream from the discharge line.

As the function of a pump may be to lift the liquid from a lower to a higher elevation, the flow direction will eventually reverse. Consequently, after a short time, the impeller of the pump will start to rotate backward. This operation type is named the zone of the turbine. When the pump operates in this zone, the rotation speed of the impeller increases in the reverse direction until it reaches a runaway speed. Thus, this increment of speed causes a reverse flow, which is named as reversed speed dissipation zone. As a result, in the suction and discharge flanges of the pump,

negative and positive pressure waves are produced. The negative pressure can cause air to come out of the solution, which will form vapor cavities.

These series of events can be modeled by the method of characteristics as boundary conditions. Then C+ and C- equations will serve carrying the information of discharge and pressure head of the pump. To achieve the necessary boundary conditions during a pump failure, turbopump characteristics should be explained in detail.

### 3.5.2 Dimensionless Pump Characteristics

When the pump operates, four parameters describe the pump characteristics. These quantities are the discharge Q, the total dynamic head H, the rotational speed of the impeller N, and the shaft torque T. Mostly, Q and N are preliminarily determined and considered as independent. Therefore, to determine values for H and T, we should make two assumptions:

1. Characteristics of the pump in steady-state also hold for unsteady flow. Although the values of Q and N change with time, their values are used to determine H and T.
2. Homologous relationships are valid.

The homologous equations are presented as (Streeter, V. L., & Wylie, 1975)

$$\frac{H_1}{(N_1 D_1)^2} = \frac{H_2}{(N_2 D_2)^2} \quad (3.10)$$

$$\frac{Q_1}{N_1 D_1^3} = \frac{Q_2}{N_2 D_2^3} \quad (3.11)$$

In the equations above, subscripts 1 and 2 refer to two units of centrifugal pumps with different sizes. When the geometrical parameters of the pumps are similar, equations (3.10) and (3.11) can be reduced.

$$\frac{H_1}{N_1^2} = \frac{H_2}{N_2^2} \quad \frac{Q_1}{N_1} = \frac{Q_2}{N_2} \quad (3.12)$$

In homologous theory, it is assumed that when the size of the unit does not change, the efficiency does not change. Then,

$$\frac{T_1 N_1}{Q_1 H_1} = \frac{T_2 N_2}{Q_2 H_2} \quad (3.13)$$

By combining the Eqs. (3.12) and (3.13), the new equations can be obtained;

$$\frac{T_1}{N_1^2} = \frac{T_2}{N_2^2} \quad \frac{H_1}{Q_1^2} = \frac{H_2}{Q_2^2} \quad \frac{T_1}{Q_1^2} = \frac{T_2}{Q_2^2} \quad (3.14)$$

It is adequate to write the equations in non-dimensional form,

$$h = \frac{H}{H_R} \quad \beta = \frac{T}{T_R} \quad \nu = \frac{Q}{Q_R} \quad \alpha = \frac{N}{N_R} \quad (3.15)$$

in which the R subscript indicated that the values are rated quantities. This means that the values of H, Q, T, and N are at their best efficiencies.

The homologous relationships can now be presented in dimensionless form,

$$\frac{h}{\alpha^2} \text{ vs. } \frac{\nu}{\alpha} \quad \frac{\beta}{\alpha^2} \text{ vs. } \frac{\nu}{\alpha} \quad \frac{h}{\nu^2} \text{ vs. } \frac{\alpha}{\nu} \quad \frac{\beta}{\nu^2} \text{ vs. } \frac{\alpha}{\nu} \quad (3.16)$$

According to homologous theory, to see the head-discharge relation for any speed of the unit, one must plot  $\nu/\alpha$  and  $h/\alpha^2$  in abscissa and ordinate form, respectively. Hence, to see the torque relations  $\nu/\alpha$  vs.  $\beta/\alpha^2$  must be plotted.

However, it needs a lot of effort to solve and find these relations since during the transient event, the quantities of the characteristics can change signs and even be zero. To overcome this problem, Marchal et al. (1965) used the equations below,

$$\frac{h}{\alpha^2 + \nu^2} \text{ vs. } \tan^{-1} \frac{\nu}{\alpha} \quad \frac{\beta}{\alpha^2 + \nu^2} \text{ vs. } \tan^{-1} \frac{\nu}{\alpha} \quad (3.17)$$

Figure 3.3 shows the polar diagram of  $\alpha$  and  $\nu$ .

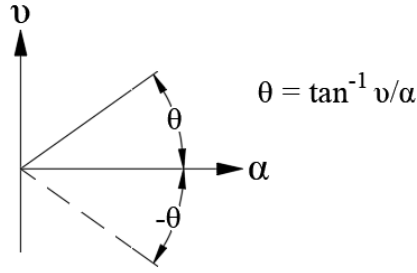


Figure 3.3. Polar diagram for  $\alpha$  and  $v$

Then, in terms of  $\alpha$ ,  $\beta$ ,  $h$ , and  $v$ , operation zones must be defined. Table 3.1 illustrates this definition.

Table 3.1 *Pump operation zones*

Zone Name	$\alpha$	$v$	Range
Turbine	$< 0$	$\leq 0$	$0 - \pi/2$
Energy Dissipation	$\geq 0$	$< 0$	$\pi/2 - \pi$
Normal	$\geq 0$	$\geq 0$	$\pi - 3\pi/2$
Reversed Speed Dissipation	$< 0$	$> 0$	$3\pi/2 - 2\pi$

Now, two curves represent the complete pump characteristics. In the polar diagram system,  $\theta = \tan^{-1} v/\alpha$  vs.  $r = h/(\alpha^2 + v^2)$  and  $r = \beta/(\alpha^2 + v^2)$  show the relationship of head and torque of a pump unit. The formulation of these curves would be,

$$WH(x) = \frac{h}{\alpha^2 + v^2} \quad WB(x) = \frac{\beta}{\alpha^2 + v^2} \quad x = \pi + \tan^{-1} \frac{v}{\alpha} \quad (3.18)$$

When solving a transient event caused by pump failure, the pump characteristic data is needed, and pump and turbine manufacturers provide these data. However, mostly, these data are not easy to be provided. Therefore, the data available in the literature are used for similar pumps. The rectangular coordinates for homologous relations are plotted in Figure (3.4).

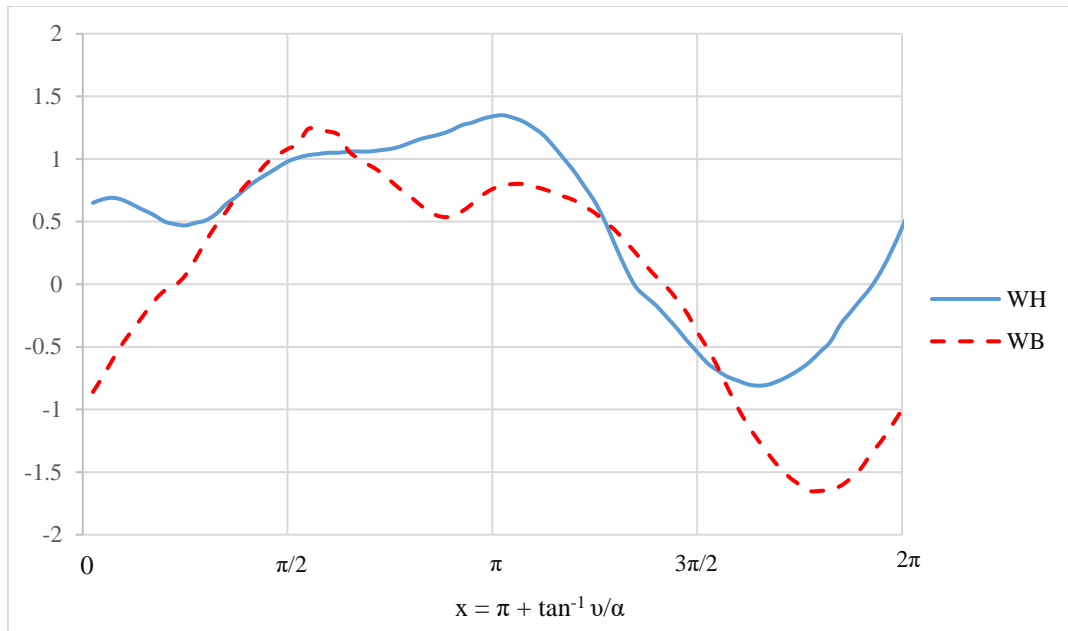


Figure 3.4. Pump characteristic curves for  $N_s = 1800$  rpm

In this study, the pump characteristic curve data presented in Figure 3.1 is used. In computation, the data is added to the program as an array of numbers with an increment of  $\pi/40$ .

### 3.5.3 Transient Equations for Pump Failure

In case of a power failure, for solving the transient event of pump operation, two equations are solved simultaneously.

1. Head balance equation through the pump and its discharge valve.
2. Torque-angular deceleration equation for rotating impeller and other masses.

#### 3.5.3.1 Head Balance Equation

In a pump boundary, three elements contribute to the head-balance equation. These elements are head value at the suction line, valve head loss, total dynamic head, and pumping head.

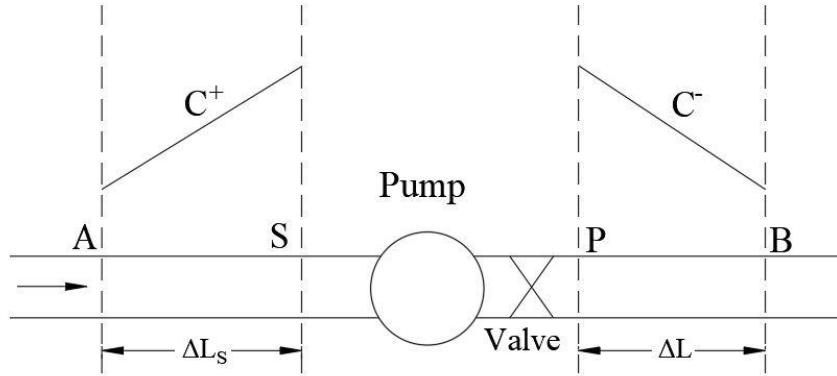


Figure 3.5. Schematic view of a pump boundary with its discharge valve

According to Figure 3.5, the head balance equation can be written as

$$H_p = H_s + tdh - (\text{valve head loss}) \quad (3.19)$$

where  $H_s$  is the piezometric head of the suction flange.  $H_p$  is the unknown head in the first section of the discharge pipe to be computed. Now,  $C^+$  characteristics can be written.

$$H_{SP(NS1)} = H_{S(NS)} - B_S [Q_{SP(NS1)} - Q_{S(NS)}] - R_S \cdot Q_{S(NS)} \left| Q_{S(NS)} \right| \quad (3.20)$$

In Eq. (3.20), NS is the last section of the suction pipe, and NS1 = NS + 1. We can rewrite the equation so that the result would be,

$$H_{SP(NS1)} = HCP - B_S \cdot Q_{SP(NS1)} \quad (3.21)$$

where,

$$B_S = \frac{a_s}{(gA_s)} \quad (3.22)$$

$R_S$  = frictional resistance,

$a_s$  = wave speed,

$A_s$  = cross-sectional area of the suction pipe,

$H_P$  = piezometric head at the first section of the discharge pipe

Therefore, C<sup>-</sup> characteristic equation for the first reach is

$$H_{P_1} = H_2 + B[Q_{P_1} - Q_2] + R \cdot Q_2 |Q_2| \quad (3.23)$$

or,

$$H_{P_1} = HCM + B \cdot Q_{P_1} \quad (3.24)$$

As long as the cross-sectional area of point A and B are the same, the continuity equation is

$$Q_{SP(NS1)} = Q_{P_1} \quad (3.25)$$

By referring to the homologous relationships in the non-dimensional form shown in Eq. (3.18), the total dynamic head can be defined.

$$tdh = H_R \cdot h = H_R (\alpha^2 + \nu^2) WH \left( \pi + \tan^{-1} \frac{\nu}{\alpha} \right) \quad (3.26)$$

In order to find the suitable vicinity of  $x = \pi + \tan^{-1} \nu/\alpha$ , it is required to replace the WH curve to a straight line. Since the data is stored in an array with small intervals, it is possible to obtain an accurate straight line that represents the approximation of the location. Hence, two contiguous data points are used to extrapolate  $\alpha$  and  $\nu$  to make the straight line. Figure 3.6 illustrates the linearization of the curve.

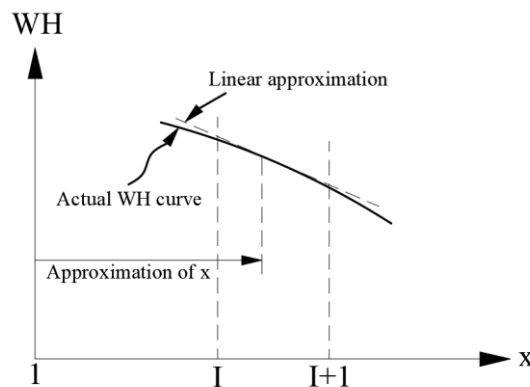


Figure 3.6. Replacement of WH curve with a straight line

In Figure 3.6,

$$I = \frac{x}{\Delta x} + 1 \quad (3.27)$$

In which the expression, I, is an integer value that indicates the data point. Then, the equation of the straight line is written.

$$WH(x) = A_0 + A_1 x \quad (3.28)$$

In which  $A_0$  and  $A_1$  can be defined from the geometry;

$$A_1 = \frac{[WH(I+1) - WH(I)]}{\Delta x} \quad A_0 = WH(I+1) - I \cdot A_1 \cdot \Delta x \quad (3.29)$$

The head loss of the valve can be written as

$$valve \ head \ loss = \frac{\Delta H v |v|}{\tau^2} \quad (3.30)$$

Now, Eq. (3.26) can be rewritten for the straight line ;

$$tdh = H_R (\alpha^2 + v^2) \left[ A_0 + A_1 \left( \pi + \tan^{-1} \frac{v}{\alpha} \right) \right] \quad (3.31)$$

In Eq. (3.30),  $\Delta H$  is the value of head loss when  $\tau = 1$  for the  $Q_R$ , which is the rated discharge. It must be mentioned that the values of  $\tau$  are available for each time step.

Finally, the head balance equation can be written as

$$F1 = HPM - B_S Q \cdot v + H_R (\alpha^2 + v^2) \left[ A_0 + A_1 \left( \pi + \tan^{-1} \frac{v}{\alpha} \right) \right] - \frac{\Delta H v |v|}{\tau^2} = 0 \quad (3.32)$$

where

$$HPM = HCP - HCM \quad Q_{P1} = v \cdot Q_R \quad BSQ = (B_S + B) Q_R$$

Eq. (3.32) is the ultimate form of head-balance equation, and the unknowns are  $\alpha$  and  $v$ . Hence, this equation is meant to be solved with the speed change equation, which is described in the next section.

### 3.5.3.2 Speed Change Calculation

As discussed in previous sections, when a transient event occurs in a pipeline with a pump, the rotational speed of the pump changes in each time step. This change of speed is made when rotating parts apply an unbalanced torque. The equation of this torque is

$$T = -\frac{WR_g^2}{g} \frac{d\omega}{dt} \quad (3.33)$$

In which

$W$  = weight of rotational parts + entrained liquid

$R_g$  = radius of gyration of the rotating mass

$\omega$  = angular velocity in radians/s

$d\omega/dt$  = angular acceleration

At the beginning of each time step,  $\Delta t$ , the unbalanced torque can be defined as  $T_0$ , and the unknown torque at the end of the time step is  $T_P$ . Moreover,

$$\omega = N_R \frac{2\pi}{60} \alpha \quad \beta_0 = \frac{T_0}{T_R} \quad \beta = \frac{T_P}{T_R} \quad (3.34)$$

According to Eqs. (3.33) and (3.34), a new equation can be written as

$$\beta = \frac{WR_g^2}{g} \frac{N_R}{T_R} \frac{\pi}{15} \frac{(\alpha_0 - \alpha)}{\Delta t} - \beta_0 \quad (3.35)$$

By defining

$$C_{31} = \frac{WR_g^2}{g} \frac{N_R}{T_R} \frac{\pi}{15} \quad (3.36)$$

Eq. (3.35) can be rewritten as

$$\beta + \beta_0 - C_{31}(\alpha_0 - \alpha) = 0 \quad (3.37)$$

By referencing to characteristic curve for torque in Figure 3.4,

$$WB(x) = \frac{\beta}{\alpha^2 + \nu^2} = B_0 + B_1 \left( \pi + \tan^{-1} \frac{\nu}{\alpha} \right) \quad (3.38)$$

Where  $B_0$  and  $B_1$  can be found like  $A_0$  and  $A_1$ , which is discussed previously. Finally, the equation of speed change can be written as

$$F2 = (\alpha^2 + \nu^2) \left[ B_0 + B_1 \left( \pi + \tan^{-1} \frac{\nu}{\alpha} \right) \right] + \beta_0 - C_{31}(\alpha_0 - \alpha) = 0 \quad (3.39)$$

Eq. (3.39) is the ultimate form of speed change equation in which the unknowns are  $\alpha$  and  $\nu$ . It should be mentioned that  $\alpha_0$  is the non-dimensional speed at the beginning of time step  $\Delta t$ .

### 3.5.4 Pumps with Discharge valve

Discharge valves are commonly used with pumps for discharging. These valves function either manually or automatically to stop the reverse flow towards the pump. Hence, an assumption must be made that when the flow is forwarding, the head loss value is constant. The head balance equation can be written for the Discharge valve as

$$F3 = HCP - HCM + H_R \alpha^2 WH \left( \frac{\pi}{\Delta x} + 1 \right) \quad (3.40)$$

In Eq. (3.40),  $\nu=0$  is set so that the positive flow is going through the Discharge valve and pump. By using the data retrieved from the WH curve in Figure 3.4, whenever  $F3$  is greater than zero, the positive flow is guaranteed.

### 3.5.5 Single Pump Boundary

In this section, head balance and speed change equations are developed for single pump boundary condition. We can use numerous numerical methods to solve these equations. For instance, the Newton-Raphson method is used to solve F1 and F2.

$$F1 + \frac{\partial F1}{\partial \nu} \Delta \nu + \frac{\partial F1}{\partial \alpha} \Delta \alpha = 0 \quad (3.41)$$

$$F2 + \frac{\partial F2}{\partial \nu} \Delta \nu + \frac{\partial F2}{\partial \alpha} \Delta \alpha = 0 \quad (3.42)$$

At the start of any iteration, the initial values for  $\nu$  and  $\alpha$  can be found.

$$\nu = 2\nu_0 - \nu_{00} \quad (3.43)$$

$$\alpha = 2\alpha_0 - \alpha_{00} \quad (3.44)$$

In Eqs. (3.43) and (3.44),  $\nu_{00}$  and  $\alpha_{00}$  are the one-time step before  $\nu_0$  and  $\alpha_0$ . Now the equations of partial derivatives can be written for this  $\nu$  and  $\alpha$ .

$$\frac{\partial F1}{\partial \nu} = -BSQ + H_R \left\{ 2\nu \left[ A_0 + A_1 \left( \pi + \tan^{-1} \frac{\nu}{\alpha} \right) \right] + A_1 \alpha \right\} - \frac{2\Delta H |\nu|}{\tau^2} \quad (3.45)$$

$$\frac{\partial F1}{\partial \alpha} = H_R \left\{ 2\alpha \left[ A_0 + A_1 \left( \pi + \tan^{-1} \frac{\nu}{\alpha} \right) \right] - \nu A_1 \right\} \quad (3.46)$$

$$\frac{\partial F2}{\partial \nu} = 2\nu \left[ B_0 + B_1 \left( \pi + \tan^{-1} \frac{\nu}{\alpha} \right) \right] - \alpha B_1 \quad (3.47)$$

$$\frac{\partial F2}{\partial \alpha} = 2\alpha \left[ B_0 + B_1 \left( \pi + \tan^{-1} \frac{\nu}{\alpha} \right) \right] - \nu B_1 + C_{31} \quad (3.48)$$

In Eq. (3.45),  $\tau$  is a known value which is a function of time. Next, Eqs. (3.41) and (3.42) should be calculated for  $\Delta \alpha$  and  $\Delta \nu$  at each time step.

$$\Delta\alpha = \frac{\left( \frac{F2}{\partial F2/\partial v} - \frac{F1}{\partial F1/\partial v} \right)}{\left( \frac{\partial F1/\partial \alpha}{\partial F1/\partial v} - \frac{\partial F2/\partial \alpha}{\partial F2/\partial v} \right)} \quad (3.49)$$

$$\Delta v = \frac{-F1}{\partial F1/\partial v} - \Delta\alpha \left( \frac{\partial F1/\partial \alpha}{\partial F1/\partial v} \right) \quad (3.50)$$

After each iteration, the results obtained for Eqs. (3.49) and (3.50) are added to the last values of  $\alpha$  and  $v$ . This procedure is repeated until a certain tolerance (TOL) is met.

$$\alpha = \alpha + \Delta\alpha \quad (3.51)$$

$$v = v + \Delta v \quad (3.52)$$

To meet the required tolerance sufficiently, the following inequality must be satisfied.

$$|\Delta\alpha| + |\Delta v| < TOL \quad (3.53)$$

In which, the value of TOL maybe around 0.0002.

After solving these equations and finishing the iterations, the values of  $A_0$ ,  $A_1$ ,  $B_0$ , and  $B_1$  must be examined. So the calculated integer will be

$$II = \frac{\pi + \tan^{-1} \frac{v}{\alpha}}{\Delta x} + 1 \quad (3.54)$$

Whenever the value of II is equal to I in Eq. (3.27), then a proper vicinity of line segments of WH and WB is represented for the solution. If the condition is not satisfied, then by replacing I with II, the procedure continues until the condition met.

### 3.6 Downstream Valve

For a valve located at downstream, the orifice equation for steady-state flow is

$$Q_0 = (C_d A_G)_0 \sqrt{2gH_0} \quad (3.55)$$

For another valve opening, the general form is

$$Q_p = C_d A_G \sqrt{2g\Delta H} \quad (3.56)$$

In Eqs. (3.55) and (3.56)

$Q_0$  = discharge of steady-state flow (m<sup>3</sup>/s)

$H_0$  = steady-state head loss across the valve (m)

$C_d$  = discharge coefficient

$A_g$  = the area of the valve (or gate) opening (m<sup>2</sup>)

$\Delta H$  = instantaneous drop in hydraulic grade line across the valve

Now a non-dimensional expression for valve opening can be written as

$$\tau = \frac{C_d A_G}{(C_d A_G)_0} \quad (3.57)$$

By dividing Eq. (3.56) by (3.55)

$$Q_p = \frac{Q_0}{\sqrt{H_0}} \tau \sqrt{\Delta H} \quad (3.58)$$

Finally, by substituting Eqs. (3.58) and (2.52), the discharge equation for the valve can be written.

$$Q_{PNS} = -BC_v + \sqrt{(BC_v)^2 + 2C_v C_p} \quad (3.59)$$

In which,

$$C_v = \frac{(Q_0 \tau)^2}{2H_0} \quad (3.60)$$

To find the value of  $H_{P(NS)}$ , either Eq. (3.58) or Eq. (2.52) can be solved.

### 3.7 Downstream Dead End

When the downstream of the system is a dead-end, it means there is no flowing liquid across this boundary. Thus,  $Q_{P(NS)}=0$  and  $H_{PNS}$  can be obtained using either Eq. (2.49) or Eq. (2.52).

### 3.8 Surge Tank

Surge tanks are protection devices that are commonly used to protect the pipeline system when a transient event occurs. Surge tanks have many shapes and connection types. Thus in this study, simple surge tank type is used as one of the boundary conditions. However, its top is open to the atmosphere. Hence, its height and diameter must be designed in a way that it can prevent liquid not to overflow.

Figure 3.7 illustrates the simple surge tank type.

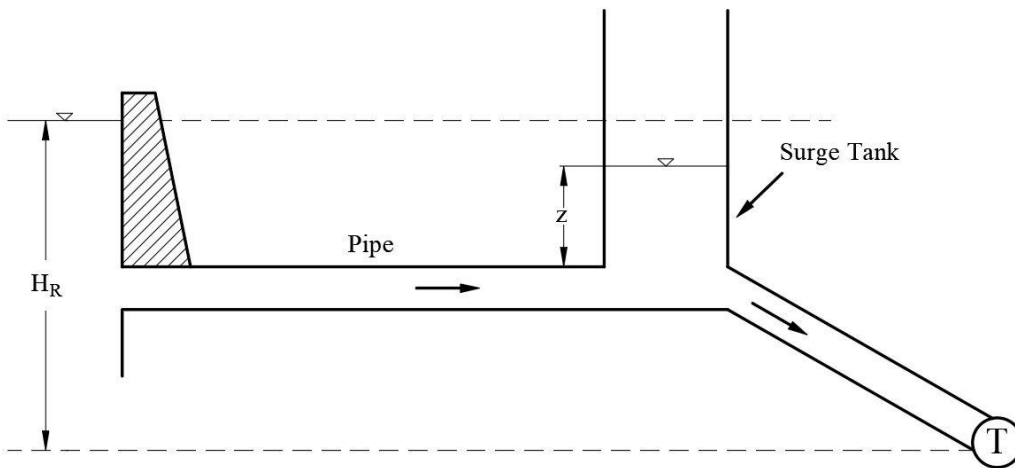


Figure 3.7. Simple surge tank

Equation of motion can be written for a simple surge tank.

$$\frac{dQ}{dt} = \frac{gA_T}{L} (-z - cQ|Q|) = F_1(Q, z, t) \quad (3.61)$$

Where

$$c = \frac{1 + k + \frac{fL}{D_T}}{2g} \quad (3.62)$$

Moreover, the continuity equation can be described as

$$\frac{dz}{dt} = \frac{1}{A_s} (Q - Q_T) = F_2(Q, z, t) \quad (3.63)$$

In these equations, both  $F_1$  and  $F_2$  are functions of  $Q$ ,  $z$ , and  $t$ . In which,  $k$  is the entrance loss coefficient,  $A_s$  is the area of the surge tank,  $A_T$  is the cross-sectional area of the pipe, and  $Q_T$  is the turbine's discharge. In this study, the Runge-Kutta method is used to solve Eqs. (3.61) and (3.63).



## CHAPTER 4

### THE SOFTWARE

A software named S-Hammer is developed to analyze fluid transient in pipelines. The code has three object Libraries, which are described in this chapter. This chapter includes a description of the main user interface, minor user interfaces, and the abilities of the software.

#### 4.1 User Interface Library

This library is formed of different windows application forms, and these forms are described.

##### 4.1.1 Main User Interface

This form is the main interface where the user works most of the time. All of the visual aspects of the software can be found in this part. There are various functions on the main windows form with different menus that are available for the user, and the features of all parts are clarified in the sections of this chapter.

The tabs of the main user interface are:

- The project tab: This is the first step in which the user starts or loads an available project, and when it started, then the project can be saved.
- The design tab: This tab includes the necessary buttons for design components, protection devices, drawing tools, and engineering libraries.
- View tab: In this section, the user can choose a theme for the user interface, and the colors of the background and grid of canvas can be adjusted.

- Calculators tab: in this tab, wave speed and friction factor calculators are available.
- Analysis tab: in this section, the user gives the initial transient conditions for the system, can start the analysis. It should be mentioned that after starting the analysis, if there is not enough data for the solver library, the user will be warned about possible deficiencies. Moreover, table and chart forms are available in this tab.
- Canvas: this is where the user draws the hydraulic system.
- Properties: after drawing the system, the user must enter the required information for all the objects here.

Figure 4.1 illustrates an image of the main form.

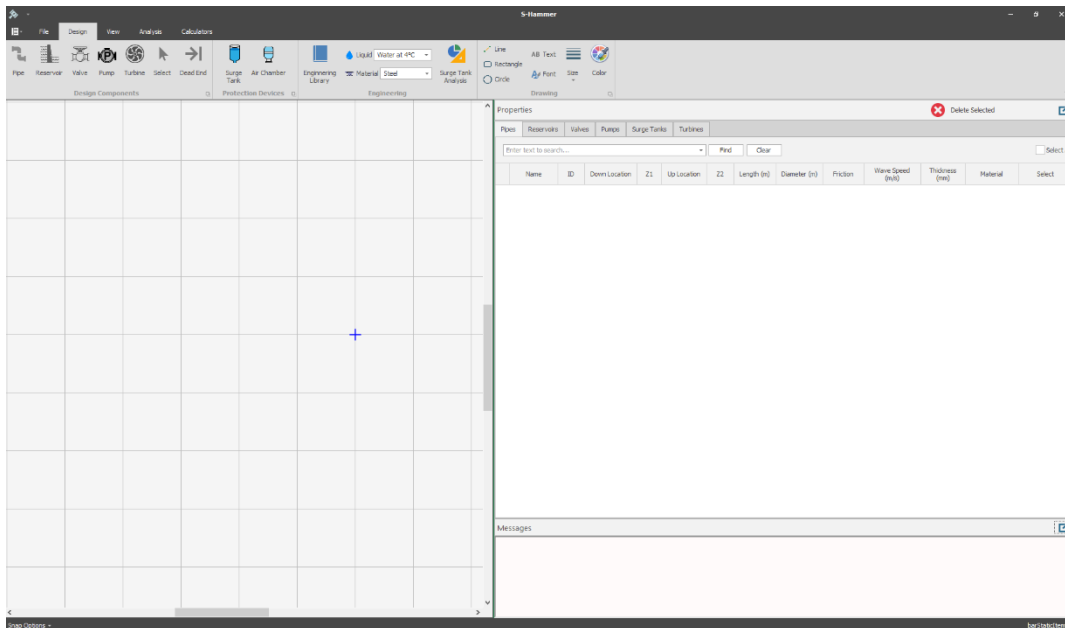


Figure 4.1. The main user interface of the software

#### 4.1.2 Design Canvas

The first step of using this software is to use the canvas section. The user can define the size of the canvas according to the design pattern, and the drawing section includes the objects below:

- Pipe: is the pipe item collection consisting of upstream and downstream points and the direction of the flow with a junction point for its upstream.
- Reservoir: is the reservoir item collection consisting of two types, which are upstream and downstream reservoir with junction point.
- Valve: is the valve item collection consisting of a junction point in the pipeline system in which the location of which pipe end is determined and operation condition is set.
- Pump: is the pump item collection consisting of a junction point in the pipeline system.
- Dead end: is the dead end item collection consisting of a junction point in the pipeline system.
- Surge Tank: is the surge tank item collection can be drawn on pipe collection, and the location on its pipe is determined.

In this section of the program, the user can select any of the objects to create a hydraulic network visually. All of the objects consist of a collection library, including their properties in which any of the objects have no limit, and the user can draw any number of them in the design stage. A sample of all the objects drawn in the canvas can be better seen in Figure 4.2;

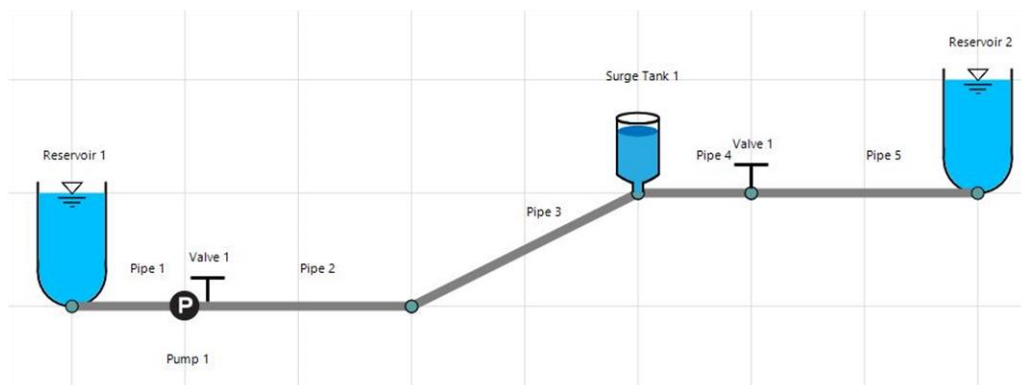


*Figure 4.2.* An example of all the objects drawn in the design canvas

### 4.1.3 Engineering Libraries

Engineering libraries include engineering objects such as liquid for the hydraulic system and material for the piping system.

#### 4.1.3.1 Material Library

In this part of the program, the user can select a pipe material from the available material collection, which is specified and set in the library. This collection includes the materials in Table 4.1 with their characteristics:

Table 4.1: *Young's Modulus of elasticity and Poisson's ratio for available pipe materials in the material collection, Chaudhry (1979)*

Material	Modulus of Elasticity, E (GPa)	Poisson's Ratio, $\mu$
Steel	207	0.27
Brass	94	0.36
Aluminium	70	0.33
Copper	120	0.34
Cast Iron	110	0.25
Transite	24	0.33
Concrete	22	0.13
Perpex Plastic	6	0.33
PVC Rigid	2.58	0.4
ABS Plastic	1.7	0.33

Apart from the material list in Table 4.1, the user can either add new materials to the collection. Figure 4.3 shows the material tab of the Engineering Library form.

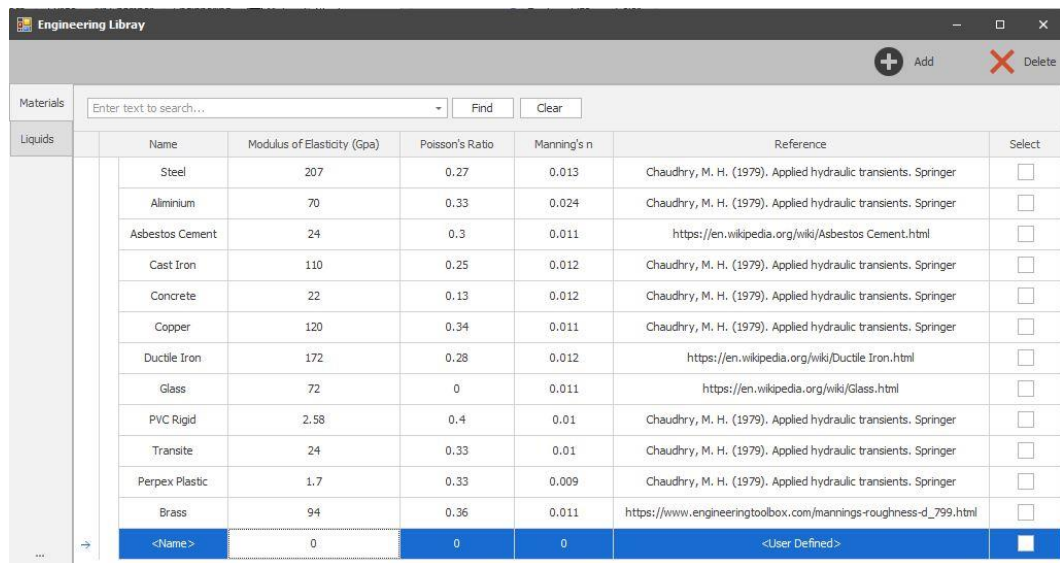


Figure 4.3. Material library interface

#### 4.1.3.2 Liquid Library

The liquid library is the part that the user can select liquid for the hydraulic system. There is an available material collection, which is specified and set in the library. This collection includes the liquids in Table 4.2 with their characteristics:

Table 4.2 Available materials in the liquid collection of the software

Name	Bulk Modulus of Elasticity (GPa)	Density (kg/m <sup>3</sup> )	Kinematic Viscosity (m <sup>2</sup> /s)	Temperature (°C)
Glycerine	4.523	1260	0.00051	20
Kerosene	1.293	810	$2.37 * 10^{-6}$	20
Mercury	2.854	13593	$1.2 * 10^{-7}$	20
Sea water with 3.3% salinity	2.337	1029	$1.4 * 10^{-6}$	10
Water at 4 °C	2.188	999.97	$1.566 * 10^{-6}$	4
Water at 20 °C	2.188	998.21	$1.004 * 10^{-6}$	20

As mentioned in the material library, in this part also, the user can add custom liquids to the library. Figure 4.4 is an illustration of the liquid tab in the engineering library form.

Name	Bulk Modulus of Elasticity (GPa)	Density	Kinematic Viscosity	Temperature (°C)	Reference	Select
Glycerine	4.522961	1260	0.00051	20	<a href="https://en.wikipedia.org/wiki/Glycerine.html">https://en.wikipedia.org/wiki/Glycerine.html</a>	<input type="checkbox"/>
Kerosene	1.292767	810	2.37E-06	20	<a href="https://en.wikipedia.org/wiki/Kerosene.html">https://en.wikipedia.org/wiki/Kerosene.html</a>	<input type="checkbox"/>
Mercury	2.85443	13593	1.2E-07	20	<a href="https://en.wikipedia.org/wiki/Mercury.html">https://en.wikipedia.org/wiki/Mercury.html</a>	<input type="checkbox"/>
Sea water with 3.3% sali...	2.337323	1029	1.4E-06	10	<a href="https://en.wikipedia.org/wiki/Sea_water.html">https://en.wikipedia.org/wiki/Sea_water.html</a>	<input type="checkbox"/>
Water at 4°C	2.188128	999.97	1.566E-06	4	<a href="https://en.wikipedia.org/wiki/Water.html">https://en.wikipedia.org/wiki/Water.html</a>	<input type="checkbox"/>
Water at 20°C	2.188128	998.21	1.004E-06	20	<a href="https://en.wikipedia.org/wiki/Water.html">https://en.wikipedia.org/wiki/Water.html</a>	<input type="checkbox"/>
<Name>	0	0	0	0	<User Defined>	<input type="checkbox"/>

Figure 4.4. Liquid library interface

#### 4.1.4 Wave Speed Calculator

This part of the software calculates the acoustic wave speed when the information needed is provided for a selected pipe. The calculation output is the result of the Eq. (2.28). For instance, Figure 4.4 shows the result of a pipe with the information below:

$$D = 2\text{m};$$

$$e = 20 \text{ mm};$$

$$E = 207 \text{ GPa};$$

$$K = 2.07 \text{ GPa};$$

$$c_1 = 1;$$

$$\rho = 1000 \text{ kg/m}^3;$$

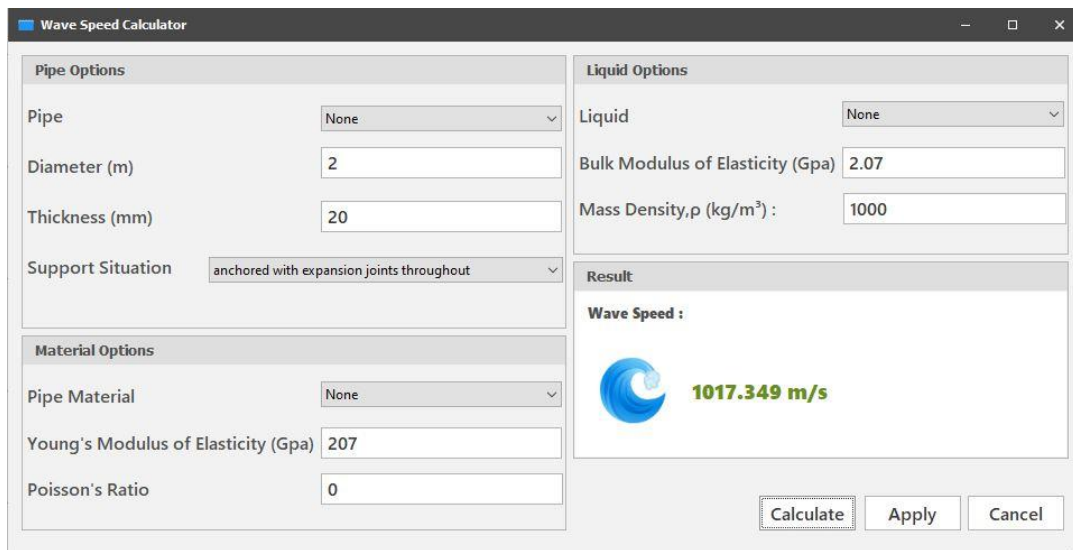


*Figure 4.5.* Wave speed calculator result for the information provided

Figure 4.4 shows that the wave speed calculated is 1017.349 m/s. In the software, pipe diameter and thickness are entered, steel pipe material is selected, water is selected as the liquid of the system, and support case (c) is decided. Finally, the user can apply the calculated wave speed for a pipe or pipes of the model.

#### **4.1.5 Object Properties Panel**

While drawing the system and adding objects to the design canvas, the properties related to the object is shown in this tab. The user can insert the required data for each object so that this information will be used when solving the transient event. Furthermore, there are different tabs for each design component. Additionally, there is a separate form that detailed data can be set or seen. The user can use this form to set the inputs of the objects, or the calculated information can also be seen. Figure 4.5 illustrates this panel.

Name	ID	Down Location	Z1	Up Location	Z2	Length (m)	Diameter (m)	$\Delta x$ (m)	Nodes	Fricti...	Wave Speed (m/s)	Thickn... (mm)	Maximum Head (m)	Minimum Head (m)	Maximum Pressure (kPa)	Minimum Pressure (kPa)	Select
Pipe 1	1	{X=-400,Y=100}	0	{X=-200,Y=100}	0	351	0.3	117	3	0.019	1170	0	516.216	85.887	516.216	85.887	<input type="checkbox"/>
Pipe 2	2	{X=-200,Y=100}	0	{X=100,Y=100}	0	483	0.2	120.75	4	0.018	1207.5	0	743.12	-61.382	743.12	-61.382	<input type="checkbox"/>
Pipe 3	3	{X=100,Y=100}	0	{X=200,Y=100}	0	115	0.15	115	1	0.018	1150	0	806.668	-74.144	806.668	-74.144	<input type="checkbox"/>

Figure 4.6. Scheme of the object properties Panel

### 4.1.6 Messages Box

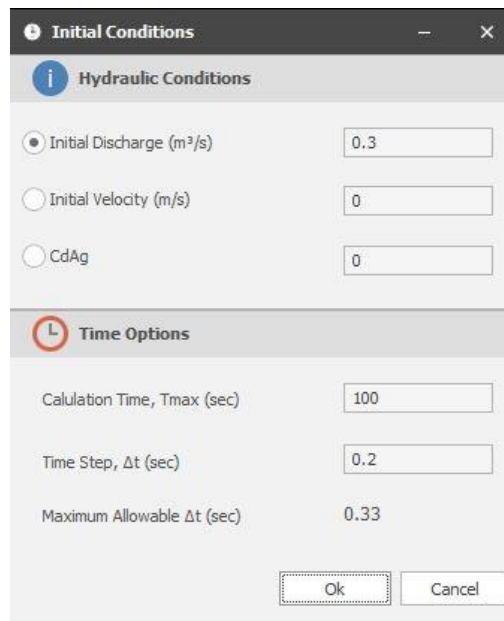
This part shows the messages for the actions done during the design by printing the steps in a text box. Also, if there is an error during the analysis, the error or warning occurred will be printed in the messages box. Figure 4.7 is an image of this section.



Figure 4.7. Message box panel

### 4.1.7 Initial Conditions

Before starting a simulation, the initial conditions of the model must be set. Hence, in the analysis panel, “Initial conditions” window must be clicked. There are two sections in this window, which are hydraulic conditions and time options. In the hydraulic conditions section, the user must choose an option to define the flow rate in the system. These options are discharge, velocity, and valve discharge coefficient times valve opening area. Figure 4.8 illustrates this window.



*Figure 4.8.* Initial conditions window

As seen in Figure 4.8, the second part of this window is to determine the maximum time and time step of the simulation. Also, the program calculates and shows the maximum allowable time step that the user can define.

#### **4.1.8 Graphical and Tabular Result Forms**

After designing and analyzing the transient in the designed hydraulic network, the user can select the windows forms to obtain the results of the analysis. These results contain graphic charts and tables.

##### **4.1.8.1 Tabular Results Form**

In this section, the tabular data of the analysis is shown, including node number, pipe number, time, discharge, head, velocity, pressure, and tau values. Functionally, the user can export and save the table into Microsoft Office Excel format. The tabular data has three different view options. Additionally, the user can select a precision for

the data numbers shown in the tables. The first view option is a time-based table, which is shown in Figure 4.9.

	Time (sec)	Object Name	Node No.	Head (m)	Discharge (m <sup>3</sup> /s)	Velocity (m/s)	Pressure (kPa)	Tau
→	0.60	Pipe-1	1	319.036	0.200	2.829	319.036	0.624
	0.60	Pipe-1	2	314.499	0.200	2.829	314.499	0.624
	0.60	Pipe-1	3	309.962	0.200	2.829	309.962	0.624
	0.60	Pipe-2	1	309.962	0.200	6.366	309.962	0.624
	0.60	Pipe-2	2	290.507	0.194	6.159	290.507	0.624
	0.60	Pipe-2	3	280.293	0.185	5.878	280.293	0.624
	0.60	Pipe-3	1	280.293	0.185	10.449	280.293	0.624
	0.60	Pipe-3	2	240.726	0.170	9.604	240.726	0.624

Figure 4.9. Time-based tabular view of the results

In this tab, the user can choose a specific time to see the results calculated for the selected time by a track bar provided.

The second view option is a pipe-based table. The user can select a pipe which is included in the transient event, and all of the data is shown for the selected pipe.

Figure 4.10. displays an image of this type of tabular view.

	Time (sec)	Object Name	Node No.	Head (m)	Discharge (m <sup>3</sup> /s)	Velocity (m/s)	Pressure (kPa)	Tau
	0.50	Pipe-2	1	309.962	0.200	6.366	309.962	0.333
	0.50	Pipe-2	2	287.504	0.200	6.366	287.504	0.333
	0.50	Pipe-2	3	290.397	0.194	6.160	290.397	0.333
	0.50	Pipe-2	4	303.535	0.184	5.871	303.535	0.333
	0.50	Pipe-2	5	331.494	0.172	5.474	331.494	0.333
	0.60	Pipe-2	1	309.962	0.200	6.366	309.962	0.200
	0.60	Pipe-2	2	312.141	0.194	6.166	312.141	0.200
	0.60	Pipe-2	3	324.315	0.185	5.885	324.315	0.200
	0.60	Pipe-2	4	351.004	0.173	5.497	351.004	0.200
	0.60	Pipe-2	5	398.281	0.155	4.947	398.281	0.200

Figure 4.10. Pipe-based tabular view of the results

Finally, the user can view all of the tabular results in all data table tab. In this tab, the result data for all time and all pipes is shown.

#### 4.1.8.2 Graphical Results Forms

In this section, the graphical results of the analysis are shown. There are two chart types in the software, which are time-based and animative charts. Both of the charts are described in this section.

##### 4.1.8.2.1 Time-Based Graphical Chart

This graphical chart depends on the time of the analysis. In all of the graphical results, the x-axis of the graphs is always time. Additionally, the user can add a secondary chart. The detailed picture of this chart is shown in Figure 4.11.

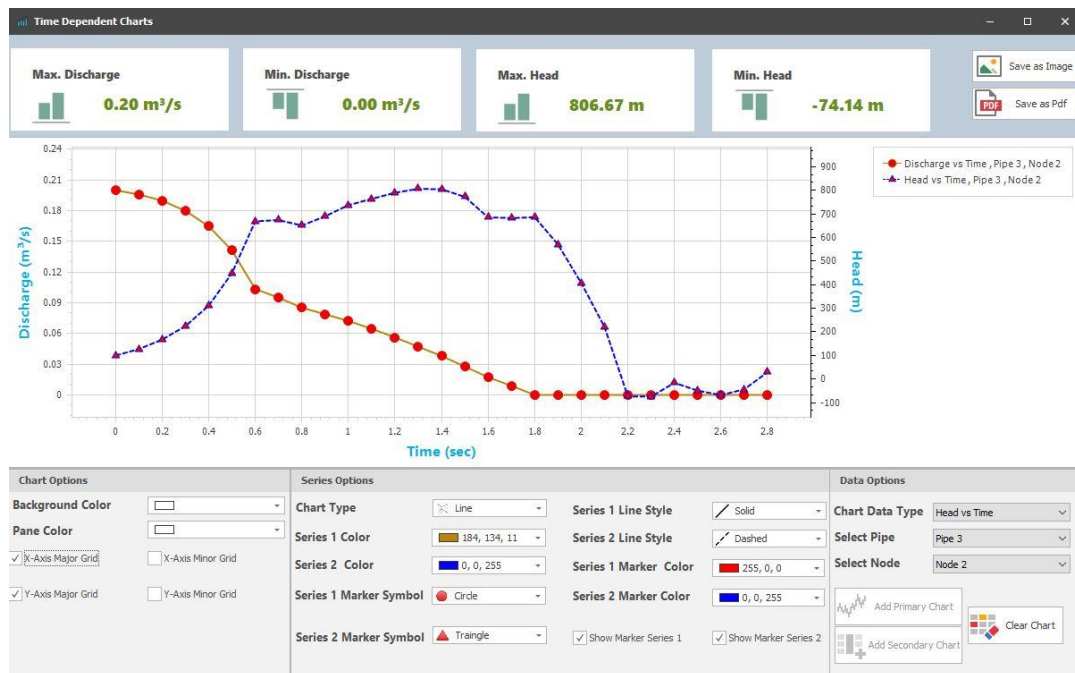


Figure 4.11. Time dependent graphical chart windows form

This form includes various options that the user can personalize. These options include charts, series, and data options. The user can change the color of the chart and activate major and minor grids for all of the axes. Moreover, the series option part has the functions named below;

- Chart Type: includes six chart types that are line, point, spline, scatter, line 3D, and spline 3D chart types.
- Series color: the user can choose any color for both primary and secondary series lines.
- Series line style: includes four different styles for both of the series lines.
- Series marker symbol: the user can enable or disable this feature and also can choose between various shapes for the points of the series.
- Series marker color: the user can select a color for the enabled marker style for both of the series.

Ultimately, in the data option, the user must select between four data types. These data types are Discharge vs. Time, Head vs. Time, Velocity vs. Time, and Pressure vs. Time. After selecting one of the chart data types, the pipe number, and the nodal point for the selected pipe must be chosen. Lastly, by adding the primary and secondary charts, the visual chart can be seen in the window. Moreover, maximum and minimum values for both of the series can be seen on the top of the form.

The graph can be saved in image or pdf formats. Also, by moving the mouse on the chart, the values of the points can be seen. Figure 4.12 illustrates this feature.

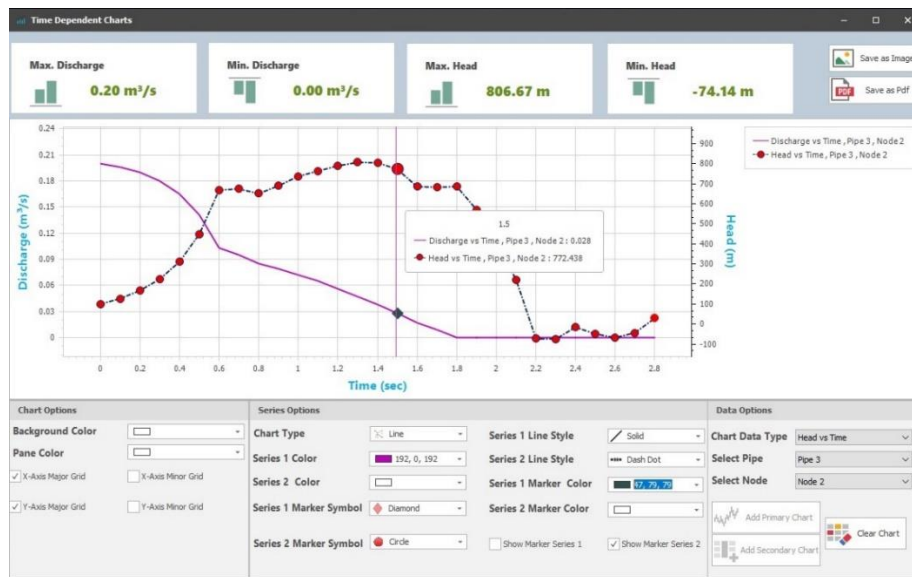


Figure 4.12. A feature of the graphical charts form

#### 4.1.8.2.2 Animation Chart

This graphical chart depends on the pipe profile of the hydraulic network. In all of the graphical results, the x-axis of the graphs is the length of the pipeline. The detailed picture of this chart is shown in Figure 4.13.

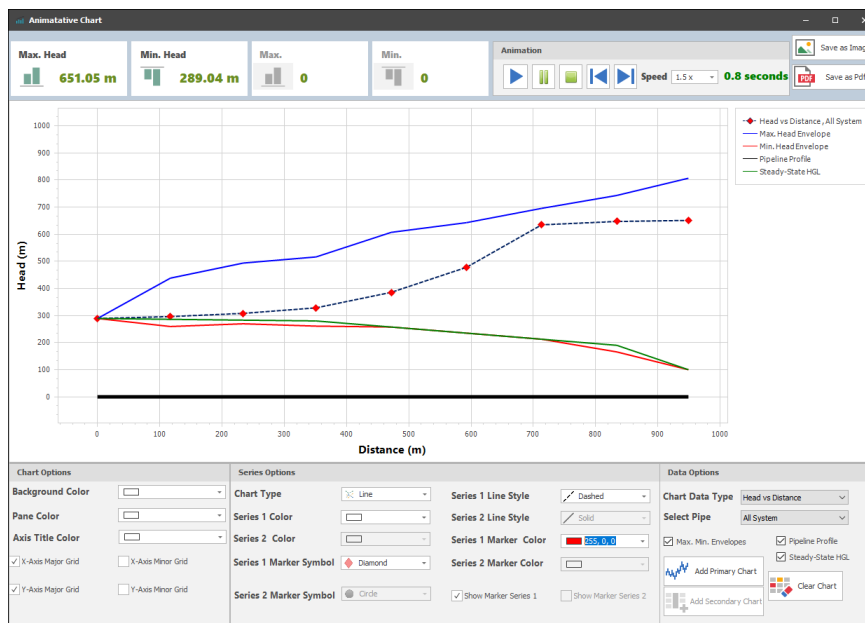


Figure 4.13. Animation graphical chart windows form

Similarly to the time-dependent chart, the user can personalize the visualization of the chart. In the data options, after selecting between Head, Discharge, Velocity, and Pressure vs. Distance chart data types, the user can either choose to add the chart for all pipeline system or a specific pipe.

Also, after drawing the chart, to visualize the motion, an animation is available for the behavior of the system. The time of the animation depends on the duration of the simulation starting from the beginning until the maximum simulation time reached. The step can be defined or calculated in the analysis. By clicking the play button, the animation will start with the user-defined speed. The animation can be paused or stopped by clicking the related buttons. Moreover, the user can see the animation step by step by pressing the next or previous time step buttons.

Additionally, as the maximum and minimum head envelopes are of particular interest to designers, these lines can be added to the chart. Similarly, the pipeline profile and steady-state HGL is also included in this chart so that the reaction of the system can be evaluated during the transient event.

## **4.2 Object Elements and Properties**

This section contains detailed information about the object collections in the program. When drawing the objects in the design canvas, all objects have a snapping feature that can help the objects to be joined. As a result, it is necessary to join the components so that the software can detect a valid pipeline system.

### **4.2.1 Pipe Object**

One of the main objects of the design system is the pipe. This object can be joined to a reservoir object. The properties of the pipe are listed below:

- Area (m<sup>2</sup>)
- Diameter (m)

- Length (m)
- Friction
- Wall thickness (mm)
- Wave speed (m/s)
- Elevation at upstream (m)
- Elevation at downstream (m)

The user must put the essential input data of each pipe in the pipe collection. Additionally, upstream and downstream points have a snap function. Figure 4.14 illustrates the pipe properties and shape of a pipe object in the program.



Figure 4.14. A scheme of pipe series and Pipe series property panel in the software

#### 4.2.2 Reservoir Object

The reservoir object consists of two types, which are upstream and downstream reservoirs. The software is able to determine the type of reservoir using the code. The properties of the reservoir are listed below:

- Reservoir head (m)

- Elevation at the junction (m)
- Loss coefficient
- Sinus wave checkbox
- Wave amplitude,  $\Delta H$  (m)
- Circular frequency,  $\omega$

The user can put the information needed in the properties panel of a reservoir object. If the sinus wave checkbox is enabled, it means that the head of the reservoir is not constant, and a sinusoidal wave causes changes in the head value. Hence, the user must enter the wave amplitude and circular frequency. Figure 4.15 illustrates both upstream and downstream reservoir shapes and properties of the upstream reservoir with a sinus wave available in the program.

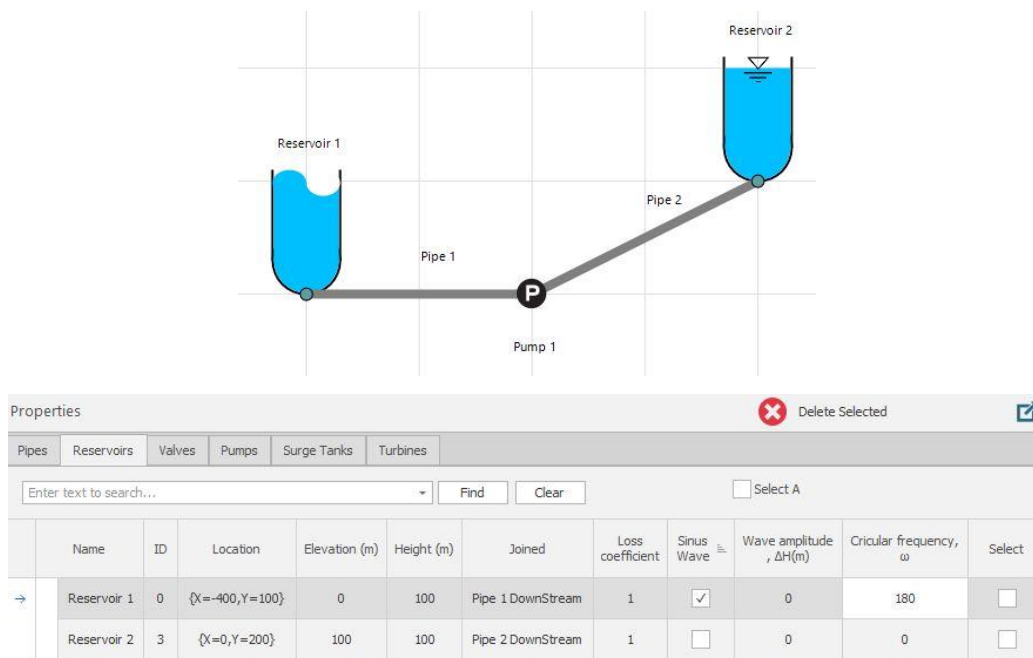


*Figure 4.15.* symbols of upstream and downstream reservoirs and upstream reservoir object properties panel

Additionally, the software is able to detect where the reservoir is attached. Attaching the objects in the software is so crucial so that the software can build a valid hydraulic system. Moreover, depending on the hydraulic system, the user must enter a value for the upstream reservoir head. However, if the downstream has a known head in

the model, the code can calculate the upstream head and apply it for the upstream reservoir.

### 4.2.3 Valve Object

One of the boundary objects of the software is the valve. This object can be joined to a pipe upstream or downstream point in the system. The code determines the location of the valve, and the user is only allowed to place the valve at junction points of the pipes. Figure 4.16 presents an illustration of a valve object and its properties.

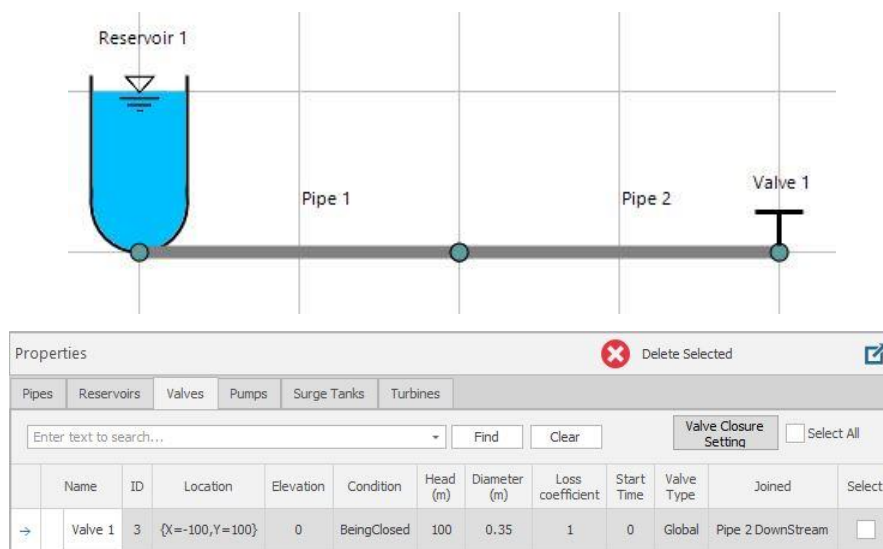


Figure 4.16. Valve objects view and its properties panel

The first property of a valve object is the condition showing with a dropdown menu, including three different functions below.

- Open condition: by selecting this item, the valve act like an open valve, effecting no impact on the system.
- Being closed condition: by selecting this item, the valve starts to operate in a closing manner during the analysis according to its closure operation, which will be explained further.
- Closed condition: whenever this item is selected, the valve object act as a dead-end in the system, and there is no motion after this boundary.

In the being closed condition, the user must click the valve closure setting button to specify a closure manner to the valve closure operation. Firstly, there must be a calculation time and time step. Then, in order to initialize the closure setting, a valve must be selected. Figure 4.17 is the schematic view of the valve closure setting window.

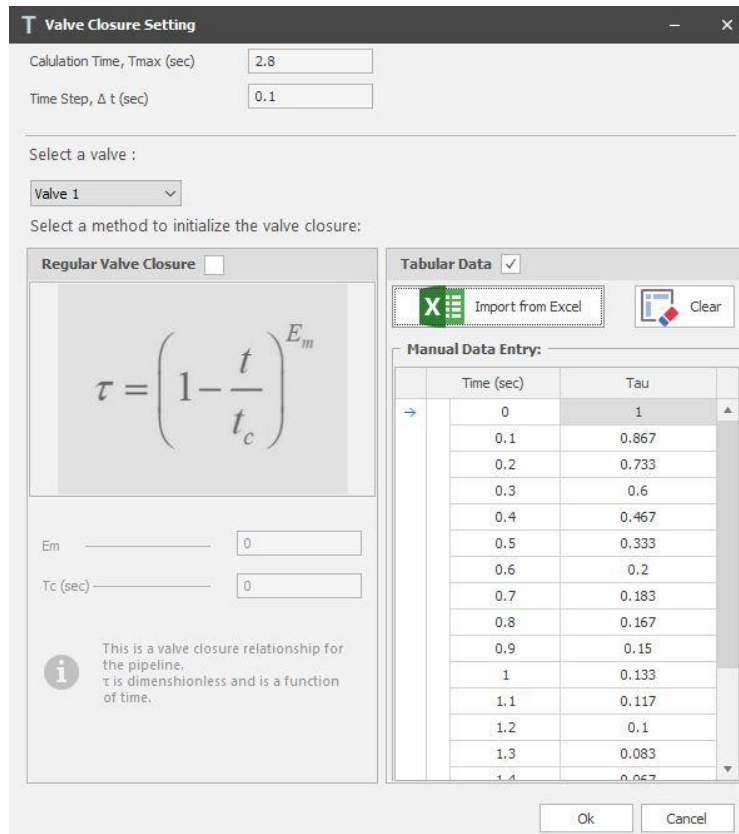


Figure 4.17. Valve object closure setting window

There are two options for the user to select. If the user selects the “Regular Valve Closure,” the program will calculate the valve closure relationship according to the equation below;

$$\tau = \left(1 - \frac{t}{t_c}\right)^{E_m} \quad (4-1)$$

In which;

$\tau$  = dimensionless valve closure coefficient

$t$  = maximum time of the operation

$t_c$  = time of the closure

$E_m$  = an exponential constant for valve closure time

$E_m = 1$  represents the condition where the valve is being closed linearly until closure time. Furthermore, it must be noticed that  $\tau$  value varies between 0 and 1, and  $\tau = 1$  means the valve is completely open, while  $\tau = 0$  represents a completely closed valve operation.

The second option for valve closure is using tabular data where the user enters the closure setting manually. To do that, the maximum time of the calculations ( $T_{max}$ ) and time interval ( $\Delta t$ ) is needed. By entering these values, a table view will be presented to the user to provide the closure data. Alternatively, the user can import tabular data from Microsoft Excel.

#### 4.2.4 Pump Object

This boundary object simulates a single pump boundary condition in the design system. The user may join the object to a pipe upstream or downstream point in the system. The code determines the location of the pump, and the user is only allowed to place the pump at junction points of the pipes. The properties of the pump are listed;

- Rated head,  $H_R$  (m),
- Rated discharge,  $Q_R$  ( $m^3/s$ ),
- Rated speed of the pump,  $N_R$  (rpm),
- $\omega_{RR}^2$  value, ( $N.m^2$ ),
- Rated torque,  $T_R$  (N.m),
- Rated pump efficiency,  $\mu_R$ ,
- Loss coefficient,
- Discharge valve availability of the pump,

- Pump trip time (sec),
- Discharge valve closure time,  $T_c$  (s)

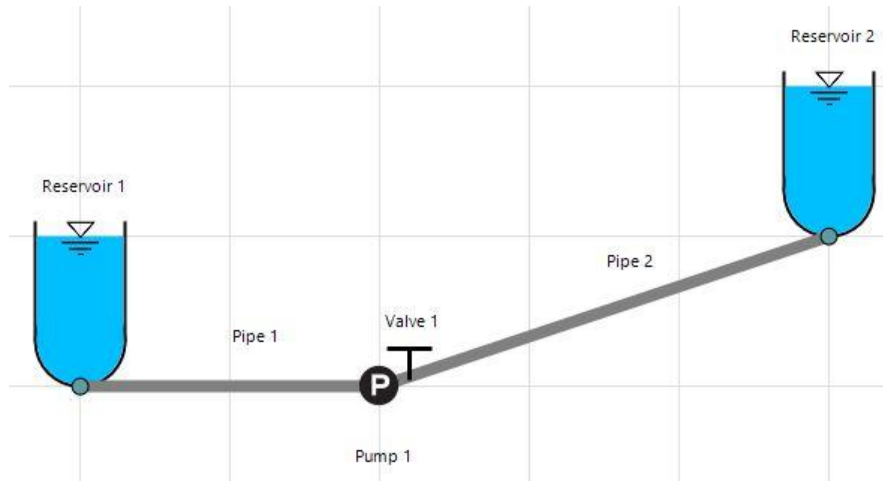


*Figure 4.18.* A sample of a system pumping water from an upstream lower reservoir to a downstream upper reservoir

In Figure 4.18, an example design shows that a single pump discharges water from an upstream reservoir to a downstream reservoir. This pump has a discharge valve on its downstream side. Hence, Figure 4.19 is the Panel where users can put the input data of the pump.

Properties													Delete Selected									
Pipes													Reservoirs		Valves		Pumps		Surge Tanks		Turbines	
Enter text to search...													Find		Clear		Select All					
	Name	ID	Elevation (m)	Joined	Loss coefficient	Rated Head (m)	Rated Discharge (m <sup>3</sup> /s)	Rated Speed (RPM)	WRR Value	Rated Torque (N.m)	Trip Time (sec)	Discharge Valve	Select									
→	Pump 1	2	0	Pipe 2 DownStream	0	75	0.25	1100	165.3	1947	5	Yes	<input type="checkbox"/>									

*Figure 4.19.* A single pump boundary object Properties

#### 4.2.5 Dead End Object

Another boundary object which is included in the software is the dead end boundary. When locating it in the downstream, simply there is no motion of flow after this

boundary. Figure 4.20 shows the schematic view of this boundary at downstream and an upstream reservoir with variable head.

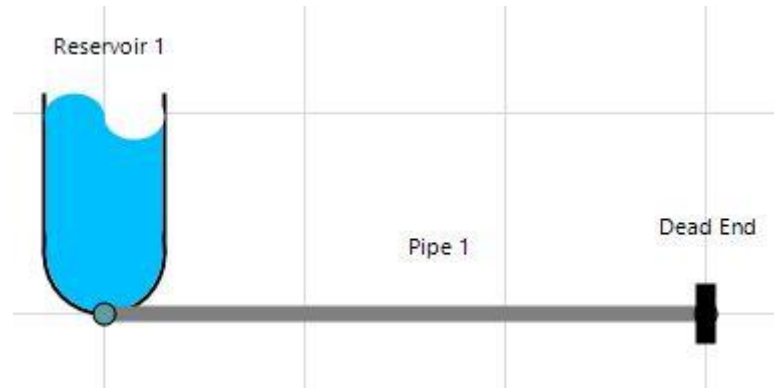


Figure 4.20. Dead end boundary view of the software

#### 4.2.6 Surge Tank Object

Surge tanks are a protective device boundary that can be placed in the pipeline system in the design stage. As protection in a transient event is so important, a comprehensive code is developed. The surge tank type that is defined to software is simple. To achieve this goal, the user can start the surge tank analysis window by adding a surge tank object to the system.

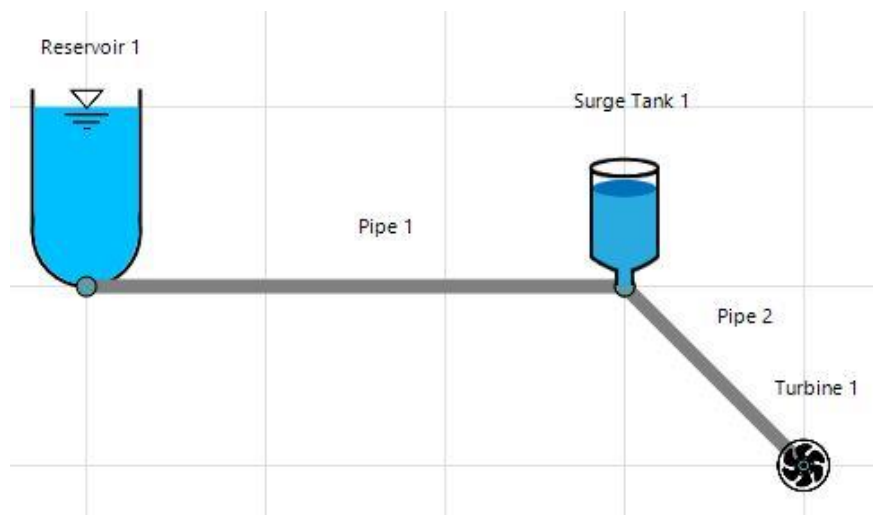


Figure 4.21. Surge tank added to the system in the design stage

After subjoining the surge tank, the surge tank designer button must be clicked, which is available in its design panel. Hence, Figure 4.22 shows the surge tank designer window.

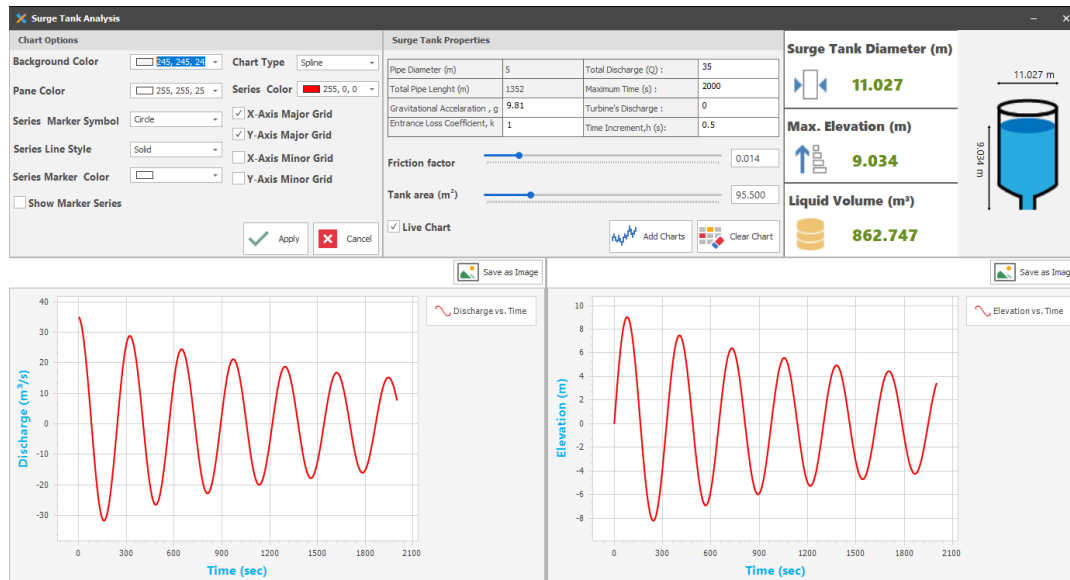


Figure 4.22. Surge tank analysis window

As shown in Figure 4.22, the user can personalize the visualization of the chart. The next step is to find the optimal tank size using the tools provided for the user. After adding essential data requirements, the user can find the optimal size by varying the values for friction factor and tank area. There are two charts presented to see the motion inside the surge tank. These charts are Discharge vs. Time and Elevation vs. Time. Additionally, the code provides information such as tank diameter, maximum elevation of liquid in the tank, and the volume of liquid to make the design more efficient. Ultimately, after finding the ideal dimensions for the tank, the user can apply the designed data to the surge tank of the hydraulic system.

## CHAPTER 5

### Validation of the Software

The verification of the software is satisfied by solving various cases and compared with different eminent sources.

#### 5.1 Single Pipe Scenario

In the first case, the application of a single-pipeline with a constant head upstream reservoir, and a closing downstream valve is tested. Figure 5.1 is the simple sketch of the case.  $H_R$  is the water surface elevation measured from the datum, which is the pipe centerline, in this case,  $Q_0$  is the steady-state discharge in the pipe, and  $H_0$  is the head loss across the partially open valve at the steady-state condition.

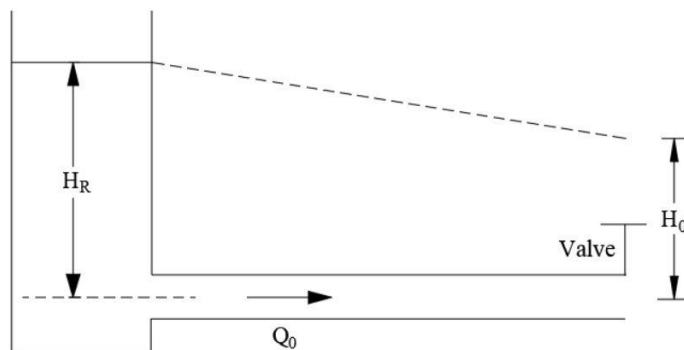


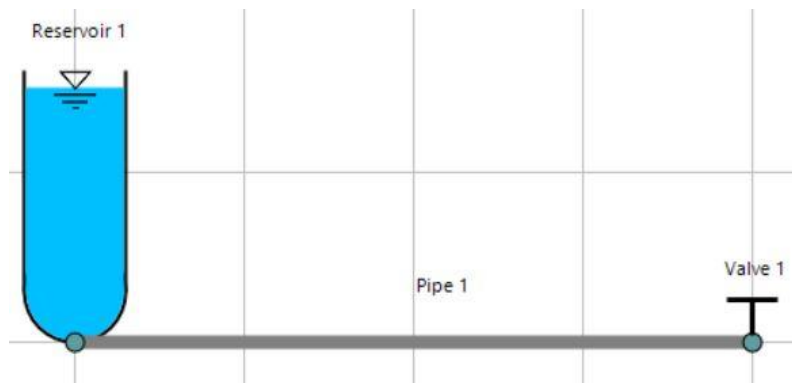
*Figure 5.1.* The definition of a water system with a Single Pipe

The details of the known data are represented below:

- Pipe Length,  $L = 600$  m
- Pipe Diameter,  $D = 0.5$  m
- Reservoir Head,  $H_R = 150$  m
- Friction Factor,  $f = 0.018$

- Wave Speed,  $a = 1200$  m/s
- Node Numbers,  $N = 5$
- Discharge Coefficient Times Valve Opening Area,  $(C_d A_g)_0 = 0.009$
- Time of the Valve Closure,  $T_c = 2.1$  seconds
- Maximum Time of the Event,  $T_{\max} = 4.3$  seconds
- Valve Closing Data = Regular Valve Closure
- Valve Closure Constant,  $E_m = 1.5$

According to the data above, the setup of the system is done, and the schematic view of the system is presented in Figures 5.2 and 5.3.



(a)

(b)

Figure 5.2. (a) Single pipeline design (b) analyze input data of the software

Properties Delete Selected

Pipes Reservoirs **Valves** Pumps Surge Tanks Turbines

Enter text to search... Find Clear Valve Closure Setting  Select All

Name	...	Location	Elevation	Condition	Head (m)	Diameter (m)	Loss coefficient	Start Time	Valve Type	Joined	Select
Valve 1	2	{X=100,Y=100}	0	BeingClosed	0	0	1	0	Global	Pipe 1 DownStream	<input type="checkbox"/>

(a)

Properties Delete Selected

Pipes Reservoirs **Valves** Pumps Surge Tanks Turbines

Enter text to search... Find Clear  Select A

Name	ID	Location	Elevation (m)	Height (m)	Loss coefficient	Sin wave	Wave amplitude, ΔH(m)	Circular frequency, ω	Joined	Select
Reservoir 1	0	{X=-300,Y=100}	0	150	0	<input type="checkbox"/>	0	0	Pipe 1 DownStream	<input type="checkbox"/>

(b)

**Valve Closure Setting**

Calculation Time, Tmax (sec)

Time Step, Δt (sec)

Select a valve :  
Valve 1

Select a method to initialize the valve closure:

Regular Valve Closure

$$\tau = \left(1 - \frac{t}{t_c}\right)^{E_m}$$

Em

Tc (sec)

This is a valve closure relationship for this pipeline. τ is dimensionless and is a function of time.

Tabular Data

Import from Excel

Manual Data Entry:

Time (sec)	Tau

Ok Cancel

(c)

Properties Delete Selected

Pipes Reservoirs **Valves** Pumps Surge Tanks Turbines

Enter text to search... Find Clear  Select A

Name	ID	Location	Elevation (m)	Height (m)	Loss coefficient	Sin wave	Wave amplitude, ΔH(m)	Circular frequency, ω	Joined	Select
Reservoir 1	0	{X=-300,Y=100}	0	150	0	<input type="checkbox"/>	0	0	Pipe 1 DownStream	<input type="checkbox"/>

(d)

Figure 5.3. Objects properties inputs, (a) Valve Object properties, (b) Reservoir object properties, (c) Valve closure setting, and (d) Pipe object properties

After inserting the necessary data into the program, the analysis is started and finished in less than 1 second. Consequently, the results obtained are presented in Figure 5.4 and Figure 5.5.

Time (sec)	Object Name	Node No.	Head (m)	Discharge (m³/s)	Velocity (m/s)	Pressure (kPa)	Tau
0.00	Pipe-1	1	150.000	0.477	2.432	150.000	1.000
0.00	Pipe-1	2	148.698	0.477	2.432	148.698	1.000
0.00	Pipe-1	3	147.395	0.477	2.432	147.395	1.000
0.00	Pipe-1	4	146.093	0.477	2.432	146.093	1.000
0.00	Pipe-1	5	144.791	0.477	2.432	144.791	1.000
0.00	Pipe-1	6	143.488	0.477	2.432	143.488	1.000
0.10	Pipe-1	1	150.000	0.477	2.432	150.000	0.929
0.10	Pipe-1	2	148.698	0.477	2.432	148.698	0.929
0.10	Pipe-1	3	147.395	0.477	2.432	147.395	0.929
0.10	Pipe-1	4	146.093	0.477	2.432	146.093	0.929
0.10	Pipe-1	5	144.791	0.477	2.432	144.791	0.929
0.10	Pipe-1	6	154.278	0.460	2.343	154.278	0.929

Figure 5.4. Tabular view of results obtained for single pipe application



Figure 5.5. Graphical results obtained at valve end for single pipe application

Finally, results obtained from the software of the present study are compared for the valve dead-end node with those from Streeter & Wylie, (1967) in Table 5.1.

Table 5.1: *Single Pipe comparison at valve end (S-Hammer & Wylie-Streeter)*

Time (s)	S-Hammer			Wylie-Streeter (1978)		
	Discharge	Head	$\tau$	Discharge	Head	$\tau$
0	0.47743	143.488	1.000	0.477	143.49	1.000
0.1	0.46012	154.277	0.929	0.460	154.28	0.929
0.2	0.44165	165.787	0.861	0.442	165.79	0.861
0.3	0.42208	178.080	0.794	0.422	178.08	0.794
0.4	0.40132	191.111	0.728	0.401	191.11	0.728
0.5	0.37945	204.929	0.665	0.379	204.93	0.665
0.6	0.35644	219.461	0.604	0.356	219.46	0.604
0.7	0.33240	234.733	0.544	0.332	234.73	0.544
0.8	0.30734	250.639	0.487	0.307	250.64	0.487
0.9	0.28141	267.174	0.432	0.281	267.17	0.432
1	0.25472	284.187	0.379	0.255	284.19	0.379
1.1	0.22105	284.869	0.329	0.221	284.87	0.329
1.2	0.18829	283.515	0.281	0.188	283.52	0.281
1.3	0.15679	279.906	0.235	0.157	279.91	0.235
1.4	0.12691	273.743	0.192	0.127	273.74	0.192
1.5	0.09905	264.803	0.153	0.099	264.80	0.153
1.6	0.07363	252.812	0.116	0.074	252.81	0.116
1.7	0.05107	237.565	0.083	0.051	237.57	0.083
1.8	0.03184	218.838	0.054	0.032	218.84	0.054
1.9	0.01642	196.449	0.029	0.016	196.45	0.029
2	0.00540	170.203	0.010	0.005	170.20	0.01
2.1	0	152.268	0	0	152.27	0
2.2	0	133.478	0	0	133.48	0
2.3	0	117.660	0	0	117.66	0
2.4	0	105.345	0	0	105.35	0
2.5	0	97.021	0	0	97.02	0
2.6	0	93.216	0	0	93.22	0

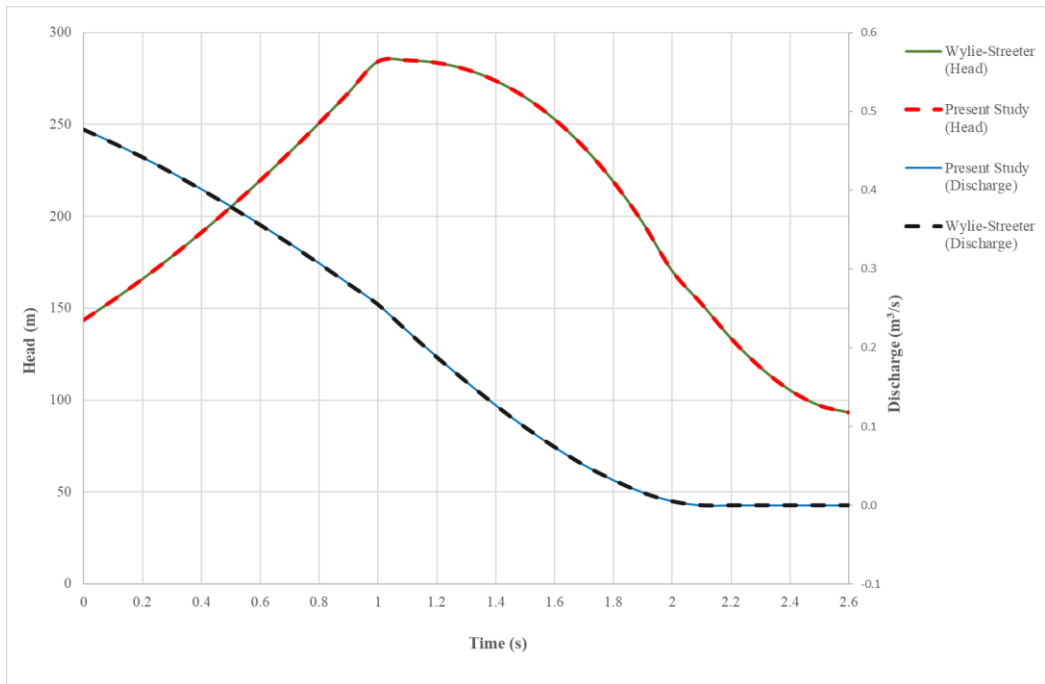


Figure 5.6. Single pipe comparison (H vs. Time) and (Q vs. Time) at valve end

## 5.1 Series Pipes Scenario

### 5.1.1 Series Pipes Comparison for a Case Study by Wylie & Streeter

Another simulation is done by comparing the results of S-Hammer with the results of a case study conducted by Wylie and Streeter (1978). Figure 5.7 shows the definition of the simulated system.

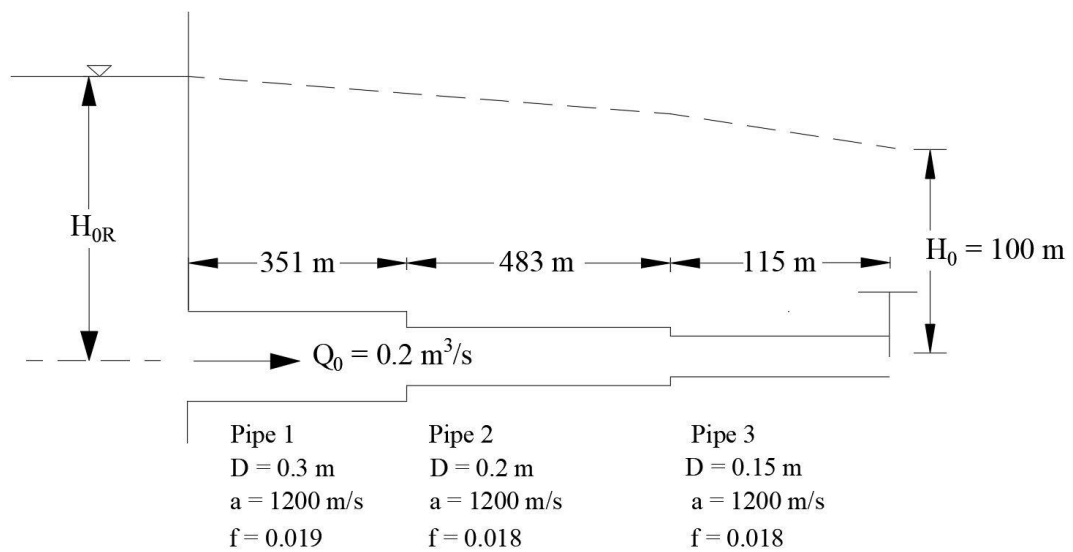
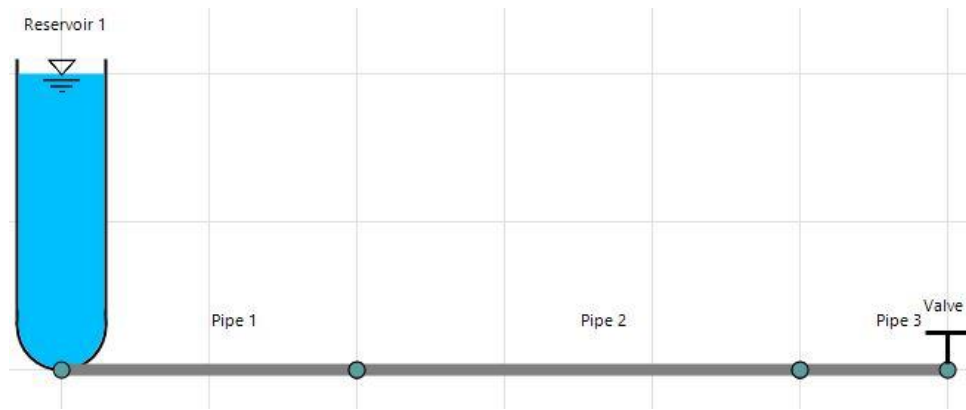


Figure 5.7. Series pipes case study, Wylie and Streeter (1978)

The information needed to start the simulation is provided in Figure 5.7. Also, the value for  $\Delta t$  is chosen as 0.1 seconds so that the results will be identical to the case study. Moreover, the values for the valve closing operation is put as tabular data. This tabular data is presented in the case study. After sketching the system and putting the provided data in the S-Hammer software, the analysis is started, and results are obtained. Figure 5.8. illustrates the sketching and pipe properties of the S-Hammer software after analysis.



Properties																		
Pipes																		
Enter text to search... Find Clear Select All																		
Name	ID	Down Location	Z1	Up Location	Z2	Length (m)	Diameter (m)	$\Delta x$ (m)	Nodes	Friction	Wave Speed (m/s)	Thickness (mm)	Maximum Head (m)	Minimum Head (m)	Maximum Pressure (kPa)	Minimum Pressure (kPa)	Select	
Pipe 1	1	{X=-400,Y=100}	0	{X=-200,Y=100}	0	351	0.3	117	3	0.019	1170	0	516.216	85.887	516.216	85.887	<input type="checkbox"/>	
Pipe 2	2	{X=-200,Y=100}	0	{X=100,Y=100}	0	483	0.2	120.75	4	0.018	1207.5	0	743.12	-61.382	743.12	-61.382	<input type="checkbox"/>	
Pipe 3	3	{X=100,Y=100}	0	{X=200,Y=100}	0	115	0.15	115	1	0.018	1150	0	806.668	-74.144	806.668	-74.144	<input type="checkbox"/>	

Figure 5.8. S-Hammer schematic view and the properties of the pipes of a case study by Wylie & Streeter

It must be mentioned that the values of the wave speed for all pipes are nominally given as 1200 m/s. However, as can be seen in Figure 5.8, wave speed values for pipes 1, 2, and 3 are adjusted during computations as 1170, 1207.5, and 1150 m/s, respectively. This is due to the grid-mesh ratio selection of the code so that the stability of the Courant condition is satisfied and does not affect the results considerably. Also, the number of nodes for each pipe is calculated according to the Courant condition. Additionally, various information such as  $\Delta x$ , maximum head, minimum head, maximum pressure, and the minimum pressure for each pipe is provided for the user.

Ultimately, a comparison of the results of S-Hammer software and Wylie and Streeter is made. These values are head and discharge values at the end junctions of the pipes. Tables 5.2 and 5.3 show these data. Figures 5.9 and 5.10 show the graphics of Head vs. Time and Discharge vs. Time at the valve end, respectively.

Table 5.2 *H vs. Time comparison for series pipes (Wylie-Streeter vs. S-Hammer)*

		Head (m)							
		Wylie-Streeter (1978)				S-Hammer			
Time(s.)	$\tau$	Reservoir	Pipe 1	Pipe 2	Pipe 3	Reservoir	Pipe 1	Pipe 2	Pipe 3
0.0	1.000	289.040	279.96	190.13	100.00	289.04	279.96	190.13	100.00
0.1	0.867	289.040	279.96	190.13	127.65	289.04	279.96	190.13	127.57
0.2	0.733	289.040	279.96	209.29	167.51	289.04	279.96	209.23	167.64
0.3	0.600	289.040	279.96	236.95	224.67	289.04	279.96	237.03	224.68
0.4	0.467	289.040	279.96	280.29	311.71	289.04	279.96	280.29	311.41
0.5	0.333	289.040	279.96	346.37	448.71	289.04	279.96	346.18	449.17
0.6	0.200	289.040	290.24	451.27	668.7	289.04	290.21	451.60	668.77
0.7	0.183	289.040	305.14	621.16	673.58	289.04	305.19	621.18	674.25
0.8	0.167	289.040	328.37	646.61	651.84	289.04	328.37	647.16	651.05
0.9	0.150	289.040	364.09	667.97	690.25	289.04	363.99	667.40	690.04
1.0	0.133	289.040	421.37	693.87	736.11	289.04	421.55	693.86	737.28
1.1	0.117	289.040	516.21	720.75	764.86	289.04	516.22	721.43	763.99
1.2	0.100	289.040	515.51	736.44	790.15	289.04	515.86	735.79	789.73
1.3	0.083	289.040	505.57	743.16	805.23	289.04	505.19	743.12	806.67
1.4	0.067	289.040	491.17	728.44	805.76	289.04	491.15	729.19	804.88
1.5	0.050	289.040	461.26	679.15	773.19	289.04	461.82	678.41	772.44
1.6	0.033	289.040	398.87	666.19	684.02	289.04	398.23	665.76	685.53
1.7	0.017	289.040	283.49	627.78	683.85	289.04	283.42	628.91	682.54
1.8	0.000	289.040	282.49	598.18	686.38	289.04	282.55	597.31	686.13
1.9	0.000	289.040	281.68	546.49	570.22	289.04	281.72	546.23	570.89
2.0	0.000	289.040	275.50	395.07	407.59	289.04	275.36	395.33	407.33
2.1	0.000	289.040	260.99	165.77	221.48	289.04	260.94	165.71	221.34

Table 5.3  $Q$  vs. Time comparison for series pipes (Wylie-Streeter vs. S-Hammer)

		Discharge (m <sup>3</sup> /s)							
		Wylie-Streeter (1978)				S-Hammer			
Time(s.)	$\tau$	Reservoir	Pipe 1	Pipe 2	Pipe 3	Reservoir	Pipe 1	Pipe 2	Pipe 3
0.0	1.000	0.200	0.200	0.200	0.200	0.200	0.200	0.200	0.200
0.1	0.867	0.200	0.200	0.200	0.196	0.200	0.200	0.200	0.196
0.2	0.733	0.200	0.200	0.195	0.190	0.200	0.200	0.195	0.190
0.3	0.600	0.200	0.200	0.188	0.180	0.200	0.200	0.188	0.180
0.4	0.467	0.200	0.200	0.177	0.165	0.200	0.200	0.177	0.165
0.5	0.333	0.200	0.200	0.161	0.141	0.200	0.200	0.161	0.141
0.6	0.200	0.200	0.194	0.135	0.103	0.200	0.194	0.135	0.103
0.7	0.183	0.200	0.185	0.093	0.095	0.200	0.185	0.093	0.095
0.8	0.167	0.200	0.171	0.088	0.085	0.200	0.171	0.088	0.085
0.9	0.150	0.188	0.188	0.085	0.079	0.188	0.150	0.085	0.079
1.0	0.133	0.171	0.117	0.077	0.072	0.171	0.117	0.077	0.072
1.1	0.117	0.144	0.061	0.068	0.065	0.144	0.061	0.068	0.065
1.2	0.100	0.103	0.051	0.059	0.056	0.103	0.050	0.059	0.056
1.3	0.083	0.037	0.040	0.048	0.047	0.037	0.041	0.048	0.047
1.4	0.067	-0.074	0.023	0.035	0.038	-0.074	0.023	0.035	0.038
1.5	0.050	-0.084	0.001	0.018	0.028	-0.084	0.000	0.018	0.028
1.6	0.033	-0.088	-0.028	0.011	0.017	-0.087	-0.028	0.011	0.017
1.7	0.017	-0.095	-0.070	0.009	0.009	-0.096	-0.070	0.009	0.009
1.8	0.000	-0.101	-0.079	-0.004	0.000	-0.101	-0.079	-0.004	0.000
1.9	0.000	-0.092	-0.082	-0.021	0.000	-0.092	-0.082	-0.021	0.000
2.0	0.000	-0.065	-0.087	-0.026	0.000	-0.065	-0.087	-0.026	0.000
2.1	0.000	-0.074	-0.083	-0.036	0.000	-0.074	-0.084	-0.036	0.000

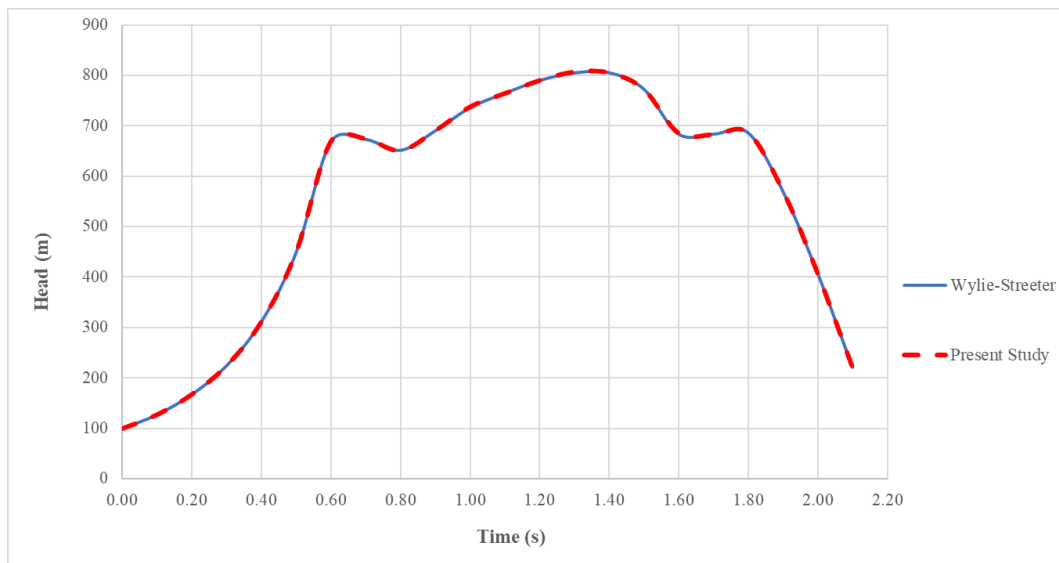


Figure 5.9. H vs. Time comparison at valve end (Wylie-Streeter vs. S-Hammer)

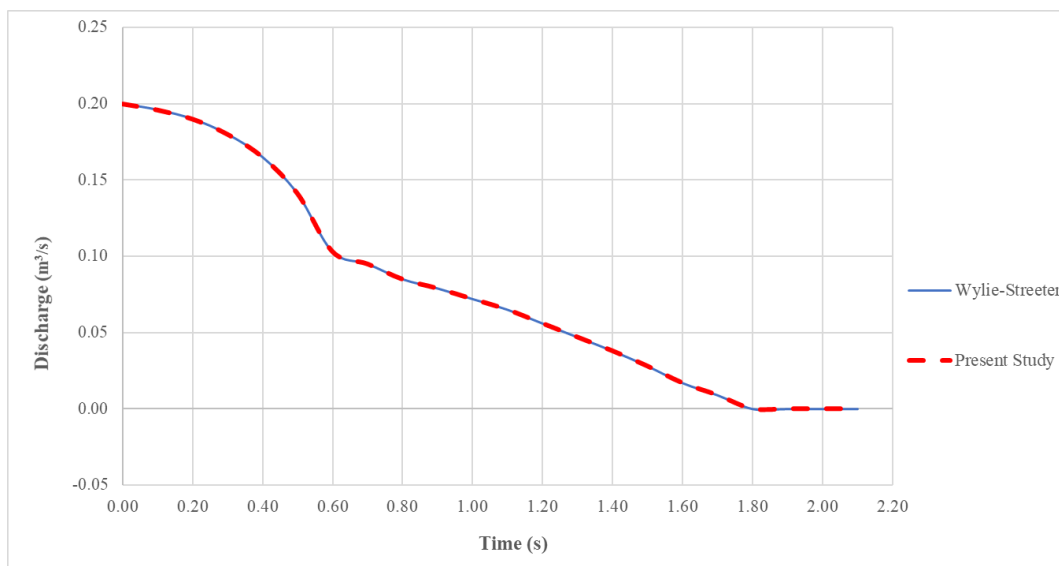


Figure 5.10. Q vs. Time comparison at valve end (Wylie-Streeter vs. S-Hammer)

Now,

By comparing the results, it is clear that the values calculated by S-Hammer are highly accurate, and coincide with those given for Wylie-Streeter's case study.

### 5.1.2 Series Pipes Comparison for a Case Study by Chaudhry

In this section, a transient problem conducted by Chaudhry (1979) is compared with S-Hammer. The detailed results of his computations are available there. The schematic view of the hydraulic system is shown in Figure 5.11 below.

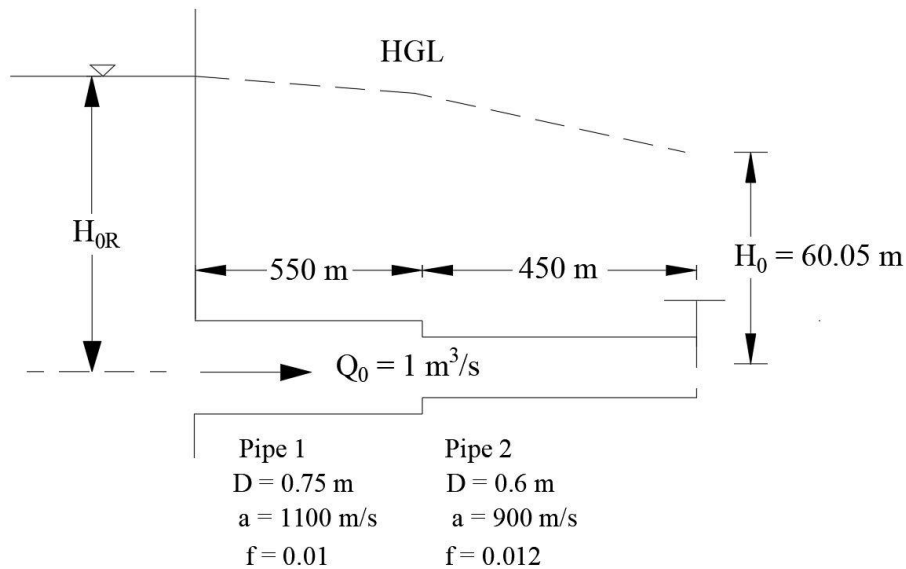


Figure 5.11. Series pipes case study by Chaudhry (1979)

The basic information needed to start the simulation is provided in Figure 5.11. Also, the value for  $\Delta t$  is chosen as 0.5 seconds, which satisfies the Courant condition, and the maximum simulation time is 10 seconds. The head value that is calculated by the code is 67.71 m for the reservoir. Moreover, the valve closure operation is lasting 6 seconds and data for this operation is inserted manually, as shown in Figure 5.12.

Tabular Data

 Import from Excel  Clear

Manual Data Entry:

Time (sec)	Tau
0	1
0.5	0.963
1	0.9
1.5	0.813
2	0.7
2.5	0.6
3	0.5
3.5	0.4
4	0.3
4.5	0.2
5	0.1
5.5	0.038
6	0
6.5	0
7	0

Figure 5.12. Manual valve closure data entry

Also, after analyzing the mentioned pipeline system, the pipe properties of the S-Hammer software and the illustration is shown in Figure 5.13.

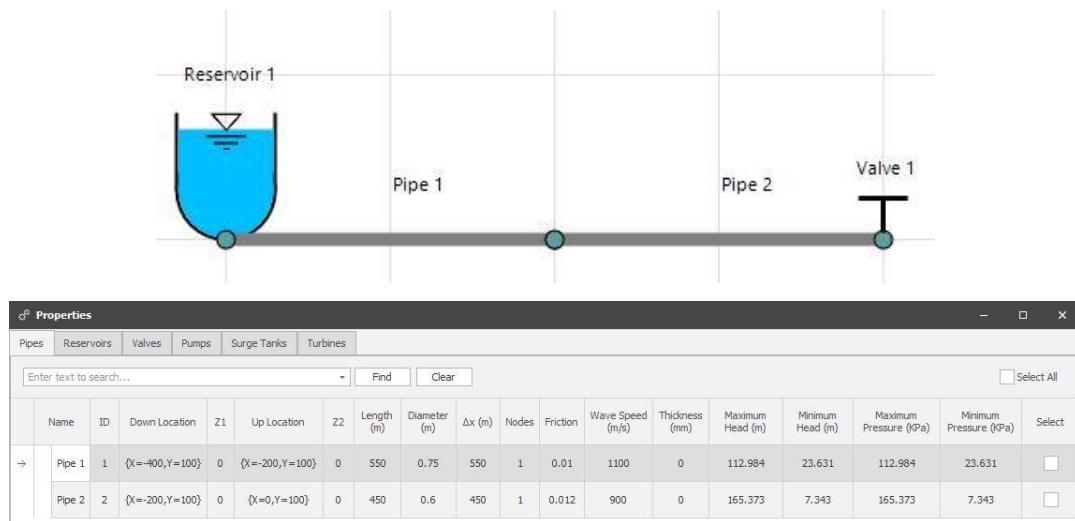


Figure 5.13. S-Hammer view and pipes properties of a case study by Chaudhry

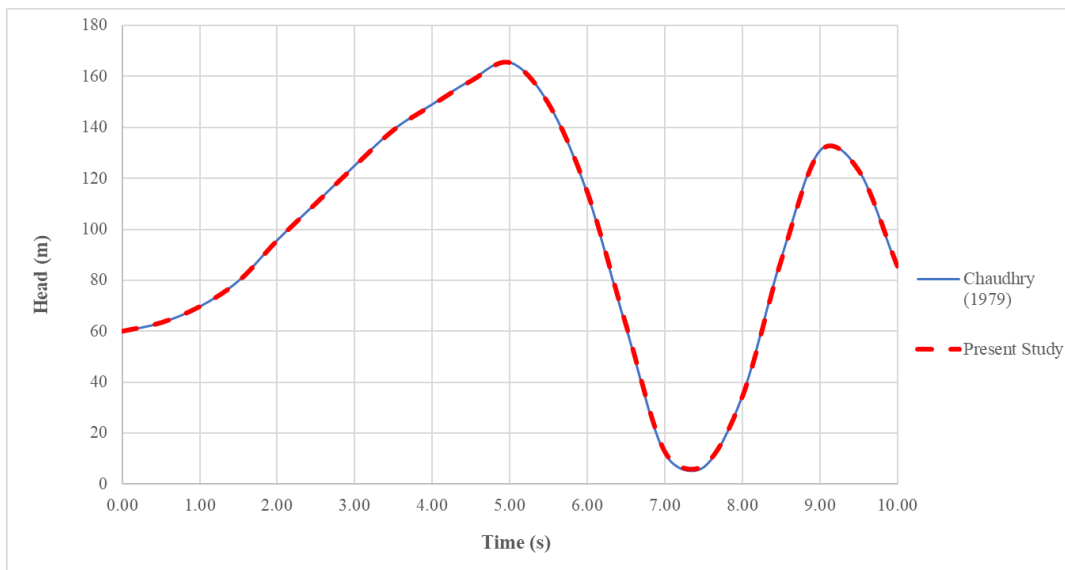
The comparison of the results of S-Hammer software and Chaudry is made. These values are head and discharge values at the end junctions of the pipes. Tables 5.4 and 5.5 show the data related to this comparison.

Table 5.4 *H vs. Time comparison for series pipes (Chaudhry vs. S-Hammer)*

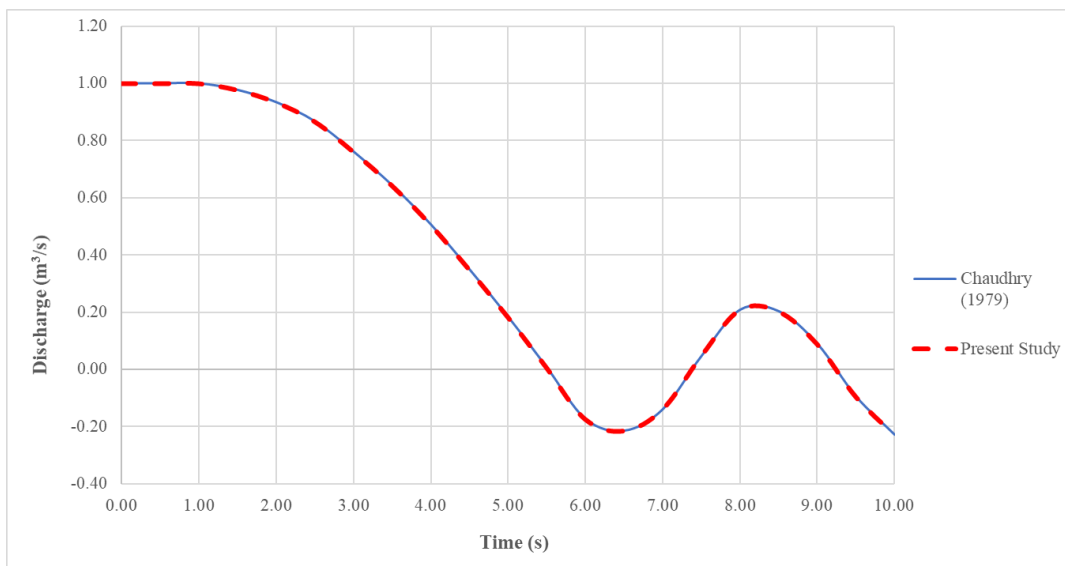
Time(s.)	$\tau$	Head (m)					
		Chaudhry (1979)			S-Hammer		
		Reservoir	Pipe 1	Pipe 2	Reservoir	Pipe 1	Pipe 2
0.000	1.000	67.70	65.78	60.05	67.706	65.790	60.050
0.500	0.963	67.70	65.78	63.46	67.706	65.790	63.417
1.000	0.900	67.70	68.73	69.78	67.706	68.694	69.765
1.500	0.813	67.70	74.16	79.88	67.706	74.169	79.785
2.000	0.700	67.70	79.92	95.83	67.706	79.919	95.759
2.500	0.600	67.70	88.25	110.41	67.706	88.248	110.330
3.000	0.500	67.70	94.95	125.13	67.706	94.994	124.951
3.500	0.400	67.70	99.18	139.2	67.706	99.139	139.027
4.000	0.300	67.70	104.4	149.14	67.706	104.335	148.847
4.500	0.200	67.70	108.47	158.61	67.706	108.365	158.276
5.000	0.100	67.70	111.20	165.65	67.706	111.068	165.373
5.500	0.038	67.70	113.07	149.46	67.706	112.984	149.041
6.000	0.000	67.70	96.01	114.28	67.706	95.795	114.306
6.500	0.000	67.70	63.25	61.79	67.706	63.366	62.024
7.000	0.000	67.70	34.25	12.33	67.706	34.663	12.567
7.500	0.000	67.70	23.55	6.75	67.706	23.631	7.343
8.000	0.000	67.70	47.63	34.76	67.706	47.750	34.687
8.500	0.000	67.70	82.89	88.45	67.706	82.753	88.068
9.000	0.000	67.70	105.95	130.93	67.706	105.514	130.692
9.500	0.000	67.70	108.01	123.42	67.706	107.972	122.944
10.000	0.000	67.70	78.38	85.12	67.706	78.400	85.281

Table 5.5 *Q vs. Time comparison for series pipes (Chaudhry vs. S-Hammer)*

		<b>Discharge (m<sup>3</sup>/s)</b>					
		<b>Chaudhry (1979)</b>			<b>S-Hammer</b>		
<b>Time(s.)</b>	<b><math>\tau</math></b>	<b>Reservoir</b>	<b>Pipe 1</b>	<b>Pipe 2</b>	<b>Reservoir</b>	<b>Pipe 1</b>	<b>Pipe 2</b>
0.000	1.000	1.000	1.000	1.000	1.000	1.000	1.000
0.500	0.963	1.000	1.000	0.989	1.000	1.000	0.990
1.000	0.900	1.000	0.988	0.97	1.000	0.989	0.970
1.500	0.813	0.977	0.967	0.937	0.977	0.967	0.937
2.000	0.700	0.935	0.922	0.884	0.934	0.922	0.884
2.500	0.600	0.867	0.847	0.814	0.867	0.847	0.813
3.000	0.500	0.761	0.755	0.722	0.761	0.754	0.721
3.500	0.400	0.643	0.633	0.609	0.643	0.633	0.609
4.000	0.300	0.506	0.496	0.473	0.506	0.495	0.472
4.500	0.200	0.35	0.344	0.325	0.349	0.344	0.325
5.000	0.100	0.183	0.177	0.166	0.183	0.177	0.166
5.500	0.038	0.006	0.004	0.059	0.006	0.004	0.060
6.000	0.000	-0.175	-0.106	0.000	-0.174	-0.104	0.000
6.500	0.000	-0.217	-0.157	0.000	-0.215	-0.157	0.000
7.000	0.000	-0.139	-0.085	0.000	-0.140	-0.084	0.000
7.500	0.000	0.047	0.035	0.000	0.046	0.034	0.000
8.000	0.000	0.208	0.126	0.000	0.208	0.124	0.000
8.500	0.000	0.205	0.148	0.000	0.203	0.148	0.000
9.000	0.000	0.088	0.054	0.000	0.089	0.054	0.000
9.500	0.000	-0.097	-0.071	0.000	-0.095	-0.070	0.000
10.000	0.000	-0.229	-0.139	0.000	-0.229	-0.137	0.000



*Figure 5.14. H vs. Time at valve end (Chaudhry vs. Present study)*



*Figure 5.15. Q vs. Time at the reservoir (Chaudhry vs. Present study)*

As seen on the tables and figures, the results are accurately similar and close to each other.

## 5.2 Pump Failure Scenarios

In this section, the results are compared with a program called Whammer. This program is developed by Wiggert (1984). It must be mentioned that the code of the S-hammer software for pump failure simulation is inspired by him. The Whammer program is developed in Fortran programming language and aimed to analyze single pump failure transient cases. To validate the S-Hammer code, the executable file of the Whammer is used, and the output data is obtained. In this comparison, three different scenarios are compared and simulated;

- Pump trip without discharge valve
- Pump trip with discharge valve closing gradually
- Pump trip with discharge valve closing suddenly

Figure 5.16 shows the hydraulic model of an example.

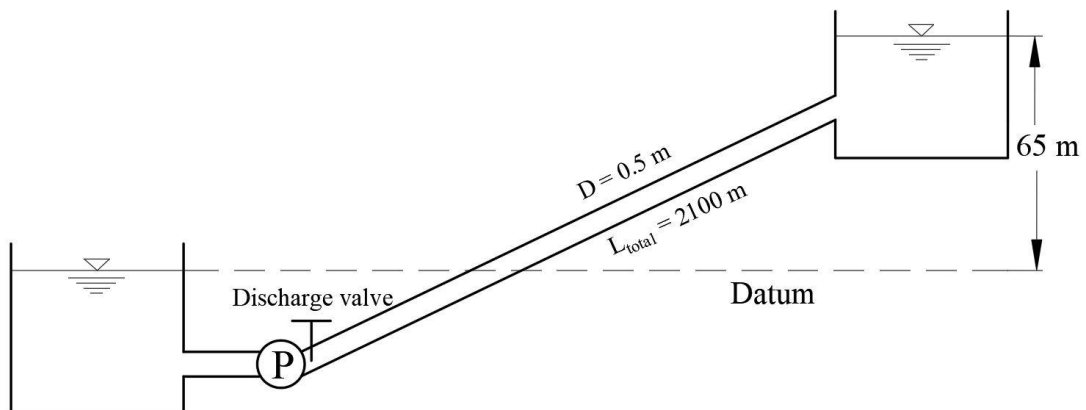


*Figure 5.16.* The hydraulic model for pump failure transient simulation

The model which is selected for simulation is formed of an upstream and downstream reservoir with a pump close to the upstream reservoir. The detailed information for input data is shown in Table 5.6.

Table 5.6 *Input data for pump failure transient simulation*

Data Title	Value	Unit
Total Pipe Length	2100	m
Pipe Diameter	0.5	m
Friction Factor	0.02	-
Wave Speed	1000	m/s
Upstream Reservoir Elevation	0	m
Downstream Reservoir Elevation	65	m
Rated Head of Pump, $H_R$	75	m
Rated Discharge of Pump, $Q_R$	0.25	m <sup>3</sup> /s
Rated Torque of Pump, $T_R$	1947.31	N.m
Rated Speed of Pump, $N_R$	1100	rpm
Rated Efficiency of Pump, $\eta_R$	0.82	-
$W_R^2$ Value of Pump	165.3	N.m <sup>2</sup>
Pump Trip Time	5	seconds

### 5.2.1 Pump Failure without Discharge valve

In this case, the pump failure is simulated. This pump trips at  $t = 5$  seconds of simulation, and there is no valve available for the pump. The maximum simulation time is chosen as 60 seconds, and the code calculated  $\Delta t = 0.525$  seconds according to the Courant condition. Results are compared and plotted on the Figures below.

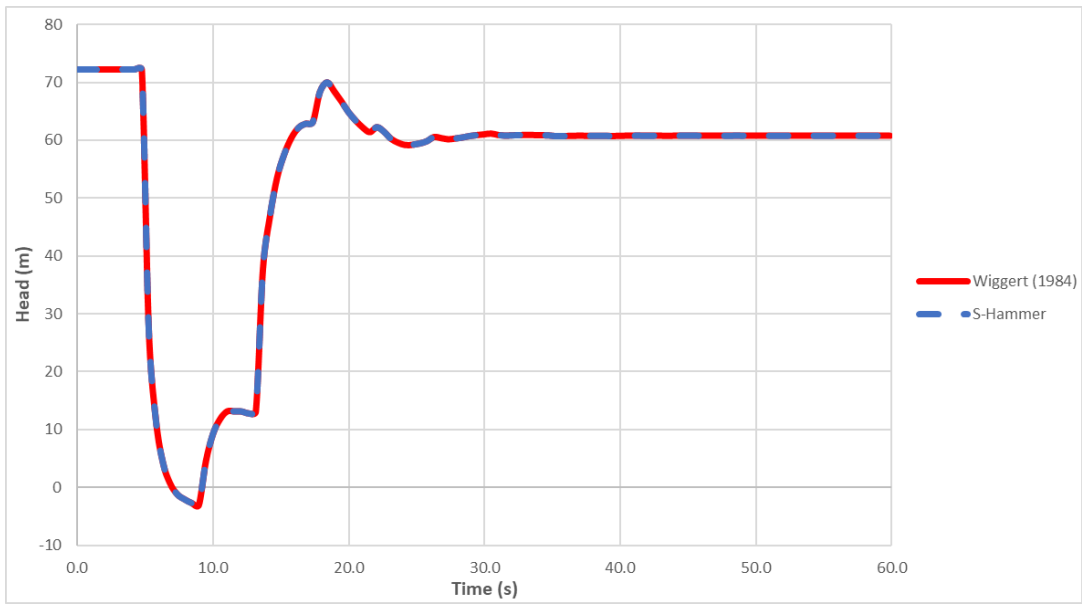


Figure 5.17. H vs. Time chart for pump failure with no discharge valve, at  $x = 0$  m

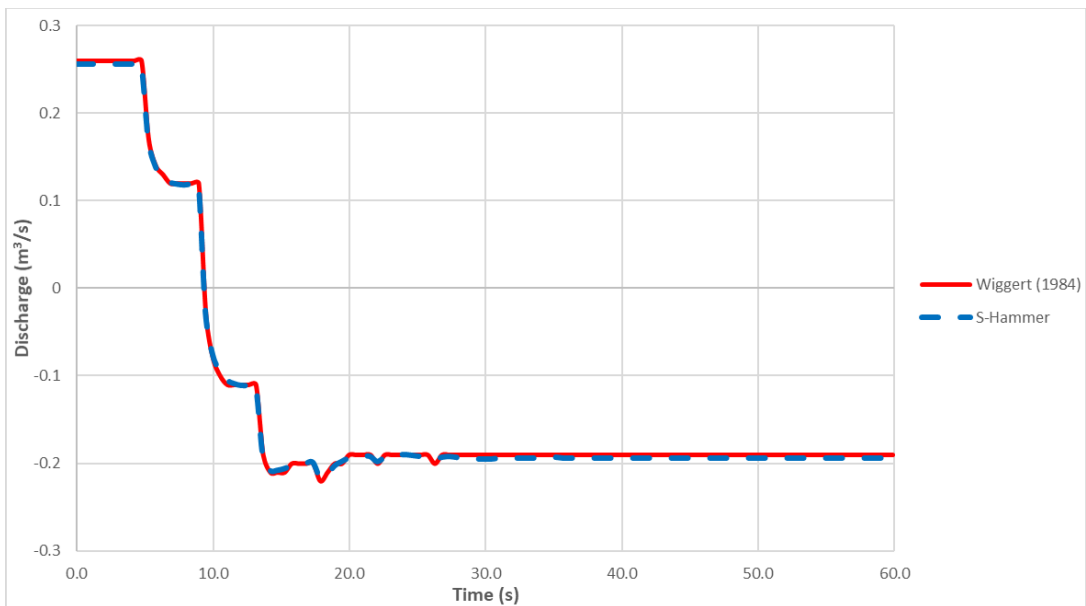


Figure 5.18. Q vs. Time chart for pump failure with no discharge valve, at  $x = 0$  m

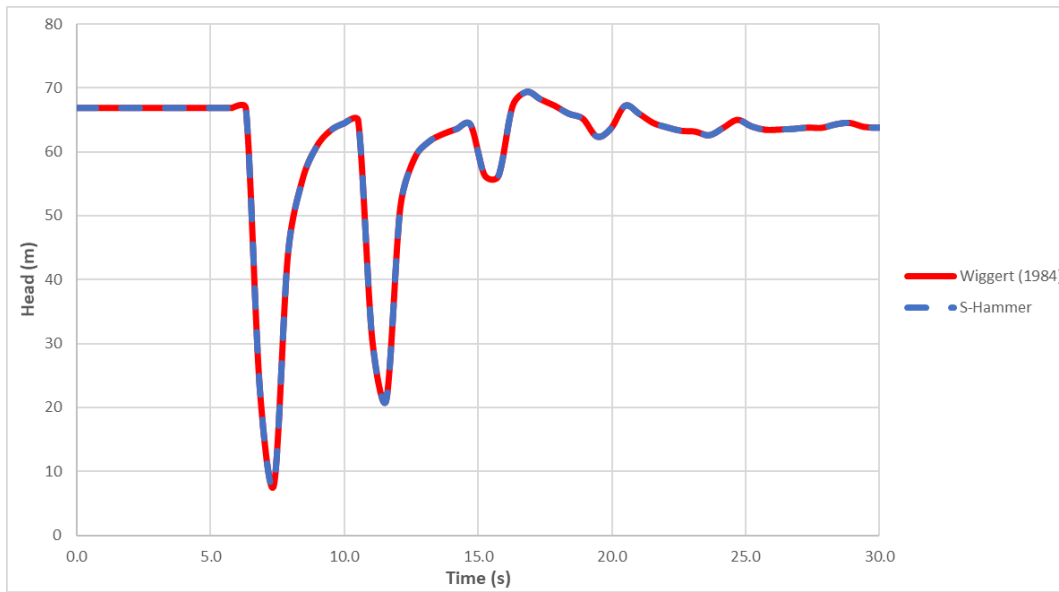


Figure 5.19. H vs. Time chart for the pump with no discharge valve, at  $x = 1575$  m

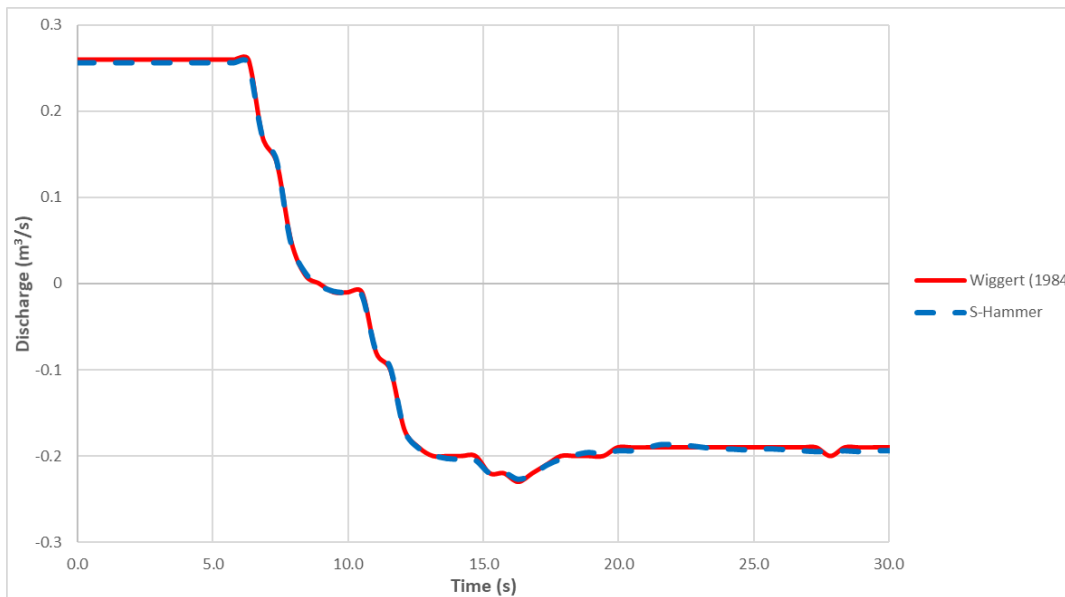


Figure 5.20. Q vs. Time chart for the pump with no discharge valve, at  $x = 1575$  m

As shown in the charts above, the results are obtained for the locations where  $x = 0$  m and  $x = 1575$  m. The results acquired from S-Hammer are very close to those from Wiggert (1984).

## 5.2.2 Pump Failure with Discharge valve Closing Gradually

In this scenario, a pump failure transient event with a valve is studied. The valve closes at a gradual rate. To define the valve closure values Eq. (4-1) is used. Closure time is selected as 8 seconds. Figure 5.21 shows the valve closure setting of the S-Hammer.

Regular Valve Closure

$$\tau = \left(1 - \frac{t}{t_c}\right)^{E_m}$$

Em

Tc (sec)

**i** This is a valve closure relationship for the pipeline.  $\tau$  is dimensionless and is a function of time.

Figure 5.21. S-Hammer valve closure setting for the pump trip with a valve

Results are compared and plotted on the Figures below.

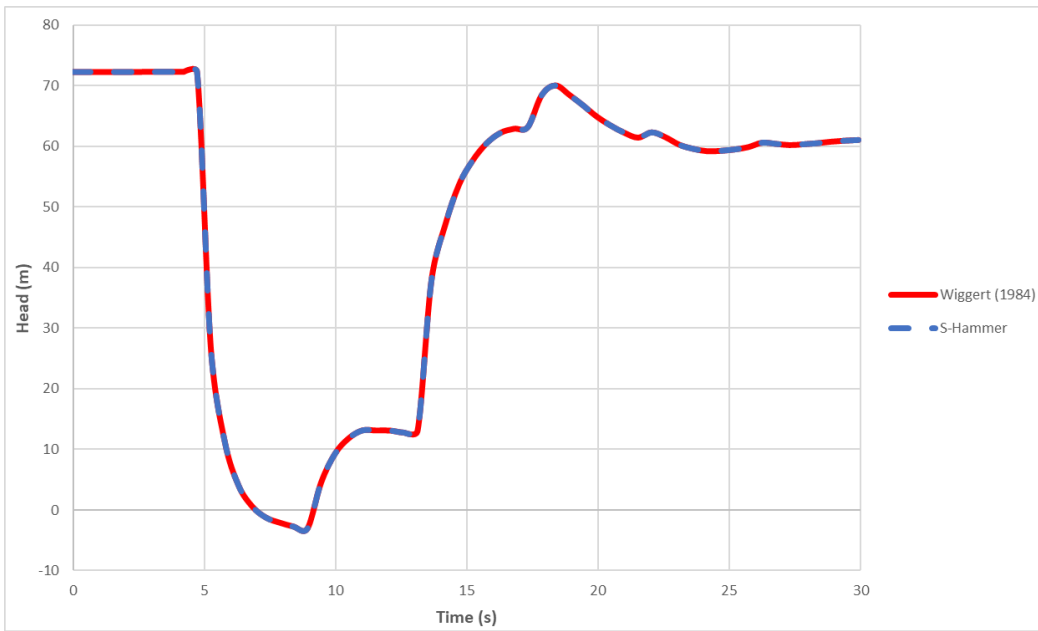


Figure 5.22. H vs. Time chart for pump failure transient event with a discharge valve and  $t_c = 8$  s, at  $x = 0$  m

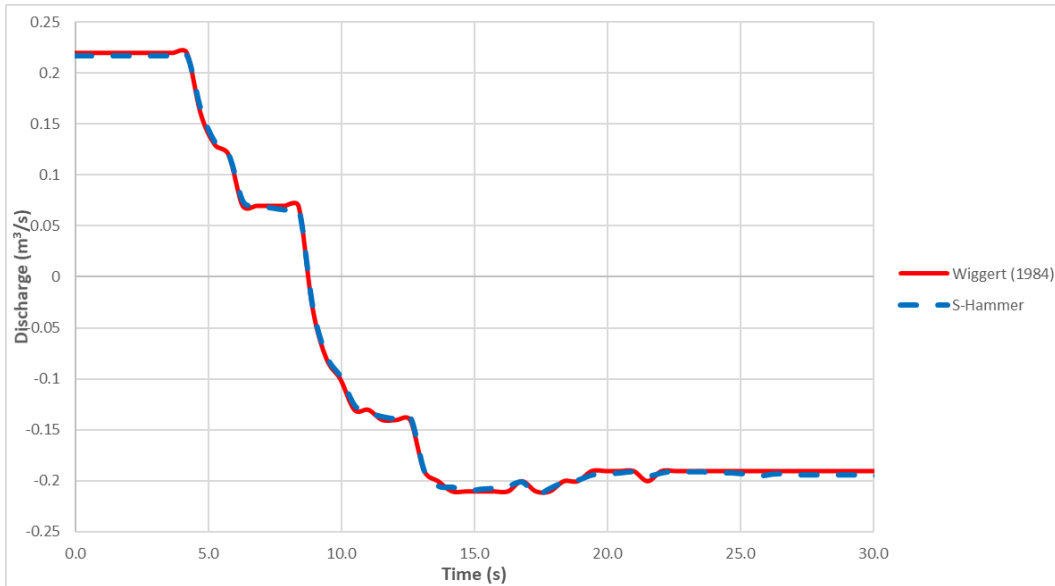


Figure 5.23. Discharge vs. Time chart for pump failure transient event with a discharge valve and  $t_c = 8$  seconds, at  $x = 0$  m

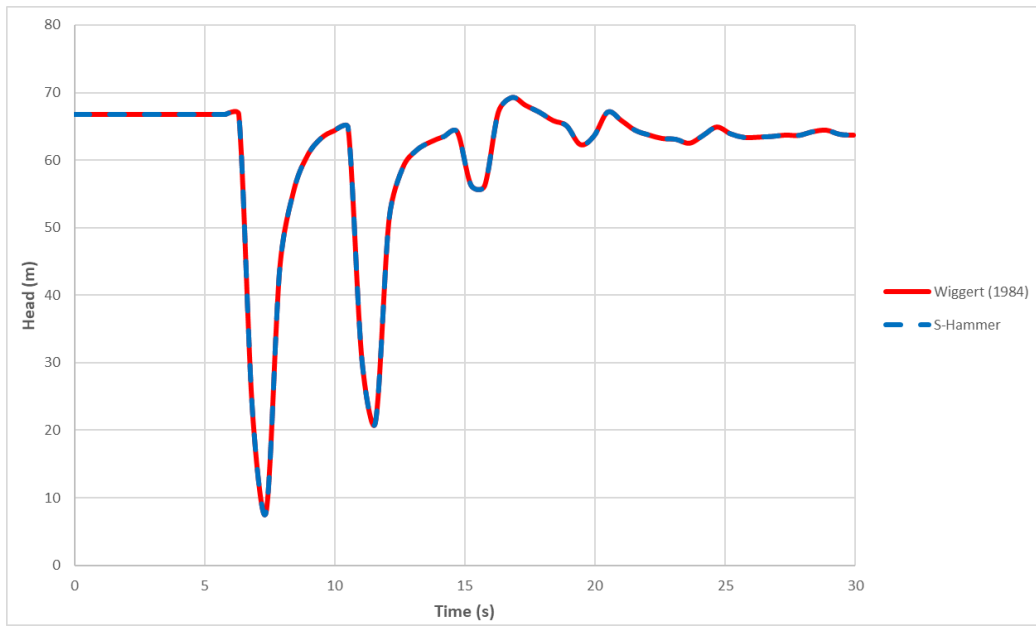


Figure 5.24. H vs. Time chart for pump failure transient event with a discharge valve and  $t_c = 8$  seconds, at  $x = 1575$  m

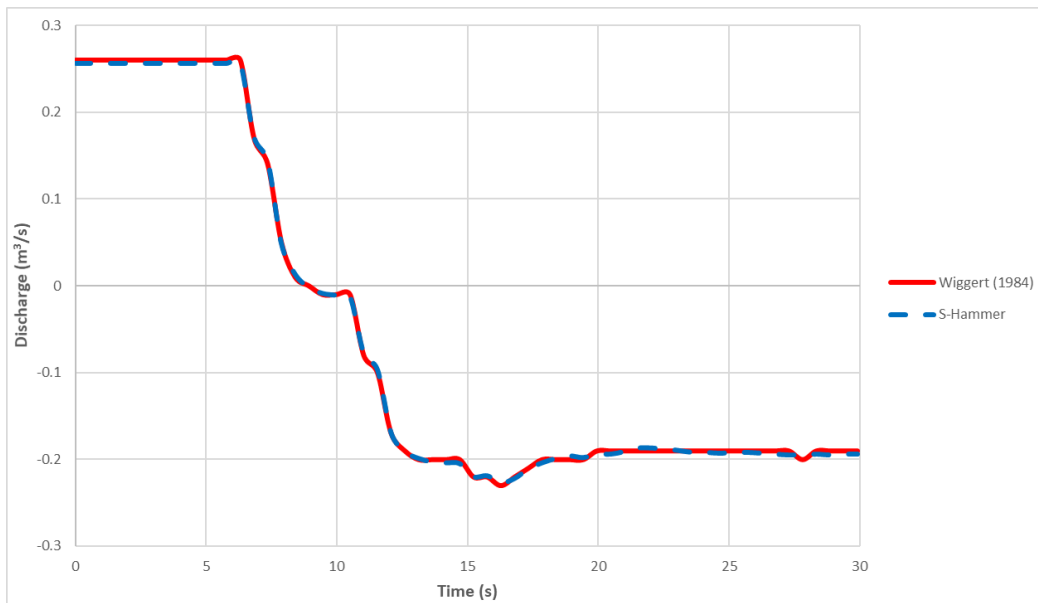


Figure 5.25. Q vs. Time chart for pump failure transient event with a discharge valve and  $t_c = 8$  seconds, at  $x = 1575$  m

### 5.2.3 Pump Failure with Discharge valve Closing Suddenly

In this section, pump failure with the discharge valve closing instantly is demonstrated. Closure time is the instant after the pump trip starts. The results are plotted and shown in the figures below.

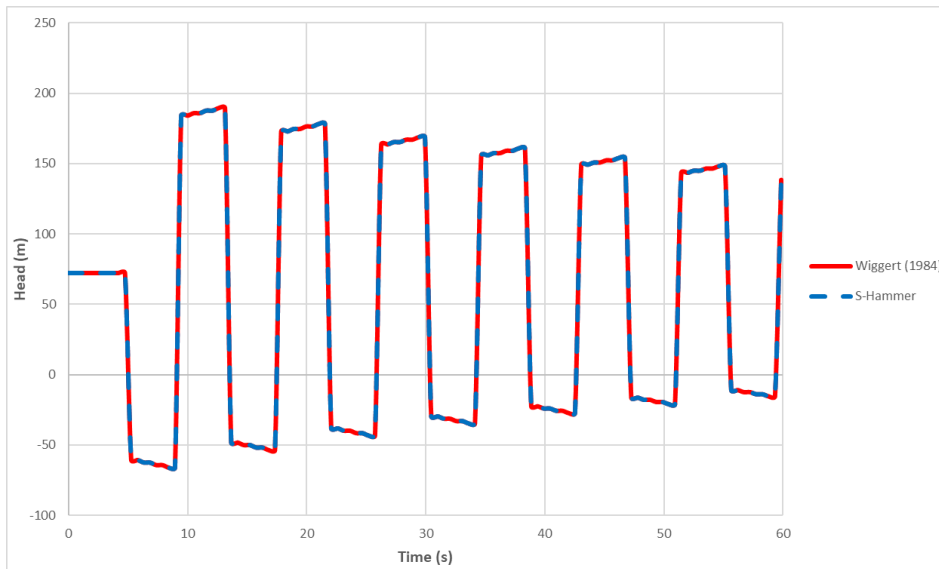


Figure 5.26. H vs. Time chart for pump failure transient event with a discharge valve closing suddenly at  $x = 0$  m

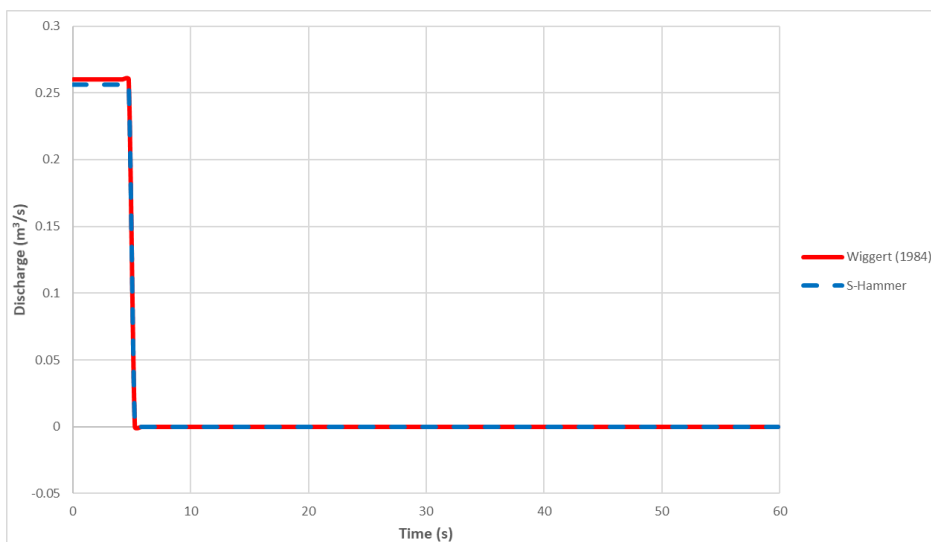


Figure 5.27. Q vs. Time chart for pump failure transient event with a discharge valve closing suddenly at  $x = 0$  m

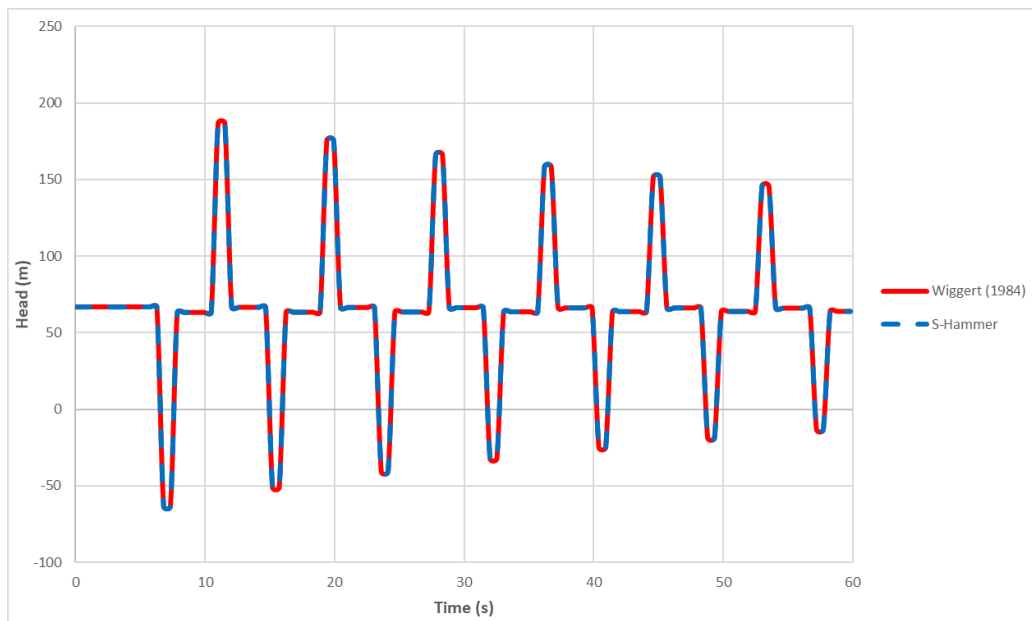


Figure 5.28. H vs. Time chart for pump failure transient event with a discharge valve closing suddenly, at  $x = 1575$  m

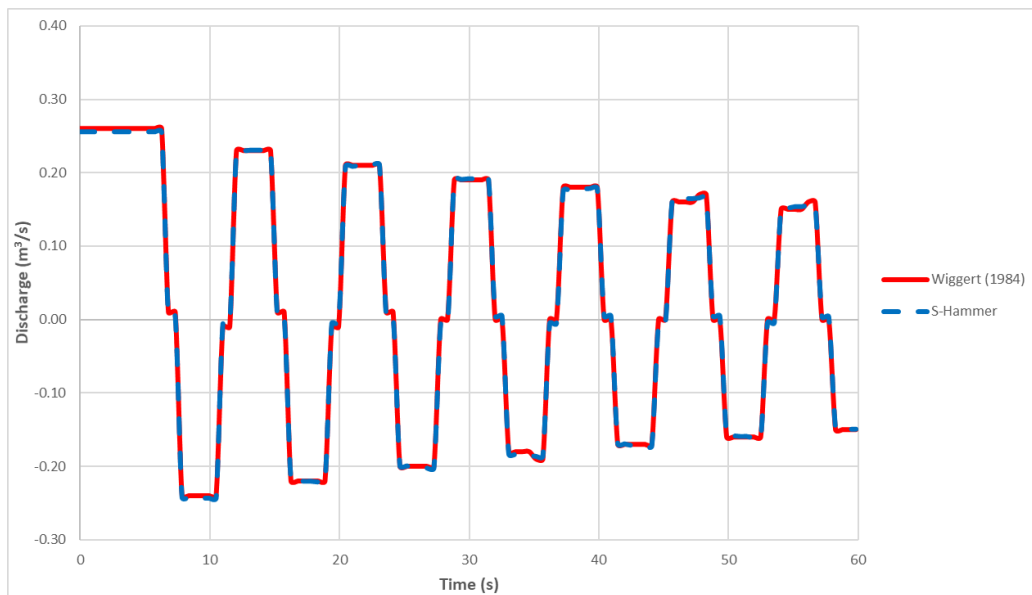


Figure 5.29. Q vs. Time chart for pump failure transient event with a discharge valve closing suddenly, at  $x = 1575$  m

### 5.3 Surge Tank Computation

In this section, a surge tank boundary condition is studied to simulate the water surface fluctuations in the surge tank and compared to those provided in the book written by (Cofcof, 2011) in which the details of the example can be found. As seen in Figure 5.30, a surge tank is located between pipe 1 (a tunnel) and pipe 2 (a penstock) in a hydropower facility. We would like to analyze the water surface fluctuations in the surge tank with the given data below. The upstream boundary condition is a large and constant head reservoir while the downstream boundary is a sudden load rejection by the turbine making the discharge zero through the turbine (i.e. since the turbine cannot operate under these circumstances, the butterfly valve not shown in the figure just upstream of the turbine is closed.) To comply with the data of Cofcof, the system is assumed to be frictionless.

The data used for the first analysis are;

$$Q = 40 \text{ m}^3/\text{s}$$

$$Q_{\text{tur}} = 0$$

$$L_{\text{tunnel}} = 4000 \text{ m}$$

$$L_{\text{penstock}} = 170 \text{ m}$$

$$D = 4 \text{ m}$$

$$f = 0$$

$$A_s = 176.625 \text{ m}^2$$

$$\text{Time interval} = 0.5 \text{ seconds}$$

$$\text{Simulation time} = 4000 \text{ seconds}$$

$$\text{Entrance loss coefficient} = 1.1$$

Figure 5.30 shows the sketch of the hydropower facility.

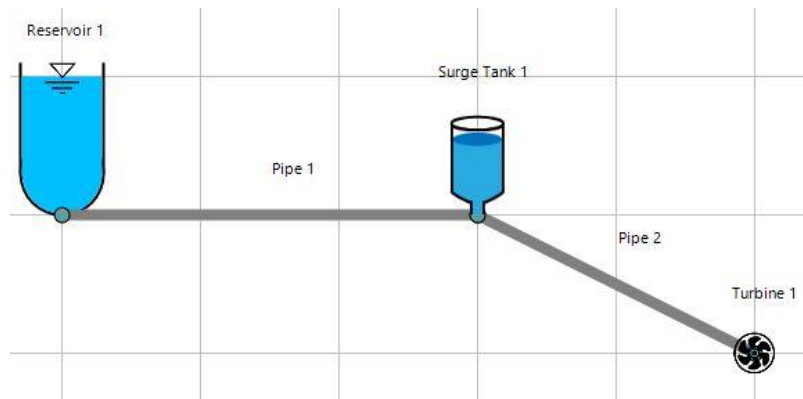


Figure 5.30. Simple surge tank model (Cofcof, 2011)

After inserting the required data into the S-hammer software, the results are obtained in the program and shown in Figure 5.31.



Figure 5.31. Simple surge tank simulations of S-Hammer

As seen in Figure 5.31, surge tank diameter is set as 15 m, and the maximum elevation for the liquid inside surge tank is calculated as 16.855 m. The simulation is done for both maximum and minimum discharge in the system and compared. The comparisons of the results are shown in Table 5.7.

Table 5.7 Simple surge tank result comparisons

Pipeline and surge tank parameters				Y <sub>max</sub> (m)		Difference (m)
D <sub>tunnel</sub> (m)	A <sub>tank</sub> (m <sup>2</sup> )	D <sub>tank</sub> (m)	Q (m <sup>3</sup> /s)	S-Hammer	Cofcof (2011)	
4	176.71	15	40	16.855	17.1	0.245
			25	10.69	10.76	0.07

As seen in Table 5.7, results are accurately similar to each other.

#### 5.4 Closure on the Cases

In this chapter, various transient scenarios have been studied and verified with some benchmarks. All cases are modeled by the code which is developed in this study. These cases include different boundary conditions. The boundaries used in validation are the upstream reservoir, a closing downstream valve, pump with and without discharge valve, and an inline simple surge tank in a hydropower plant.

To be able to simulate the transient problem in the software, the initial steady-state conditions first should be calculated. Then, the unknown head and discharge values in the solution domain (x-t space) can be computed by using appropriate upstream and downstream boundaries defined by the user.

## CHAPTER 6

### CONCLUSIONS

In this study, a program was developed to solve and analyze transients in pipelines with a number of user-defined transient scenarios (i.e. boundary conditions). The scenarios were selected carefully as they commonly occur in the engineering practice and their proper considerations in the problem and measures to be taken if necessary are essential for safe and reliable operations of such systems. To solve the transient equations, a widely known approach, the method of characteristics was used in the code. In the previous chapters of this thesis, the theoretical background of this method and derivation of its equations were clarified. Various boundary conditions were used in the code, and these boundaries are single pipe, series pipes, upstream reservoir with constant and variable head, single centrifugal pump, downstream valve closing, downstream dead-end, and a simple surge tank in a power plant.

The developed computer software has a visual user interface with numerous capabilities. The software finishes the analysis quickly and presents tabular and graphical results. Animations showing how the head or discharge varies with time over a pipeline can be performed. Detailed information about the program was explained in its relevant chapter. As long as one defines an accurate model, there is no restriction in either the size of the model or the number of the components. Also, the program runs accurately in terms of the system processor and memory, so sophisticated computers are not needed to run the program.

When analyzing a transient event with computer code, numerical stability is essential and critical. As long as the Courant condition is satisfied, no convergence problems are observed in the present study. One must select the properties of the designed system and its grid generation properly by paying great care to this aspect. For instance, the time increment selection plays a crucial role in terms of accuracy. To get more accurate results, with a smaller time increment, more accurate and precise

results can be obtained at the cost of more CPU time. This would be an important aspect to consider, especially for sophisticated hydraulic systems where there are many numbers of pipes, and the boundary conditions are complex. As the newly developed software is planned to be improved and become more advanced in future studies, this aspect will be given more attention. Also, the capabilities of the code are intended to be enhanced by using more complex real applications.

The validation of the results obtained by the software was verified by comparing them with some well-known benchmarks. The comparisons are made graphically and numerically. Results showed that the output of the present study agrees with those of the benchmarks.

The logical structure of the program is user-friendly, and it is independent of any external application. To help users in working with the software, a user manual was prepared to guide them properly. It should be mentioned and emphasized that the program needs to be improved by adding more protection devices as new boundary conditions to compete in this field.

## REFERENCES

- Afshar, M. H., & Rohani, M. (2008). Water hammer simulation by implicit method of characteristic. *International Journal of Pressure Vessels and Piping*, 85(12), 851–859.
- Bozkuş, Z. (2008). Water hammer Analyses of Çamlidere-Ivedik Water Treatment Plant (IWTP) Pipeline. *Teknik Dergi*, 19(2), 4409–4422.
- Calamak, M., & Bozkus, Z. (2012). Protective measures against waterhammer in run-of-river hydropower plants. *Teknik Dergi*, 23(4), 6187–6202.
- Chaudhry, M. H. (1979). *Applied hydraulic transients*. Springer.
- Cofcof, Ş. (2011). *Denge Bacaları*. Dolsar Müh. Ltd. Şti, Ankara.
- Dalgıç, H. (2017). *Development of a computer code to analyse fluid transients in pressurized pipe systems*. Master's Thesis, Middle East Technical University, Ankara, Turkey.
- Dinçer, A. E. (2013). Investigation of Waterhammer Problems in the Penstocks of Pumped-Storage Power Plants. Master's thesis, Middle East Technical University, Ankara, Turkey.
- Dursun S. (2013) Numerical Investigation of Protection Measures against Water Hammer in the Yeşilvadi Hydropower Plant. Master's thesis, Middle East Technical University, Ankara, Turkey.
- Dinçer, A. E., & Bozkuş, Z. (2016). Investigation of Waterhammer Problems in Wind-Hydro Hybrid Power Plants. *Arabian Journal for Science and Engineering*, 41(12), 4787–4798.
- Karney, Bryan W, & McInnis, D. (1992). Efficient calculation of transient flow in simple pipe networks. *Journal of Hydraulic Engineering*, 118(7), 1014–1030.

- Karney, Bryan William. (1984). *Analysis of fluid transients in large distribution networks*. University of British Columbia.
- Koç, G. (2007). *Simulation of flow transients in liquid pipeline systems*. Master's Thesis, Middle East Technical University, Ankara, Turkey.
- Marchal, M. G. Flesch, P. S. (1965). The calculation of waterhammer problems by means of the digital computer. *Proc. Intern. Symp. Waterhammer Pumped Storage Projects, ASME, Chicago, USA*.
- Seleznev, V. S., Liseikin, A. V, Bryksin, A. A., & Gromyko, P. V. (2014). What Caused the Accident at the Sayano–Shushenskaya Hydroelectric Power Plant (SSHPP): A Seismologist's Point of View. *Seismological Research Letters*, 85(4), 817–824.
- Streeter, V. L., & Wylie, E. B. (1978). *Fluid Mechanics*. McGraw-Hill.
- Streeter, V. L., & Wylie, E. B. (1967). *Hydraulic transients*. Mcgraw-hill.
- Thorley, D. (2004). *Fluid Transients in Pipeline Systems*. Professional Engineering Publishing Limited, London and Bury St Edmunds, UK
- Wylie, E. B. and Streeter, V. L. with Suo, L. (1993). *Fluid Transients in Systems*. New Jersey: Prentice-Hall
- Wiggert, D. C. (1984). *Single Pipeline Water Hammer Program*. Michigan State University.

## APPENDICES

### A. USER MANUAL

In this section, step by step instructions about the use of the software will be provided.

1. Open S-Hammer application.
2. From the file tab, click the new project, and from the new project form, write the name for the project and select a location.

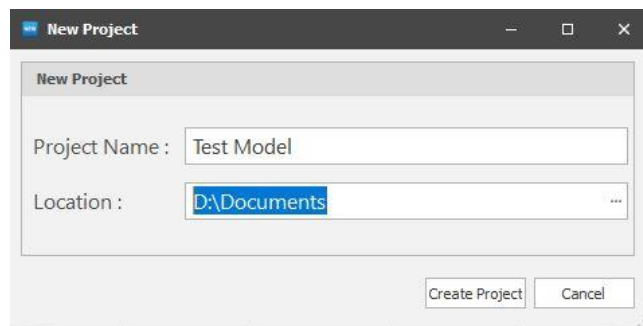


*Figure A.1.* New project windows form

3. From the design tab, click a component to start drawing the model on canvas.



*Figure A.2.* Design tab and design components list

4. Draw a desired accurate hydraulic model.

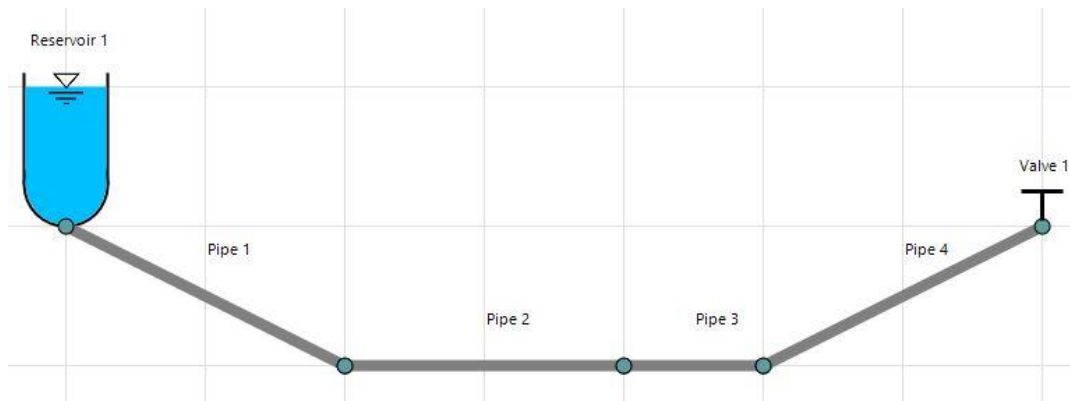


Figure A.3. A sample hydraulic system drawn in S-Hammer

As seen in Figure A.3, a valid hydraulic system must be drawn. The boundaries included in the example are the reservoir at upstream and a valve at the downstream end.

5. Go to the properties tab and insert pipe information. For instance, Figure A.4 illustrates relevant information of pipes entered in the tab menu.

Properties									
Pipes									
Reservoirs									
Valves									
Pumps									
Surge Tanks									
Turbines									
Enter text to search... Find Clear <input type="checkbox"/> Select All									
	Name	ID	Length (m)	Diameter (m)	Friction	Wave Speed (m/s)	Thickness (mm)	Material	Select
→	Pipe 1	7	500	0.3	0.019	1200	0	Steel	<input type="checkbox"/>
	Pipe 2	8	500	0.2	0.018	1200	0	Steel	<input type="checkbox"/>
	Pipe 3	9	200	0.2	0.018	1200	0	Steel	<input type="checkbox"/>
	Pipe 4	10	500	0.3	0.019	1200	0	Steel	<input type="checkbox"/>

Figure A.4. Pipe properties inserted to a sample model

6. In the next step, insert the initial conditions of the steady-state flow.
  - Go to the analysis tab and click initial conditions button. Select and enter one of the hydraulic conditions. Next, enter the simulation time options, as shown in Figure A.4.

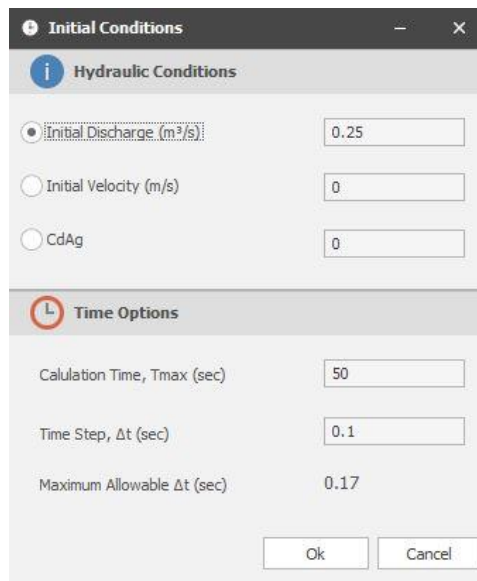


Figure A.5. Initial conditions options of a sample model

- Select the valve condition as “Being closed”, go to the valve closure setting in the valve properties tab and select a valve and its closure setting type. In this case, regular closure is chosen, and the required data is entered, as shown in Figure A.6.

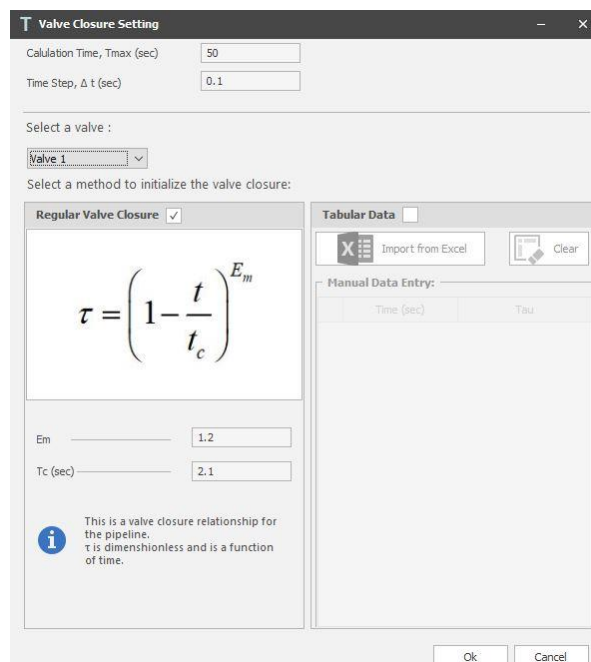


Figure A.6. Valve closure setting of a sample model

- Now steady-state head value must be entered. It is possible in two different options. One can choose to enter the head value at upstream or downstream. In this model, the upstream boundary is a reservoir, and the downstream boundary is a valve. So, we can enter either reservoir head or valve head. The steady-state head value at the valve end is selected as 140 m.
7. Now that we entered all of the required data go to the analysis tab, and click the compute button. If an error occurs, the application will warn you about the problem. But if there is no problem with the analysis, the message will appear in the messages box, as shown in Figure A.7.



Figure A.7. Messages printed for an example model

8. After a successful analysis, now it's time to see the results.
- To see the full information about pipes after analysis, go to properties sidebar and click maximize.

Name	ID	Length (m)	Diameter (m)	$\Delta x$ (m)	Nodes	Friction	Wave Speed (m/s)	Maximum Head (m)	Minimum Head (m)	Maximum Pressure (kPa)	Minimum Pressure (kPa)	Select
Pipe 1	7	500	0.3	125	4	0.019	1250	704.819	158.157	6911.248	1550.841	<input type="checkbox"/>
Pipe 2	8	500	0.2	125	4	0.018	1250	1011.027	-92.45	9913.833	-906.538	<input type="checkbox"/>
Pipe 3	9	200	0.2	100	2	0.018	1000	1075.979	-201.619	10550.734	-1977.017	<input type="checkbox"/>
Pipe 4	10	500	0.3	125	4	0.019	1250	1119.173	-204.387	10974.281	-2004.159	<input type="checkbox"/>

Figure A.8. Properties of example model after analysis

- To see the transient solution results, go to the analysis tab, and on the results section click the tables button.

- On the tables window, on the time-based table by varying the trackbar, choose the desired time, and click show table button to see the results, as shown in Figure A.9.

	Time (sec)	Object Name	Node No.	Head (m)	Discharge (m <sup>3</sup> /s)	Velocity (m/s)	Pressure (kPa)	Tau
→	23.00	Pipe-1	1	383.817	-0.058	-0.820	3763.600	0.000
	23.00	Pipe-1	2	415.270	-0.041	-0.574	4072.017	0.000
	23.00	Pipe-1	3	416.804	-0.041	-0.585	4087.053	0.000
	23.00	Pipe-1	4	422.220	-0.038	-0.544	4140.165	0.000
	23.00	Pipe-1	5	347.394	0.003	0.044	3406.446	0.000
	23.00	Pipe-2	1	347.394	0.003	0.100	3406.446	0.000
	23.00	Pipe-2	2	247.275	-0.022	-0.688	2424.710	0.000
	23.00	Pipe-2	3	247.954	-0.022	-0.691	2431.363	0.000
	23.00	Pipe-2	4	258.387	-0.019	-0.611	2533.671	0.000
	23.00	Pipe-2	5	198.239	-0.004	-0.137	1943.877	0.000
	23.00	Pipe-3	1	198.239	-0.004	-0.137	1943.877	0.000
	23.00	Pipe-3	2	198.777	-0.004	-0.132	1949.151	0.000
	23.00	Pipe-3	3	197.482	-0.004	-0.119	1936.453	0.000
	23.00	Pipe-4	1	197.482	-0.004	-0.053	1936.453	0.000
	23.00	Pipe-4	2	200.194	-0.002	-0.032	1963.040	0.000
	23.00	Pipe-4	3	183.247	0.007	0.101	1796.863	0.000
	23.00	Pipe-4	4	168.032	-0.001	-0.018	1647.674	0.000
	23.00	Pipe-4	5	165.714	0.000	0.000	1624.948	0.000

Figure A.9. Time-based table results for the example model

- On the pipe-based table tab, select a pipe and click the show table button. In this case, pipe three is selected, and the results are sorted by node number.

	Time (sec)	Object Name	Node No.	Head (m)	Discharge (m <sup>3</sup> /s)	Velocity (m/s)	Pressure (kPa)	Tau
→	0.00	Pipe-4	1	160.197	0.250	3.537	1570.849	0.000
	0.10	Pipe-4	1	160.197	0.250	3.537	1570.849	0.000
	0.20	Pipe-4	1	160.197	0.250	3.537	1570.849	0.000
	0.30	Pipe-4	1	160.197	0.250	3.537	1570.849	0.000
	0.40	Pipe-4	1	726.871	0.075	1.067	7127.479	0.000
	0.50	Pipe-4	1	726.871	0.075	1.067	7127.479	0.000
	0.60	Pipe-4	1	739.729	0.080	1.125	7253.560	0.000

Figure A.10. Pipe-based table results for the example model

- To see the graphical results, on the main window, go to analysis tab and select time-dependent charts. On this window, you can personalize the appearance of the graph and legends whenever it is wanted. On the data options panel, select chart data type. Next, choose the pipe number and its node number and click ‘Add Primary Chart’ button.

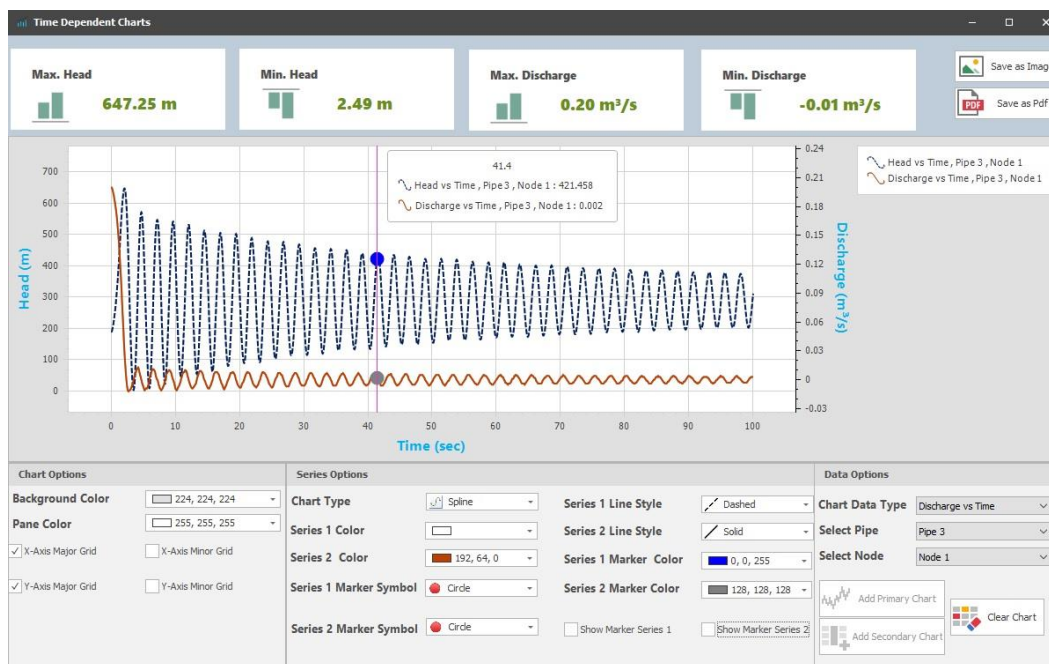


Figure A.11. Time-dependent graphical chart for the example model

If required, a secondary legend can be added by changing the chart data information and clicking ‘Add Secondary Chart’ button. Moreover, by moving the mouse on the data points, detailed information about the point values is shown in Figure A.11.

- Another option is to see the graphical results along with the distance of the pipeline system and animate it. To do so, on the main window, go to charts panel and click ‘Animative Charts’ button.
- On the chart window, as mentioned previously, personalize the charts and legend and choose desired data information to plot the graph.

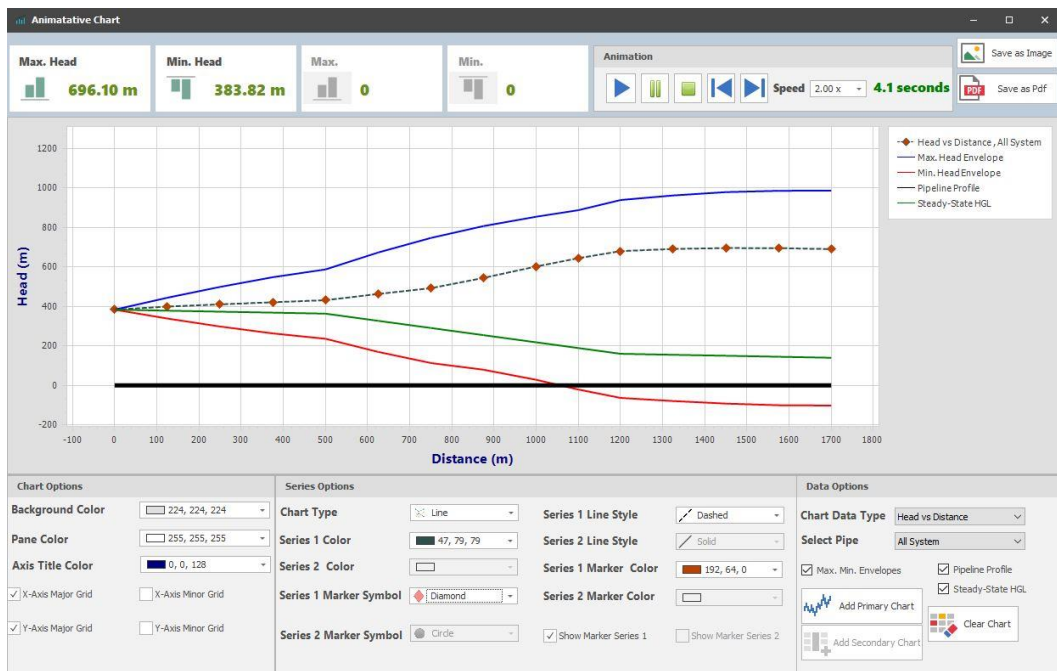


Figure A.12. Animative chart result for the example model

After plotting the chart, on the animation panel, select a speed rate for animation and click start animation button to see the transient event through the pipeline.

9. After all of the steps are done, the user can save the project so that it can be modified or reused later.